2 WINDINGS OF ELECTRICAL MACHINES

The operation principle of electrical machines is based on the interaction between the magnetic fields and the currents flowing in the windings of the machine. The winding constructions and connections together with the currents and voltages fed into the windings determine the operating modes and the type of the electrical machine. According to their different functions in an electrical machine, the windings are grouped for instance as follows:

- armature windings,
- other rotating-field windings (e.g. stator or rotor windings of induction motors)
- field (magnetizing) windings,
- damper windings
- commutating windings, and
- compensating windings.

Armature windings are rotating-field windings, into which the rotating-field-induced voltage required in energy conversion is induced. According to IEC 60050-411, the armature winding is a winding in a synchronous, DC, or single-phase commutator machine, which, in service, receives active power from or delivers active power to the external electrical system. This definition also applies to a synchronous compensator if the term 'active power' is replaced by 'reactive power'. The air gap flux component caused by the armature current linkage is called the armature reaction.

An armature winding determined under these conditions can transmit power between an electrical network and a mechanical system. Magnetizing windings create a magnetic field required in the energy conversion. All machines do not include a separate magnetizing winding; for instance in asynchronous machines, the stator winding both magnetizes the machine and acts as a winding, where the operating voltage is induced. The stator winding of an asynchronous machine is similar to the armature of a synchronous machine; however, it is not defined as an armature in the IEC standard. In this material, the asynchronous machine stator is therefore referred to as a rotating-field stator winding, not an armature winding. Voltages are also induced to the rotor of an asynchronous machine, and currents significant in the torque production are created. However, the rotor itself takes only a rotor's dissipation power (I^2R) from the air gap power of the machine, this power being proportional to the slip; therefore, the machine can be considered stator fed, and depending on the rotor type, the rotor is called either a squirrel cage rotor or a wound rotor. In DC machines, the function of a rotor armature winding is to perform the actual power transmission, the machine being thus rotor fed. Field windings do not normally participate in energy conversion, double-salient pole reluctance machines maybe excluded: in principle, they have nothing but magnetizing windings, but the windings also perform the function of the armature. In DC machines, commutating and compensating windings are windings, the purpose of which is to create auxiliary field components to compensate the armature reaction of the machine and thus improve its performance characteristics. Similarly as the previously described windings, these windings do not participate in energy conversion in the machine either. The damper windings of synchronous machines are a special case among different winding types. Their primary function is to damp undesirable phenomena, such as oscillations and fields rotating opposite to the main field. Damper windings are important during the transients of controlled synchronous drives, in which the damper windings keep the air gap flux linkage instantaneously constant. In the asynchronous drive of a synchronous machine, the damper windings act like cage windings of asynchronous machines.

The most important windings are categorized according to their geometrical characteristics and internal connections as follows:

- phase windings,
- salient pole windings, and
- commutator windings

Windings, in which separate coils embedded in slots form a single or poly-phase winding, constitute a large group of AC armature windings. However, a similar winding is also employed in the magnetizing of non-salient pole synchronous machines. In commutator windings, individual coils contained in slots form a single or several closed circuits, which are connected together via a commutator. Commutator windings are employed only as armature windings of DC and AC commutator machines. Salient pole windings are normally concentrated field windings, but may also be used as armature windings for instance in fractional slot permanent magnet machines and in double-salient reluctance machines. Concentrated stator windings are used as an armature winding also in small shaded-pole motors.

In the following, the windings applied in electrical machines are classified according to the two main winding types, viz. slot windings and salient pole windings. Both types are applicable both to direct and alternating current cases, Table 2.1.

Table 2.1. Different types of windings or permanent magnets used instead of a field winding in the most common machine types.

	Stator winding	**Rotor winding**	**Compensating winding**	**Commutating winding**	**Damper winding**
Salient pole synchronous machine	poly-phase distributed rotating-field slot winding	salient pole winding	-	-	short-circuited cage winding
Non-salient pole synchronous machine	poly-phase distributed rotating-field slot winding	slot winding	-	-	solid rotor core or short-circuited cage winding
Synchronous reluctance machine	poly-phase distributed rotating-field slot winding	-	-	-	short-circuited cage winding possible
Permanent magnet synchronous machine, PMSM, $q > 0.5$	poly-phase distributed rotating-field slot winding	permanent magnets	-	-	solid rotor or short-circuited cage winding, or e.g. aluminium plate in the air gap possible
Permanent magnet synchronous machine, PMSM, $q \leq 0.5$	poly-phase concentrated pole winding	permanent magnets	-	-	Damping should be harmful because of excessive losses
Double-salient reluctance machine	poly-phase concentrated pole winding	-	-	-	-
Induction motor, IM	poly-phase distributed rotating-field slot winding	cast or soldered cage winding, squirrel cage winding	-	-	-
Solid rotor IM	poly-phase distributed rotating-field slot winding	solid rotor made of steel, may be equipped with squirrel cage	-	-	-
Slip-ring asynchronous motor	poly-phase distributed rotating-field slot winding	poly-phase distributed rotating-field slot winding	-	-	-

DC machine	salient pole winding	rotating-field commutator slot winding	slot winding	salient pole winding	-

2.1 Basic Principles

2.1.1 Salient Pole Windings

Fig. 2.1 illustrates a synchronous machine with a salient pole rotor. To magnetize the machine, direct current is fed through brushes and slip rings to the windings located on the salient poles. The main flux created by the direct current flows from the pole shoe to the stator and back simultaneously penetrating the poly-phase slot winding of the stator. The dotted lines in the figure depict the paths of the main flux. Such a closed path of a flux forms the magnetic circuit of a machine.

One turn of a coil is a conductor that constitutes a single turn around the magnetic circuit. A coil is a part of winding that consists of adjacent series-connected turns between the two terminals of the coil. Figure 2.1a illustrates a synchronous machine with a pole with one coil per pole, whereas in Figure 2.1b, the locations of the direct (d) and quadrature (q) axes are shown.

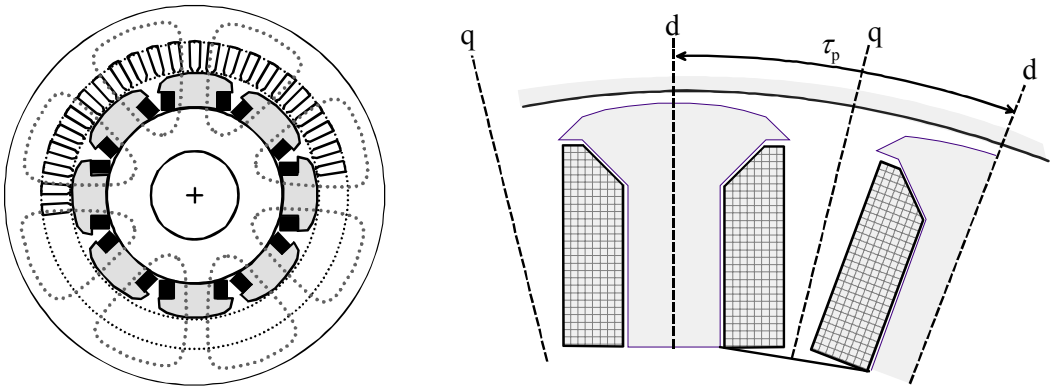

Figure 2.1. a) Salient pole synchronous machine (p = 4). The black areas around two pole bodies form a salient pole winding. b) Single poles with windings, d $\hat{=}$ direct axis, q $\hat{=}$ quadrature axis. In salient pole machines, these two magnetically different, rotor-geometry-defined axes have a remarkable effect on the machine behaviour; the issue will be discussed later.

A group of coils is a part of winding that magnetizes the same magnetic circuit. In Fig. 2.1a, the coils at the different magnetic poles (N and S alternating) form in pairs a group of coils. The number of field winding turns magnetizing one pole is N_f.

The salient pole windings located on the rotor or on the stator are mostly used for the DC magnetizing of a machine. The windings are then called magnetizing or sometimes excitation windings. With a direct current, they create a time-constant current linkage Θ. The part of this current linkage consumed in the air gap, that is, the magnetic potential difference of the air gap $U_{m,\delta}$, may be, for simplicity, regarded as constant between the quadrature axes, and it changes its sign at the quadrature axis q, Fig. 2.2.

A significant field of application for salient pole windings is doubly salient reluctance machines. In these machines, a solid salient pole is not utilizable, since the changes of flux are rapid when operating at high speeds. At simplest, DC pulses are fed to the pole windings with power switches. In the air gap, direct current creates a flux that tries to turn the rotor in a direction where the

magnetic circuit of the machine reaches its minimum reluctance. The torque of the machine tends to be pulsating, and to reach an even torque, the current of a salient pole winding should be controllable so that the rotor can rotate without jerking.

Salient pole windings are employed also in the magnetizing windings of the DC machines. All series, shunt, and compound windings are wound on salient poles. The commutating windings are also of the same type as salient pole windings.

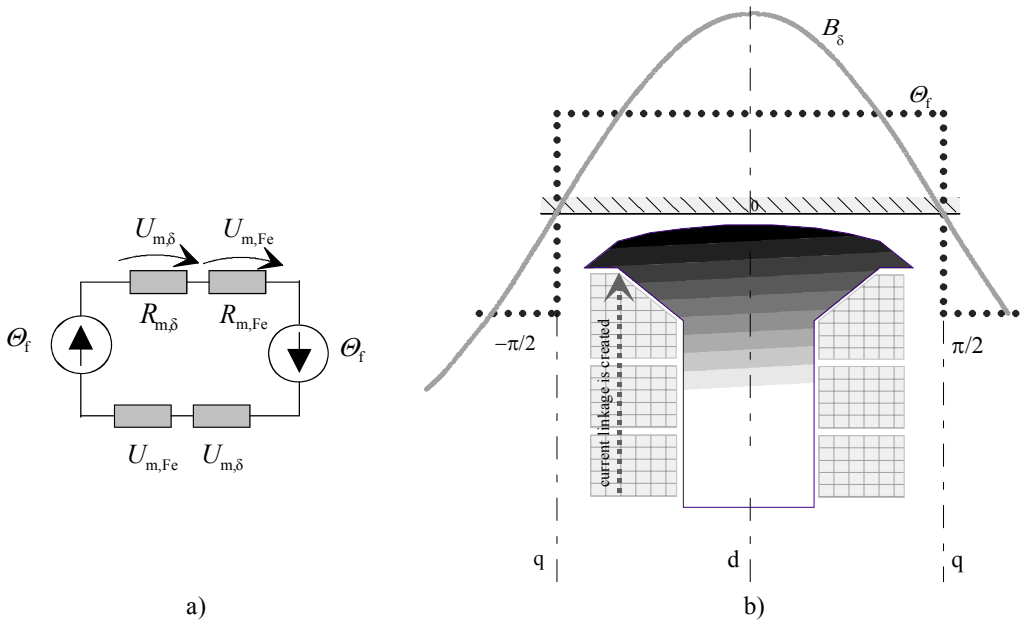

Figure 2.2. a) Equivalent magnetic circuit. The current linkages Θ_f created by two adjacent salient pole windings. Part $U_{m,\delta}$ is consumed in the air gap. b) The behaviour of the air gap flux density B_δ. Thanks to the appropriate design of the pole shoe, the air gap flux density varies cosinusoidally even though it is caused by the constant magnetic potential difference in the air gap $U_{m,\delta}$. The air gap magnetic flux density B_δ has its peak value on the d-axis and is zero on the q-axis. The current linkage created by the pole is accumulated by the ampere turns on the pole.

EXAMPLE 2.1: Calculate the field winding current that can ensure a maximum magnetic flux density of B_δ = 0.82 T in the air gap of a synchronous machine if there are 95 field winding turns per pole. It is assumed that the air gap magnetic flux density of the machine is sinusoidal along the pole shoes and the magnetic permeability of iron is infinite ($\mu_{Fe} = \infty$) in comparison with the permeability of air $\mu_0 = 4\pi \cdot 10^{-7}$ H/m. The minimum length of the air gap is 3.5 mm.

SOLUTION: If $\mu_{Fe} = \infty$, the magnetic reluctance of iron parts and the iron magnetic potential difference is zero. Now, the whole field current linkage $\Theta_f = N_f I_f$ is spent in the air gap to create the required magnetic flux density:

$$\Theta_f = N_f I_f = U_{m,\delta} = H_\delta \delta = \frac{B_\delta}{\mu_0}\delta = \frac{0.82}{4\pi \cdot 10^{-7}} 3.5 \cdot 10^3 \text{ A}$$

If the number of turns is N_f = 95, the field current is

$$I_f = \frac{\Theta_f}{N_f} = \frac{0.82}{4\pi \cdot 10^{-7}} 3.5 \cdot 10^{-3} \frac{1}{95} \text{A} = 24 \text{ A}$$

It should be noticed that calculation of this kind is appropriate for an approximate calculation of the current linkage needed. In fact, about 60–90 % of the magnetic potential difference in electrical

machines is spent in the air gap, and the rest in the iron parts. Therefore, in a detailed design of electrical machines, it is necessary to take into account all the iron parts with appropriate material properties. A similar calculation is valid for DC machines with the exception that in DC machines the air gap is usually constant under the poles.

2.1.2 Slot Windings

Here we concentrate on symmetrical, three-phase AC distributed slot windings, in other words, rotating-field windings. However, first, we discuss the magnetizing winding of a rotor of a non-salient pole synchronous machine, and finally turn to commutator windings, compensating windings, and damper windings. Because unlike in the salient pole machine, the length of the air gap is now constant, we may create a cosinusoidally distributed flux density in the air gap by producing a cosinusoidal distribution of current linkage with an AC magnetizing winding, Fig. 2.3. The cosinusoidal distribution, instead of sinusoidal, is used because we want the flux density to reach its maximum on the direct-axis, where $\alpha = 0$.

In the case of Fig. 2.3, the function of the magnetic flux density approximately follows the curve function of the current linkage distribution $\Theta(\alpha)$. In machine design, an equivalent air gap δ_e is applied, the target being to create a cosinusoidally alternating flux density into the air gap

$$B(\alpha) = \frac{\mu_0}{\delta_e}\Theta(\alpha) \tag{2.1}$$

The concept of equivalent air gap δ_e will be discussed later.

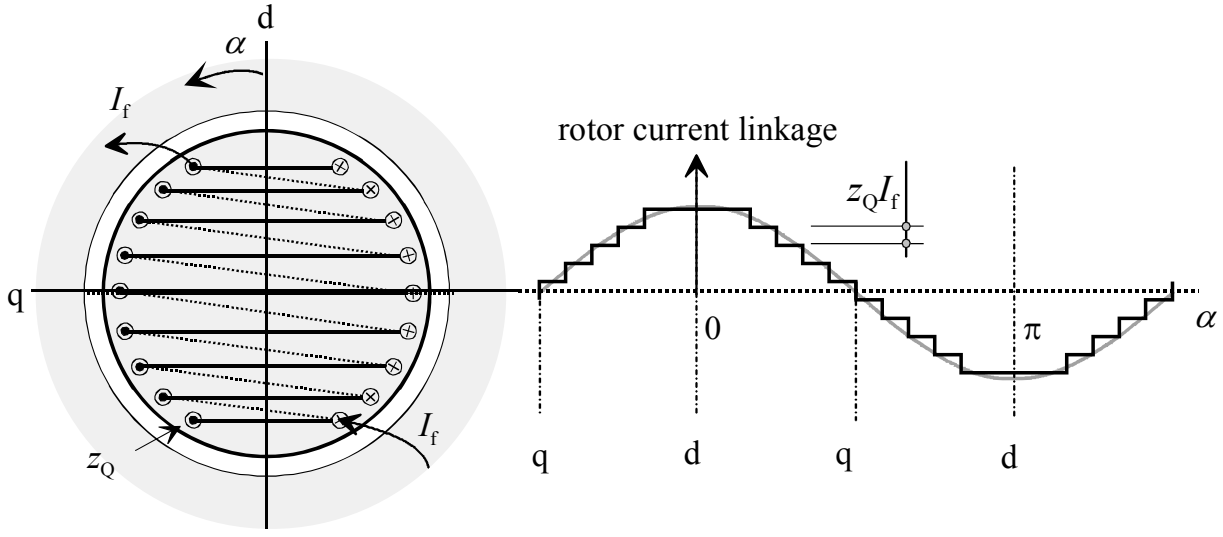

Figure 2.3. Current linkage distribution created by two-pole non-salient pole winding and the fundamental of the current linkage. There are z_Q conductors in each slot, and the excitation current in the winding is I_f. The height of a single step of the current linkage is $z_Q I_f$.

The slot pitch τ_u and the slot angle α_u are the core parameters of the slot winding. The slot pitch is measured in metres, whereas the slot angle is measured in electrical degrees. The number of slots being Q and the diameter of the air gap D, we may write

$$\tau_{\mathrm{u}} = \frac{\pi D}{Q}; \quad \alpha_{\mathrm{u}} = p\frac{2\pi}{Q}. \tag{2.2}$$

The slot pitch being usually constant in non-salient pole windings, the current sum ($z_{\mathrm{Q}}I_{\mathrm{f}}$) in a slot has to be of a different magnitude in different slots (in a sinusoidal or cosinusoidal manner to achieve a sinusoidal or cosinusoidal variation of current linkage along the surface of the air gap.). Usually, there is a current of equal magnitude flowing in all turns in the slot, and therefore, the number of conductors z_{Q} in the slots has to be varied. In the slots of the rotor in Fig. 2.3, the number of turns is equal in all slots, and a current of equal magnitude is flowing in the slots. We may see that by selecting z_{Q} slightly differently in different slots, we can improve the stepped waveform of the figure to better approach the cosinusoidal form. The need for this depends on the induced voltage harmonic content in the stator winding. The voltage may be of almost pure sinusoidal waveform despite the fact that the air gap flux density distribution should not be perfectly sinusoidal. This depends on the stator winding factors for different harmonics. In synchronous machines, the air gap is usually relatively large, and correspondingly, the flux density on the stator surface changes more smoothly (neglecting the influence of slots) than the stepped current linkage waveform of Fig. 2.3. Here, we apply the well-known finding that if 2/3 of the rotor surface are slotted and 1/3 is left slotless, not only the third harmonic component but any of its multiple harmonics called triplen harmonics are eliminated in the air gap magnetic flux density, and also the low-order odd harmonics (5^{th}, 7^{th}) are suppressed.

2.1.3 End Windings

Figure 2.4 illustrates how the arrangement of the coil end influences the physical appearance of the winding. The windings a and b in the figure are of equal value with respect to the main flux, but their leakage inductances diverge from each other because of the slightly different coil ends. When investigating the winding a of Fig. 2.4, we note that the coil ends form two separate planes at the endfaces of the machine. This kind of a winding is therefore called a two-plane winding. The coil ends of the type are depicted in Fig. 2.4e. In the winding of Fig. 2.4b, the coil ends are overlapping, and therefore, this kind of winding is called a diamond winding (lap winding). Figures 2.4c and d illustrate three-phase stator windings that are identical with respect to the main flux, but in Fig. 2.4c, the groups of coil are non-divided, and in Fig. 2.4d, the groups of coil are divided. In Fig. 2.4c, an arbitrary radius r is drawn across the coil end. It is shown that at any position, the radius intersects only coils of two phases, and the winding can thus be constructed as a two-plane winding. A corresponding winding constructed with distributed coils (Fig. 2.4d) has to be a three-plane arrangement, since now the radius r may intersect the coil ends of the windings of all the three phases.

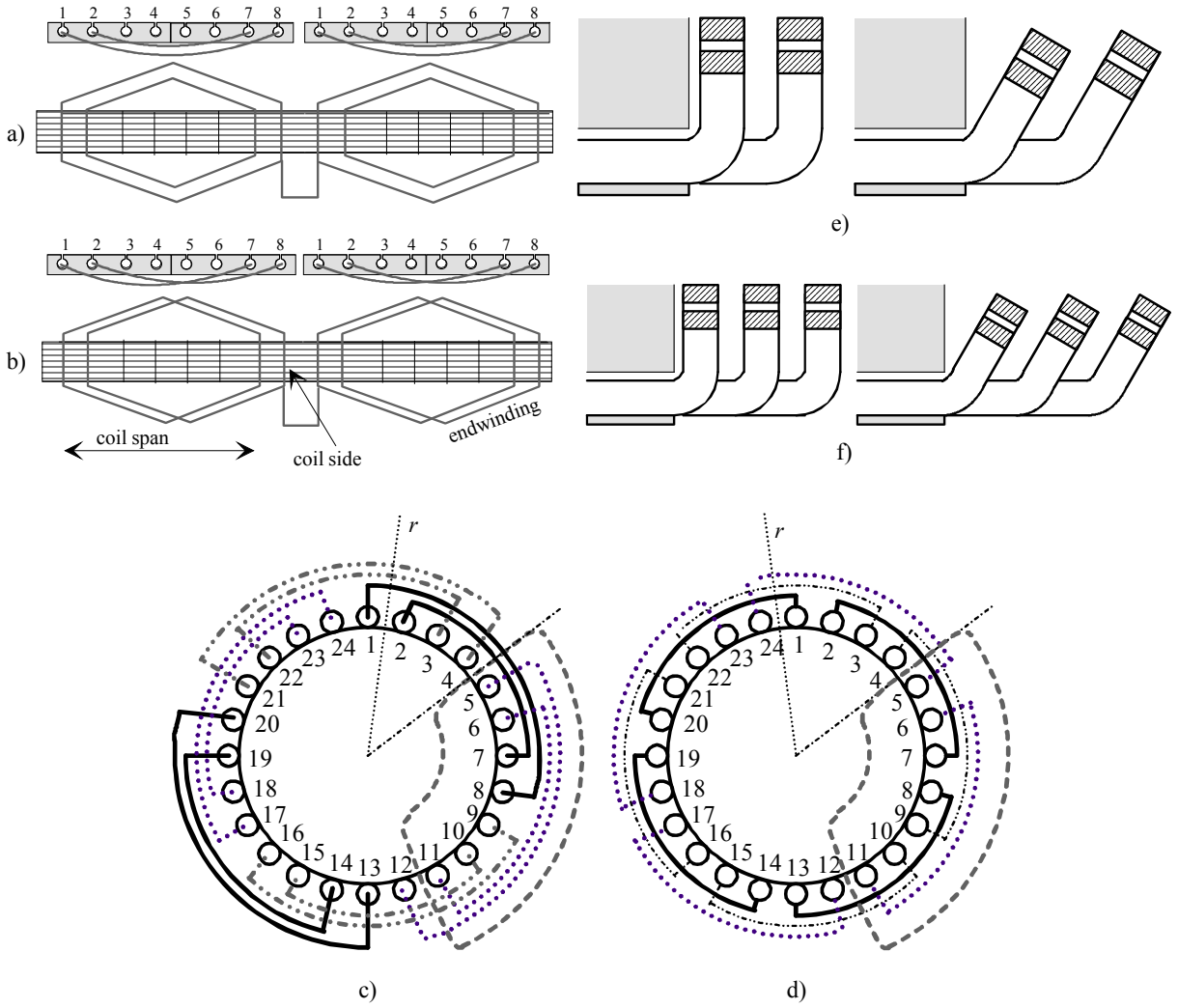

Figure 2.4. a) Concentric winding and b) a diamond winding. In a two-plane winding, the coil spans differ from each other. In the diamond winding, all the coils are of equal width. c) A two-plane three-phase four-pole winding with non-divided groups of coil. d) A three-plane three-phase four-pole winding with divided groups of coils. Figures c and d illustrate also a single main flux path. e) Profile of an end winding arrangement of a two-plane winding. f) Profile of an end winding of a three-plane winding. The radii *r* in the figures illustrate that in a winding with non-divided groups, an arbitrary radius may intersect only two phases, and in a winding with divided groups, the radius may intersect all the three phases. The two- or three-plane windings will result correspondingly.

The part of a coil located in a single slot is called a coil side, and the part of the coil outside the slot is termed a coil end. The coil ends together constitute the end windings of the winding.

2.2 Phase Windings

Next, poly-phase slot windings that produce the rotating field of poly-phase AC machines are investigated. In principle, the number of phases *m* can be selected freely, but the use of a three-phase supply network has led to a situation in which also most electrical machines are of the three-phase type. Another, extremely common type is two-phase electrical machines that are operated with a capacitor start and run motor in a single-phase network. A symmetrical two-phase winding is in principle the simplest AC winding that produces a rotating field.

A configuration of a symmetrical poly-phase winding can be considered as follows: the periphery of the air gap is evenly distributed over the poles so that we can determine a pole arc, which covers 180 electrical degrees and a corresponding pole pitch, τ_p, which is expressed in metres

$$\tau_p = \frac{\pi D}{2p}. \tag{2.3}$$

Figure 2.5 depicts the division of the periphery of the machine into phase zones of positive and negative values. In the figure, the number of pole pairs $p = 2$, and the number of phases $m = 3$.

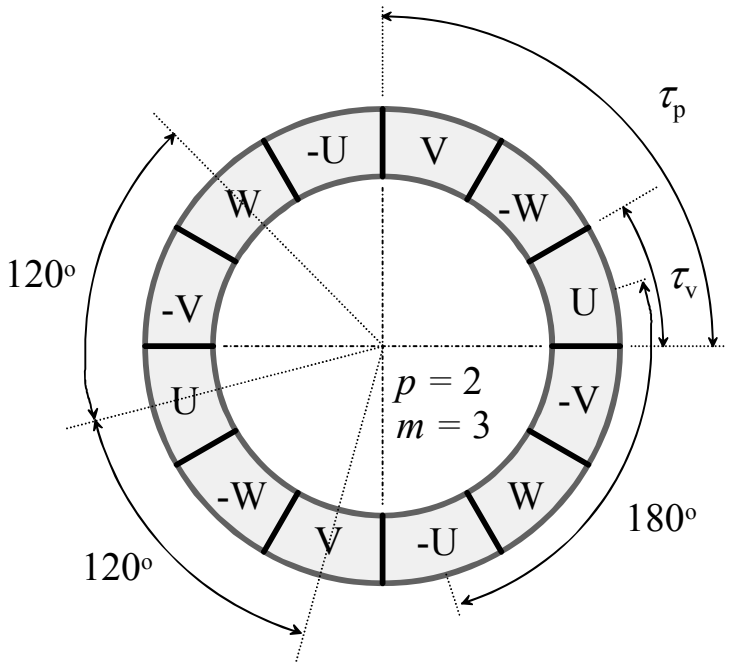

Figure 2.5. Division of the periphery of a three-phase four-pole machine into phase zones of positive and negative values. Pole pitch is τ_p and phase zone distribution τ_v. When the windings are located in the zones, the instantaneous currents in the positive and negative zones are flowing in opposite directions.

Phase zone distribution is written as

$$\tau_v = \frac{\tau_p}{m}. \tag{2.4}$$

The number of zones will thus be $2pm$. The number of slots per each such zone is expressed by the term q, as a number of slots per pole and phase

$$q = \frac{Q}{2pm}. \tag{2.5}$$

Here Q is the number of slots in the stator or in the rotor. In integral slot windings, q is an integer. However, q can also be a fraction. In that case, the winding is called a fractional slot winding.

The phase zones are distributed symmetrically to different phase windings so that the phase zones of the phases U, V, W, ... are positioned on the periphery of the machine at equal distances in electrical degrees. In a three-phase system, the angle between the phases is 120 electrical degrees. This is illustrated by the periphery of Fig. 2.5, where we have 2×360 electrical degrees because of four

poles. Now, it is possible to label every phase zone. We start for instance with the positive zone of the phase U. The first positive zone of the phase V shall be 120 electrical degrees from the first positive zone of the phase U. Correspondingly, the first positive zone of the phase W shall be 120 electrical degrees from the positive zone of the phase V etc. In Fig. 2.5, there are two pole pairs, and hence we need two positive zones for each phase U, V, and W. In the slots of each, now labelled phase zones, there are only the coil sides of the labelled phase coil, in all of which the current flows in the same direction. Now, if their direction of current is selected positive in the diagram, the unlabelled zones become negative. Negative zones are labelled by starting from the distance of a pole pitch from the position of the positive zones. Now U and –U, V and –V, W and –W are at the distance of 180 electrical degrees from each other.

2.3 Three-Phase Integral Slot Stator Winding

The armature winding of a three-phase electrical machine is usually constructed in the stator, and it is spatially distributed in the stator slots so that the current linkage created by the stator currents is distributed as sinusoidally as possible. The simplest stator winding that produces a noticeable rotating field comprises three coils, the sides of which are divided into six slots, because if $m = 3$, $p = 1$, $q = 1$, then $Q = 2pmq = 6$; see Figs. 2.6 and 2.7.

EXAMPLE 2.2: Create a three-phase, two-pole stator winding with $q = 1$. Distribute the phases in the slots and illustrate the current linkage created based on the instant values of phase sinusoidal currents. Draw a phasor diagram of the slot voltage and sum the voltages of the individual phases. Create a current linkage waveform in the air gap for the time instant t_1 when the phase U voltage is in its positive maximum and for t_2, which is 30° shifted.

SOLUTION: If $m = 3$, $p = 1$, $q = 1$, then $Q = 2pmq = 6$, which is the simplest case of three-phase windings. The distribution of the phases in the slots will be explained based on Fig. 2.6. Starting from the slot 1, we insert there the positive conductors of the phase U forming the zone U1. The pole pitch expressed in the number of slots per pole, or in other words, 'the coil span expressed in the number of slot pitches y_Q' is

$$y_Q = \frac{Q}{2p} = \frac{6}{2} = 3 .$$

Then, the zone U2 will be one pole pitch shifted from U1 and will be located in the slot 4, because $1 + y_Q = 1 + 3 = 4$. The beginning of the phase V1 is 120°shifted from U1, which means the slot 3, and its end V2 is in the slot 6 (3 + 3 = 6). The phase W1 is again shifted form V1 by 120°, which means the slot 5, and its end is in the slot 2; see Fig. 2.6a. The polarity of instantaneous currents is shown at the instant, when the current of the phase U is in its positive maximum value flowing in the slot 1, depicted as a cross (tail of arrow) in U1 (current flowing away from the observer). Then, U2 is depicted by a dot (a point of arrow) in the slot 4 (current flowing towards the observer). At the same instant in V1 and W1, there are also dots, because the phases V and W are carrying negative current values (see 2.6d), and therefore V2 and W2 are positive, indicated by crosses. In this way, a sequence of slots with inserted phases is as follows: U1, W2, V1, U2, W1, V2, if $q = 1$.

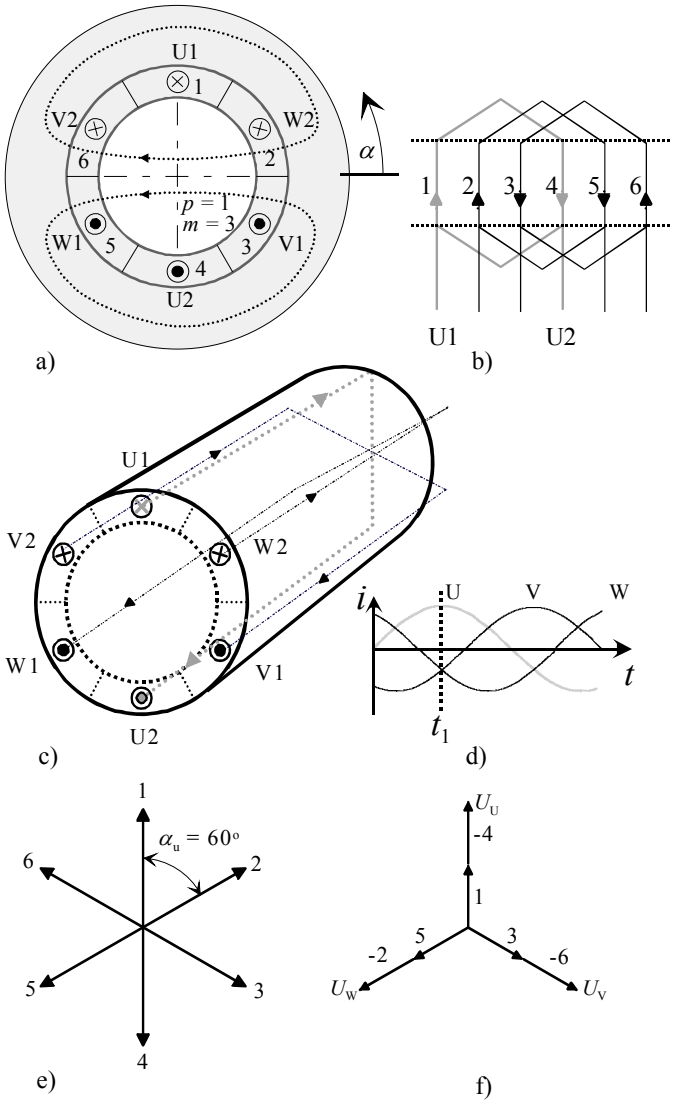

Figure 2.6. The simplest three-phase winding that produces a rotating field. a) A cross-sectional surface of the machine and a schematic view of the main flux route at the observation instant t_1, b) a developed view of the winding in a plane, and c) a three-dimensional view of the winding. The figure illustrates how the winding penetrates the machine. The coil end at the rear end of the machine is not illustrated as in reality, but the coil comes directly from a slot to another without travelling along the rear endface of the stator. The ends of the phases U, V, and W at the terminals are denoted U1-U2, V1-V2, and W1-W2. d) The three-phase currents at the observed time instant t_1 when $i_W = i_V = -1/2\ i_U$. ($i_U+i_V+i_W = 0$), e) a voltage phasor diagram for the given three-phase system, f) the total phase voltage for individual phases. The voltage of the phase U is created by summing the voltage of the slot 1 and the negative voltage of slot 4, and therefore the direction of the voltage phasor in the slot 4 is taken opposite with the denotation −4. We can see the sum of voltages in both slots and the phase shift by 120° of the V and W phase voltages.

The cross-section of the stator winding in Fig. 2.6a shows fictitious coils with current directions resulting in the magnetic field represented by the force lines and arrows.

The phasor diagram in Fig. 2.6e includes six phasors. To determine their number, the largest common divider of Q and p denoted t has to be found. In this case, for $Q = 6$ and $p = 1$, $t = 1$, and therefore, the number of phasors is $Q/t = 6$. The angle between the voltage phasors in the adjacent slots is given by expression

$$\alpha_u = \frac{360° p}{Q} = \frac{360° \cdot 1}{6} = 60° ,$$

which results in the numbering of the voltage phasors in slots as shown in Fig. 2.6e. Now, the total phase voltage for individual phases has to be summed. The voltage of the phase U is created by the positive voltage in the slot 1, and the negative voltage in the slot 4. The direction of the voltage phasor in the slot 4 is taken opposite with the denotation –4. We can see the sum of voltages in both slots of the phase U, and the phase shift of 120° of the V and W phase voltages in Fig. 2.6f.

The current linkage waveforms for this winding are illustrated in Fig. 2.7b and c for the time instants t_1 and t_2, between which the waveforms proceed by 30°. The procedure of drawing the figure can be described as follows: We start observation at $\alpha = 0$. We assume the same constant number of conductors z_Q in all slots.

The current linkage value on the left in Fig. 2.7b is changed stepwise at the slot 2, where the phase W is located and is carrying a current with a cross sign. This can be drawn as a positive step of Θ with a certain value ($\Theta(t_1) = i_{uW}(t_1)z_Q$). Now, the current linkage curve remains constant until we reach the slot 1, where the positive currents of the phase U are located. The instantaneous current in the slot 1 is the phase U peak current. The current sum is indicated again with a cross sign. The step height is now twice the height in the slot 2, because the peak current is twice the current flowing in the slot 2. Then, in the slot 6, there is again a positive half step caused by the phase V. In the slot 5, there is a current sum indicated by a dot, which means a negative Θ step. The same is repeated with all slots, and when the whole circle has been closed, Fig. 2.7b. When this procedure is repeated for one period of the current, we obtain a travelling wave for the current linkage waveform. Fig. 2.7c shows the current linkage waveform after 30 degrees. Here we can see that if the instantaneous value of a slot current is zero, the current linkage does not change, and the current linkage remains constant; see the slots 2 and 5. We can also see that the Θ profiles in b and c are not similar, but the form is changed depending on the time instant at which it is investigated.

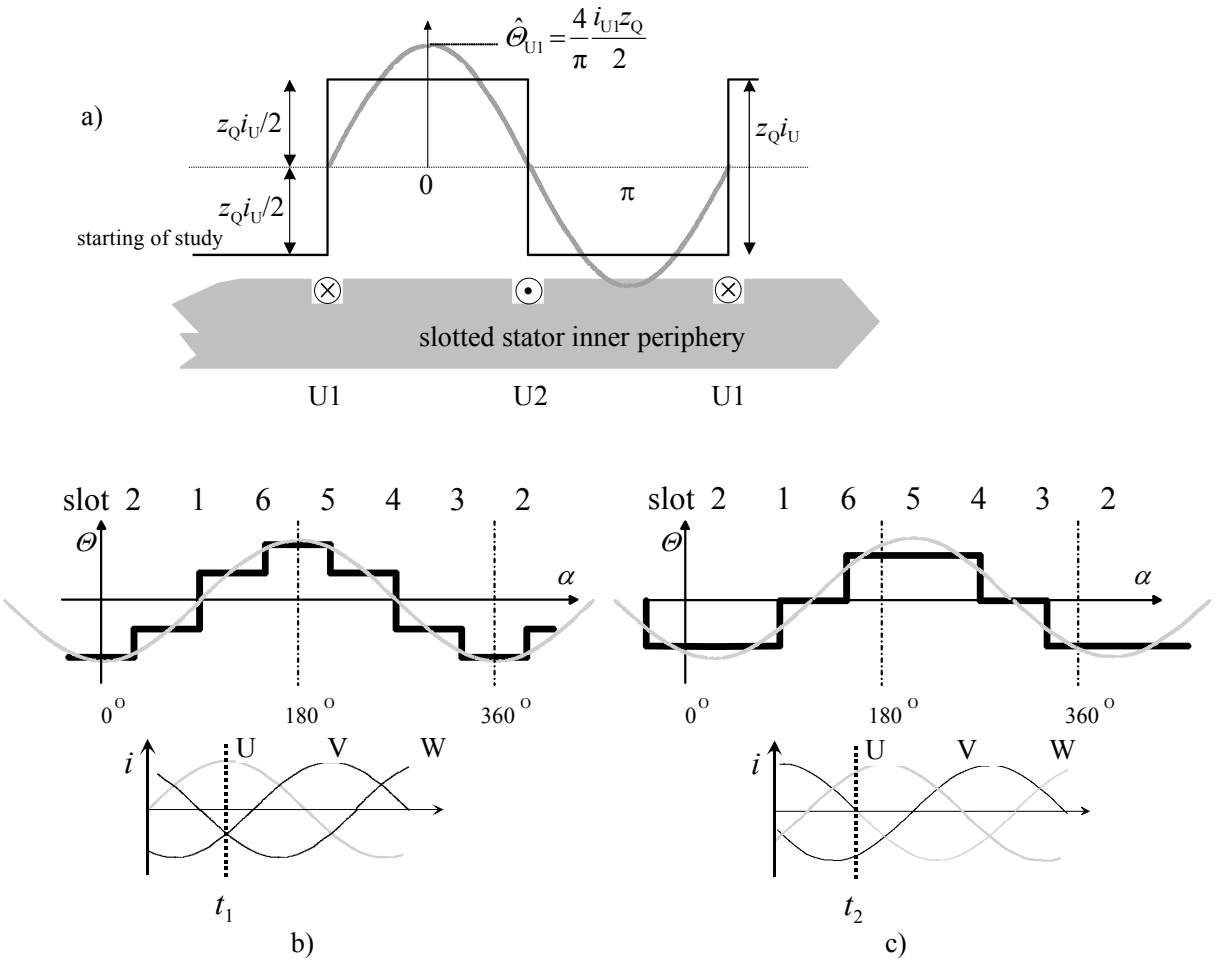

Figure 2.7. Current linkages Θ created by a simple three-phase q = 1 winding, a) only the phase U is fed by current and observed. A rectangular waveform of current linkage with its fundamental component is shown to explicate the staircase profile of the current linkages below. If all three phases are fed and observed in two different current situations ($i_U+i_V+i_W = 0$) at two time instants t_1 and t_2, see b) and c) respectively. The figure illustrates also the fundamental of the staircase current linkage curves. The stepped curves are obtained by applying Ampère's law in the current-carrying teeth zone of the electrical machine. Note that as time elapses from t_1 to t_2, the three phase currents change and also the position of the fundamental component changes. This indicates clearly the rotating-field nature of the winding. The angle α and the numbers of slots refer to the previous figure, in which we see that the maximum flux density in the air gap lies between the slots 6 and 5. This coincides with the maximum current linkage shown in this figure. This is valid if no rotor currents are present.

Figure 2.7 shows that the current linkage produced with such a simple winding deviates considerably from sinusoidal waveform. Therefore, in electrical machines, more coil sides are usually employed per pole and phase.

EXAMPLE 2.3: Consider an integral slot winding, where p = 1 and q = 2, m = 3. Distribute the phase winding into the slots, make an illustration of the windings in the slots, draw a phasor diagram and show the phase voltages of the individual phases. Create a waveform of the current linkage for this winding and compare it with that in Fig. 2.7.

SOLUTION: The number of the slots needed for this winding is $Q = 2pmq = 2 \cdot 3 \cdot 2 = 12$. The cross-sectional area of such a stator with 12 slots and embedded conductors of individual phases is illustrated in Fig. 2.8a. The distribution of the slots into the phases is made in the same order as in Example 2.2, but now q = 2 slots per pole and phase. Therefore, the sequence of the slots for the

phases is as follows: U1, U1, W2, W2, V1, V1, U2, U2, W1, W1, V2, V2. The direction of the current in the slots will be determined in the same way as above in Example 2.2. The coils wound in individual phases are shown in Fig. 2.8b. The pole pitch expressed in number of slot pitches is

$$y_{\mathrm{Q}} = \frac{Q}{2p} = \frac{12}{2} = 6$$

Figure 2.8c shows how the phase U is wound to keep the full pitch equal to 6 slots. In Fig. 2.8d, the average pitch is also 6, but the individual steps are $y_{\mathrm{Q}} = 5$ and 7, which gives the same average result for the value of induced voltage.

The phasor diagram has 12 phasors, because $t = 1$ again. The angle between two phasors of adjacent slots is

$$\alpha_{\mathrm{u}} = \frac{360° p}{Q} = \frac{360° \cdot 1}{12} = 30°$$

The phasors are numbered gradually around the circle. Based on this diagram, the phase voltage of all phases can be found. Figures 2.8f and g show that the voltages are the same independent of the way how separate coil sides are connected in series. In comparison with the previous example, the geometrical sum is now less than the algebraic sum. The phase shifting between coil side voltages is caused by the distribution of the winding in more than one slots, here in two slots per each pole. This reduction of the phase voltage is expressed by means of a distribution winding factor; this will be derived later.

The waveform of the current linkage for this winding is given in Fig. 2.9. We can see that it is much closer to a sinusoidal waveform than in the previous example with $q = 1$.

In undamped permanent magnet synchronous motors, also such windings can be employed, the number of slots per pole and phase of which is clearly less than one, for instance $q = 0.4$. In that case, a well-designed machine looks like a rotating-field machine when observed at its terminals, but the current linkage produced by the stator winding deviates so much from the fundamental that, because of excessive harmonic losses in the rotor, no other rotor type comes into question.

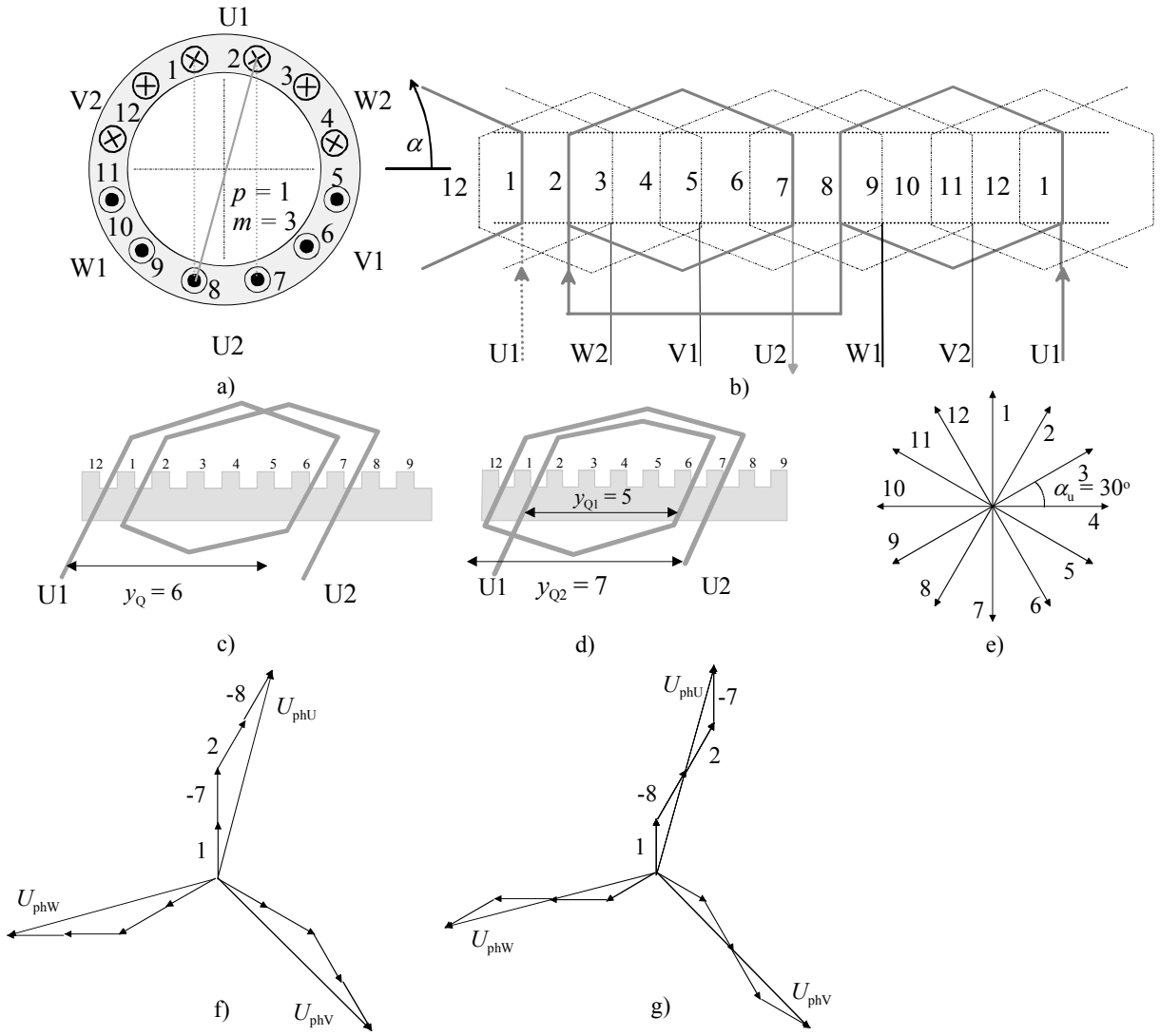

Figure 2.8. Three-phase two-pole winding with two slots per pole and phase, a) a stator with 12 slots, the number of slots per pole and phase $q = 2$. b) Divided coil groups, c) full-pitch coils of the phase U, d) average full-pitch coils of phase U, e) a phasor diagram with 12 phasors, one for each slot, f) sum phase voltage of individual phases corresponding to Fig. c, g) a sum phase voltage of individual phases corresponding to Fig. d.

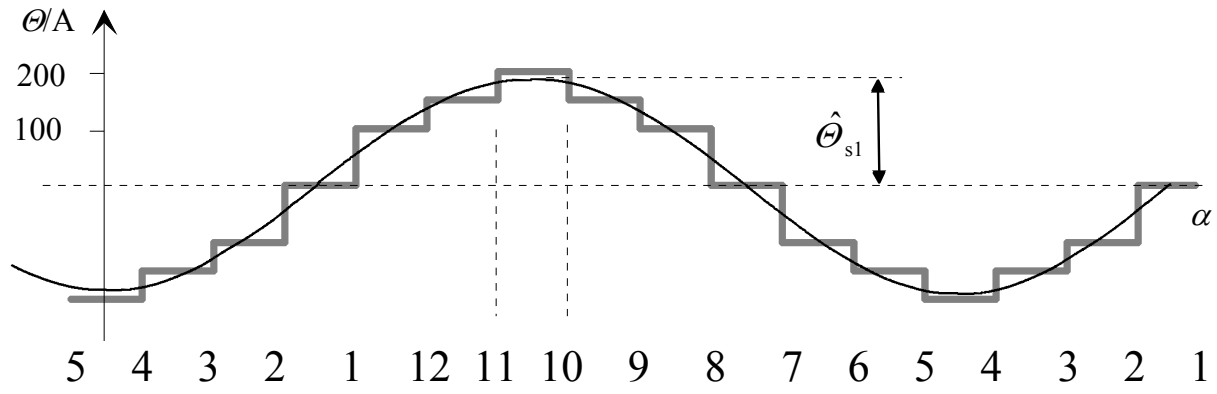

Figure 2.9. Current linkage $\Theta_s = f(\alpha)$ created by the winding on the surface of the stator bore of Fig. 2.8 at a time $i_W = i_V = -1/2\ i_U$. The fundamental Θ_{s1} of Θ_s is given as a sinusoidal curve. The numbering of the slots is also given.

When comparing Fig. 2.9 (q = 2) with Fig. 2.7 (q = 1), it is obvious that the higher the term q (slots per pole and phase) is, the more sinusoidal the current linkage of the stator winding is.

As we can see in Fig. 2.7a, the current linkage amplitude of the fundamental component for one full-pitch coil is

$$\hat{\Theta}_{1U} = \frac{4}{\pi}\frac{z_Q \hat{i}_U}{2}. \tag{2.6}$$

If the coil winding is distributed into more slots, and $q > 1$ and $N = pqz_Q$, the winding factor must be taken into account:

$$\hat{\Theta}_{1U} = \frac{4}{\pi}\frac{Nk_{w1}\hat{i}_U}{2}. \tag{2.7}$$

In a $2p$-pole machine ($2p$>2), the current linkage for one pole is:

$$\hat{\Theta}_{1U} = \frac{4}{\pi}\frac{Nk_{w1}\hat{i}_U}{2p}. \tag{2.8}$$

This expression can be rearranged with the number of conductors in a slot. In one phase, there are $2N$ conductors, and they are embedded in the slots belonging to one phase Q/m. Therefore, the number of conductors in one slot will be:

$$z_Q = \frac{2N}{Q/m} = \frac{2mN}{2pqm} = \frac{N}{pq} \tag{2.9}$$

and

$$\frac{N}{p} = qz_Q \tag{2.10}$$

Then N/p presented in Eq. (2.8) and in the following can be introduced by qz_Q.:

$$\hat{\Theta}_{1U} = \frac{4}{\pi}\frac{Nk_{w1}\hat{i}_U}{2p} = \frac{4}{\pi}qz_Q\frac{k_{w1}\hat{i}_U}{2}. \tag{2.11}$$

It can be also expressed with the effective value of sinusoidal phase current if there is a symmetrical system of phase currents:

$$\hat{\Theta}_{1U} = \frac{4}{\pi}\frac{Nk_{w1}}{2p}\sqrt{2}I. \tag{2.12}$$

For an m-phase rotating-field stator or rotor winding, the amplitude of current linkage is $m/2$ times higher:

$$\hat{\Theta}_1 = \frac{m}{2}\frac{4}{\pi}\frac{Nk_{w1}}{2p}\sqrt{2}I \tag{2.13}$$

and for three-phase stator or rotor winding, the current linkage amplitude of the fundamental component for one pole is:

$$\hat{\Theta}_1 = \frac{3}{2}\frac{4}{\pi}\frac{Nk_{w1}}{2p}\sqrt{2}I = \frac{3}{\pi}\frac{Nk_{w1}}{p}\sqrt{2}I \tag{2.14}$$

For a stator current linkage amplitude $\hat{\Theta}_{s\nu}$ of the harmonic ν of the current linkage of a poly-phase ($m > 1$) rotating-field stator winding (or rotor winding), when the effective value of the stator current is I_s, we may write

$$\hat{\Theta}_{s\nu} = \frac{m}{2}\frac{4}{\pi}\frac{k_{w\nu}N_s}{p\nu}\frac{1}{2}\sqrt{2}I_s = \frac{mk_{w\nu}N_s}{\pi p\nu}\hat{i}_s . \tag{2.15}$$

EXAMPLE 2.4: Calculate the amplitude of the fundamental component of stator current linkage, if N_s= 200, k_{w1} = 0.96, m = 3, p = 1 and $i_{sU}(t) = \hat{i} = 1\,\text{A}$, the effective value for a sinusoidal current being $I_s = \left(1/\sqrt{2}\right)$ A = 0.707 A.

SOLUTION: For the fundamental, we obtain $\hat{\Theta}_{s1}$ = 183.3 A, because:

$$\hat{\Theta}_1 = \frac{3}{2}\frac{4}{\pi}\frac{Nk_{w1}}{2p}\sqrt{2}I_s = \frac{3}{\pi}\frac{Nk_{w1}}{p}\sqrt{2}I_s = \frac{3}{\pi}\cdot\frac{200\cdot 0.96}{1}\sqrt{2}\cdot 0.707\text{A} = 183.3\ \text{A}.$$

2.4 Voltage Phasor Diagram and Winding Factor

Since the winding is spatially distributed in the slots on the stator surface, the flux (which is proportional to the current linkage Θ) penetrating the winding does not intersect all windings simultaneously, but with a certain phase shift. Therefore, the electromotive force (emf) of the winding is not calculated directly with the number of turns N_s, but the winding factors $k_{w\nu}$ corresponding to the harmonics are required. The emf of the fundamental induced in the turn is calculated with the flux linkage Ψ by applying Faraday's induction law $e = -Nk_{w1}\mathrm{d}\Phi/\mathrm{d}t = -\mathrm{d}\Psi/\mathrm{d}t$ (see Eqs. 1.3, 1.7 and 1.8) We can see that the winding factor correspondingly indicates the characteristics of the winding to produce harmonics, and it has thus to be taken into account when calculating the current linkage of the winding (Eq. 2.15). The common distribution of all the current linkages created by all the windings together produces a flux density distribution in the air gap of the machine, which, when moving with respect to the winding, induces voltages to the conductors of the winding. The phase shift of the induced electromotive force in different coil sides is investigated with a voltage phasor diagram. The voltage phasor diagram is presented in electrical degrees. If the machine is for instance a four-pole one, p = 2, the voltage vectors have to be distributed along two full circles in the stator bore. Figure 2.10 a) illustrates the voltage phasor diagram of a two-pole winding of Fig. 2.8.

In Fig. 2.10a, the phasors 1 and 2 are positive and 7 and 8 are negative for the phase under consideration. Hence, the phasors 7 and 8 are turned by 180 degrees to form a bunch of phasors. For harmonic ν (excluding slot harmonics that have the same winding factor as the fundamental) the directions of the phasors of the coil sides vary more than in the figure, because the slot angles $\alpha_{\underline{u}}$ are replaced with the angles $\nu\alpha_{\underline{u}}$.

According to Fig. 2.10b, when calculating the geometric sum of the voltage phasors for a phase winding, the symmetry line for the bunch of phasors, where the negative phasors have been turned opposite, must be found. The angles α_ρ of the phasors with respect to this symmetry line may be used in the calculation of the geometric sum. Each phasor contributes to the sum with a component proportional to $\cos\alpha_\rho$.

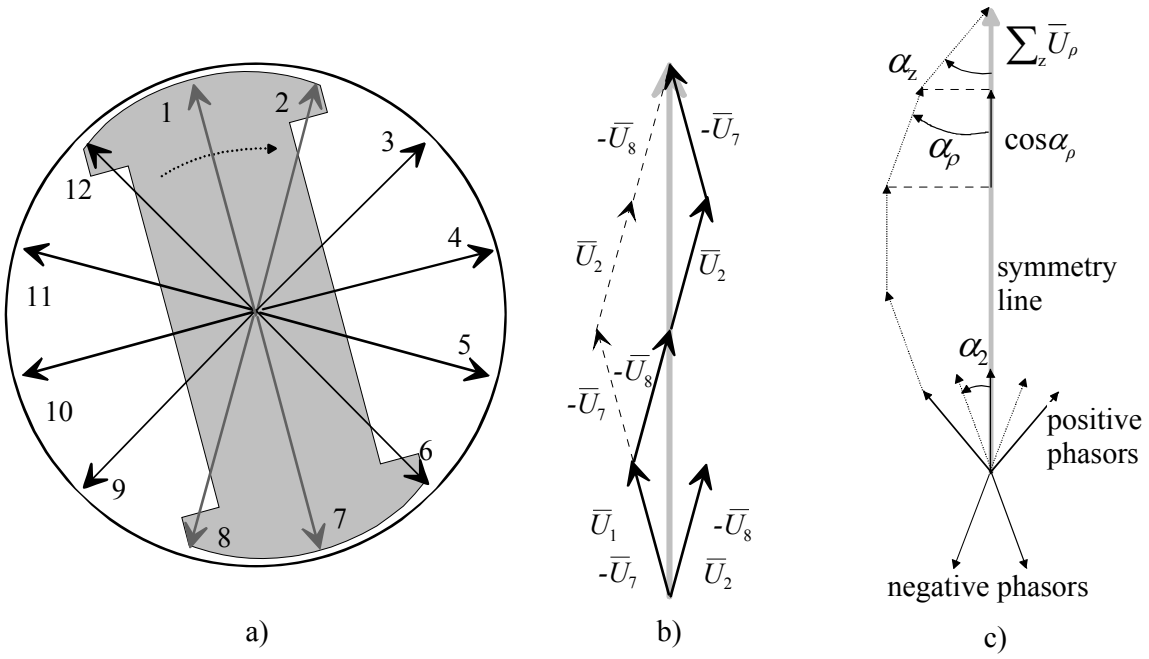

Figure 2.10. a) and b) Fundamental voltage phasor diagram for the winding of Fig. 2.8 Q_s = 12, p = 1, q_s = 2. A maximum voltage is induced in the bars in the slots 1 and 7 at the moment depicted in the figure, when the rotor is rotating clockwise. The figure illustrates also the calculation of the voltage in a single coil with the radii of the voltage phasor diagram. c) General application of the voltage phasor diagram in the determination of the winding factor (fractional slot winding since the number of phasors is uneven). The phasors of negative coil sides are turned 180°, and then the summing of the resulting bunch of phasors is calculated according to Eq. (2.16). A symmetry line is drawn in the middle of the bunch, and each phasor forms an angle α_ρ with the symmetry line. The geometric sum of all the phasors lies on the symmetry line.

We can now write a general presentation for the winding factor k_{wv} of a harmonic ν, by employing the voltage phasor diagram

$$k_{wv} = \frac{\sin\frac{\nu\pi}{2}}{Z}\sum_{\rho=1}^{Z}\cos\alpha_\rho \,. \qquad (2.16)$$

Here Z is the total number of positive and negative phasors of the phase in question, ρ is the ordinal number of a single phasor, and ν is the ordinal number of the harmonic under observation. The coefficient $\sin\frac{\nu\pi}{2}$ in the equation only influences the sign (of the factor). The angle of a single phasor α_ρ can be found from the voltage phasor diagram drawn for the specific harmonic, and it is the angle between an individual phasor and the symmetry line drawn for a specific harmonic (c.f. Fig. 2.10b). This voltage vector diagram solution is universal and may be used in all cases, but the numerical values of Eq. (2.16) do not always have to be calculated directly from this equation, or with the voltage phasor diagram at all. In simple cases, we may apply equations introduced later. However, the voltage phasor diagram forms the basis for the calculations, and therefore its utilization is discussed further when analyzing different types of windings.

If we are in Fig. 2.10a considering a currentless stator of a synchronous machine, a maximum voltage can be induced to the coil sides 1 and 7 at the middle of the pole shoe, when the rotor is rotating at no load inside the stator bore (which corresponds to the peak value of the flux density, but the zero value of the flux penetrating the coil), where the derivative of the flux penetrating the coil reaches its peak value, the voltage induction being at its highest at that moment. If the rotor

rotates clockwise, a maximum voltage is induced in the coil sides 2 and 8 in a short while, and so on. The voltage phasor diagram then describes the amplitudes of voltages induced in different slots and their temporal phase shift.

The series-connected coils of the phase U travel e.g. from the slot 1 to the slot 8 (coil 1) and from the slot 2 to the slot 7 (coil 2). Thus a voltage, which is the difference of the phasors $\underline{U}_1$ and $\underline{U}_8$, is induced in the coil 1. The total voltage of the phase is thus

$$\underline{U}_\mathrm{U} = \underline{U}_1 - \underline{U}_8 + \underline{U}_2 - \underline{U}_7 . \tag{2.17}$$

The figure also indicates the possibility of connecting the coils in the order 1–7 and 2–8, which gives the same voltage but a different end winding. The winding factor $k_{\mathrm{w}1}$ based on the distribution of the winding for the fundamental is calculated here as a ratio of the geometric sum and the sum of absolute values as follows:

$$k_{\mathrm{w}1} = \frac{\textit{geometric sum}}{\textit{sum of absolute values}} = \frac{\underline{U}_1 - \underline{U}_8 + \underline{U}_2 - \underline{U}_7}{|\underline{U}_1| + |\underline{U}_8| + |\underline{U}_2| + |\underline{U}_7|} = 0.966 \le 1 . \tag{2.18}$$

EXAMPLE 2.5: Equation (2.16) indicates that the winding factor for the harmonics may also be calculated using the voltage phasor diagram. Derive the winding factor for the seventh harmonic of the winding in Fig 2.8.

SOLUTION: We now draw a new voltage phasor diagram based on Fig. 2.10 for the seventh harmonic, Fig. 2.11.

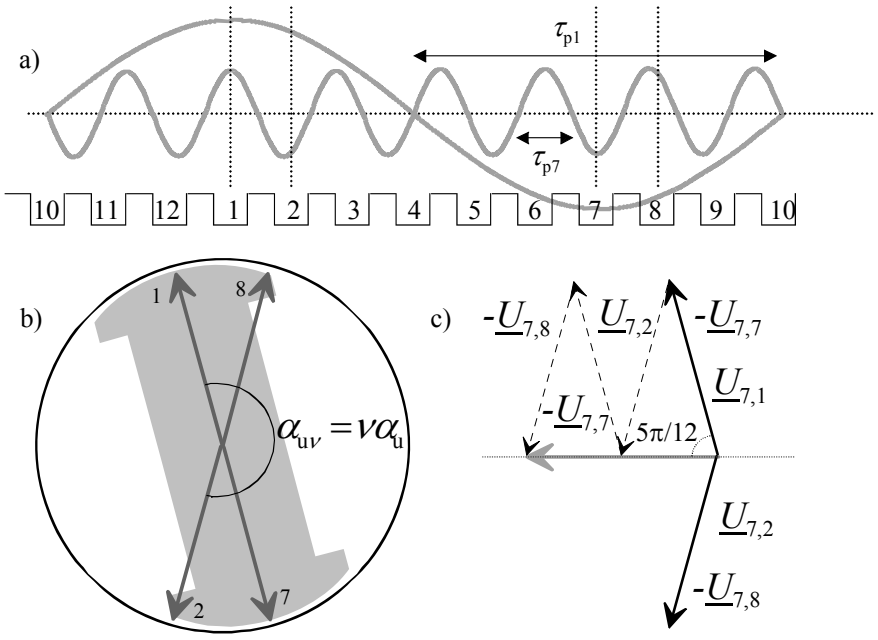

Fig. 2.11. Deriving the harmonic winding factor, a) the fundamental and the seventh harmonic field in the air gap over the slots, b) voltage phasors for the seventh harmonic of a full pitch q = 2 winding (slot angle $\alpha_{\mathrm{u}7}$ = 210°), and c) the symmetry line and the sum of the voltage phasors. The phasor angles α_ρ with respect to the symmetry line are α_ρ = 5π/12 or –5 π /12.

The slots 1 and 2 belong to the positive zone of the phase U and the slots 7 and 8 to the negative zone measured by the fundamental. In Fig. 2.11, we see that the pole pitch of the seventh harmonic

is one seventh of the fundamental pole pitch. Deriving the phasor sum for the seventh harmonic is started for instance with the voltage phasor of the slot 1. This phasor remains in its original position. The slot 2 is physically and by fundamental located 30° clockwise from the slot 1, but as we are now studying the seventh harmonic, the slot angle measured in degrees for it is 7×30°=210°, which can also be seen in the figure. The phasor for the slot 2 is, hence, located 210° from the phasor 1 clockwise. The slot 7 is located at 7×180°=1260° from the slot 1. Since 1260° = 3×360° + 180° the phasor 7 remains opposite to the phasor 1. The phasor 8 is located 210° clockwise from the phasor 7 and will find its place 30° clockwise from the phasor 1. By turning the negative zone phasors by π and applying Eq. (2.17) we obtain

$$k_{\mathrm{w7}} = \frac{\sin\frac{7\pi}{2}}{4}\sum_{\rho=1}^{4}\cos\alpha_{\rho} = \frac{\sin\frac{7\pi}{2}}{4}\left(\cos\frac{-5\pi}{12}+\cos\frac{+5\pi}{12}+\cos\frac{-5\pi}{12}+\cos\frac{+5\pi}{12}\right) = -0.2588.$$

It is not necessary to apply the voltage phasor diagram, but also simple equations may be derived to directly calculate the winding factor. In principle, we have three winding factors: a distribution factor, a pitch factor, and a skewing factor. The latter may also be taken into account by a leakage inductance. The winding factor derived based on the shifted voltage phasors in the case of distributed winding is called the distribution factor with the subscript ‘d’. This factor is always $k_{\mathrm{d1}} \leq 1$. The value $k_{\mathrm{d1}} = 1$ can be reached when $q = 1$, in which case the geometric sum equals the sum of absolute values, see Fig. 2.6f. If $q \neq 1$, then $k_{\mathrm{d1}} < 1$. In fact, it means that the total phase voltage is reduced by this factor (see Example 2.6).

If each coil is wound as a full-pitch winding, the coil pitch is in principle the same as the pole pitch. However, the voltage of the phase with full-pitch coils is reduced because of the winding distribution with the factor k_{d}. If the coil pitch is shorter than the pole pitch and the winding is not a full-pitch winding, the winding is called a short-pitch winding, or a chorded winding (see Fig. 2.15). Note that the winding in Fig. 2.8 is not a short-pitch winding, even though the coil may be realized from the slot 1 to the slot 8 (shorter than pole pitch) and not from the slot 1 to the slot 7 (equivalent to pole pitch). This is because the full-pitch coils together produce the same current linkage as the shorter coils together. A real short-pitching is obviously employed in the two-layer windings. Short-pitching is another reason why the voltage of the phase winding may be reduced. The factor of such reduction is called the pitch factor k_{p}. The total winding factor is given as:

$$k_{\mathrm{w}} = k_{\mathrm{d}} \cdot k_{\mathrm{p}} . \tag{2.19}$$

Equations to calculate the distribution factor k_{d} will be derived now; see Fig. 2.12. The equations are based on the geometric sum of the voltage phasors in a similar way as in Figs. 2.10 and 2.11.

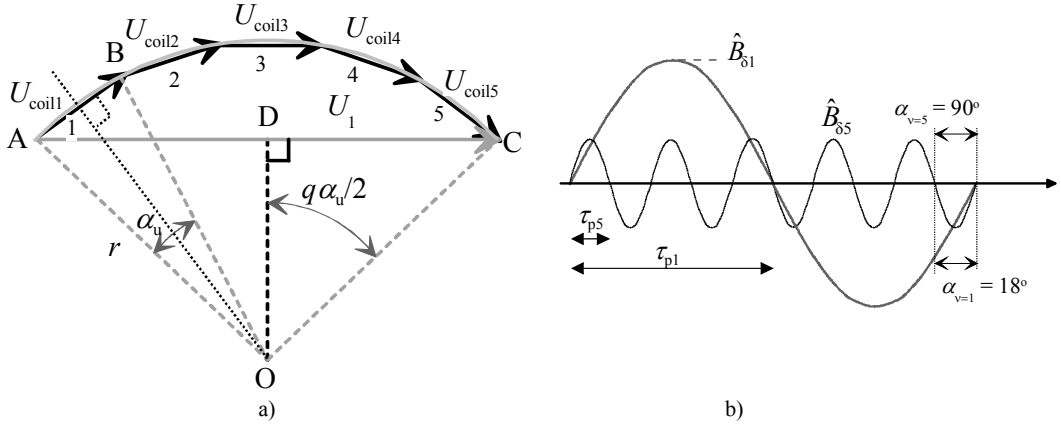

Figure 2.12. a) Determination of the distribution factor with a polygon with q = 5, b) the pole pitch for the fundamental and the fifth harmonic. The same physical angles for the fifth and the fundamental are shown as an example.

The distribution factor for the fundamental component is given as

$$k_{d1} = \frac{geometric\ sum}{sum\ of\ absolute\ values} = \frac{U_1}{qU_{coil1}}. \tag{2.20}$$

According to Fig. 2.12, we may write for the triangle ODC

$$\sin\frac{q\alpha_u}{2} = \frac{\frac{U_1}{2}}{r} \Rightarrow U_1 = 2r\sin\frac{q\alpha_u}{2}, \tag{2.21}$$

and for the triangle OAB

$$\sin\frac{\alpha_u}{2} = \frac{\frac{U_{v1}}{2}}{r} \Rightarrow U_{v1} = 2r\sin\frac{\alpha_u}{2}. \tag{2.22}$$

We may now write for the distribution factor

$$k_{d1} = \frac{U_1}{qU_{v1}} = \frac{2r\sin\frac{q\alpha_u}{2}}{q2r\sin\frac{\alpha_u}{2}} = \frac{\sin\frac{q\alpha_u}{2}}{q\sin\frac{\alpha_u}{2}}. \tag{2.23}$$

This is the basic expression for the distribution factor for the calculation of the fundamental in a closed form. Since the harmonic components of the air gap magnetic flux density are present, the calculation of the distribution factor for the ν^{th} harmonic will be carried out applying the angle $\nu\alpha_u$; see Fig. 2.11b and 2.12b:

$$k_{dv} = \frac{\sin\nu\frac{q\alpha_u}{2}}{q\sin\nu\frac{\alpha_u}{2}}. \tag{2.24}$$

EXAMPLE 2.6: Repeat Example 2.5 using Eq. (2.24)

SOLUTION: $k_{\mathrm{dv}} = \dfrac{\sin \nu \dfrac{q\alpha_{\mathrm{u}}}{2}}{q \sin \nu \dfrac{\alpha_{\mathrm{u}}}{2}} = \dfrac{\sin 7 \dfrac{2\dfrac{\pi}{6}}{2}}{2 \sin 7 \dfrac{\pi}{6 \cdot 2}} = \dfrac{\sin \dfrac{7\pi}{6}}{2 \sin \dfrac{7\pi}{12}} = -0.2588$. The result is the same as above.

The expression for the fundamental may be rearranged:

$$k_{\mathrm{d1}} = \frac{\sin \dfrac{Q}{2pm} \dfrac{2\pi p}{2Q}}{q \sin \dfrac{2\pi p}{2 \cdot 2pmq}} = \frac{\sin \dfrac{\pi/2}{m}}{q \sin \dfrac{\pi/6}{q}}. \tag{2.25}$$

For three-phase machines $m = 3$, the expression is as follows:

$$k_{\mathrm{d1}} = \frac{\sin(\pi/6)}{q \sin \dfrac{\pi/6}{q}} = \frac{1}{2q \sin \dfrac{\pi/6}{q}}. \tag{2.26}$$

This simple expression of the distribution factor for the fundamental is most often employed for practical calculation.

EXAMPLE: 2.7 Calculate the phase voltage of a three-phase four-pole synchronous machine with the stator bore diameter of 0.30 m, the length of 0.5 m, and the speed of rotation 1500 rpm. The excitation creates the air gap fundamental flux density $\hat{B}_{\delta 1} = 0.8\,\mathrm{T}$. There are 36 slots, in which a one-layer winding with three conductors in each slot is embedded.

SOLUTION: According to the Lorentz law, an instantaneous value of the induced electric field strength in a conductor is $\boldsymbol{E} = \boldsymbol{v} \times \boldsymbol{B}_{\mathrm{o}}$. In one conductor embedded in a slot of an AC machine, we may get the induced voltage by integrating: $e_{\mathrm{1c}} = B_{\delta}\, l' v$ where B_{δ} is the local air- gap flux density value of the rotating magnetic field, l' is the effective length of the of stator iron stack, and v is the speed at which the conductor travels in the magnetic field, see Fig 2.13.

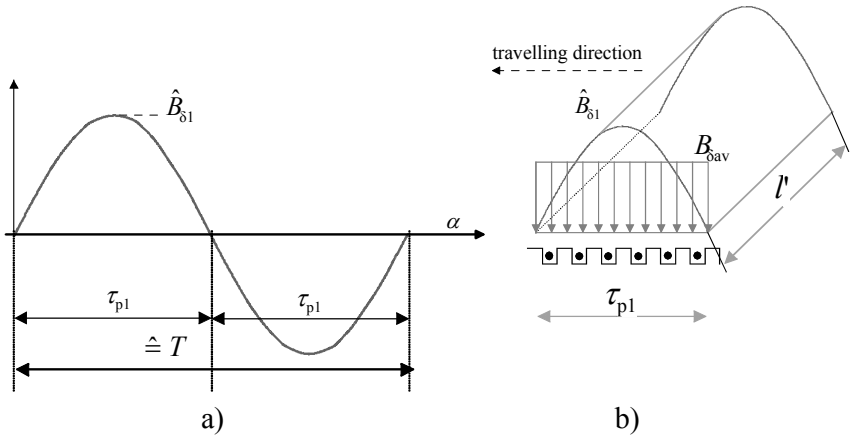

Figure 2.13 a) Flux density variation in the air gap. One flux density period travels two pole pitches during one time period *T*. b) The flux distribution over one pole and the conductors in slots.

During one period T, the magnetic flux density wave travels two pole pitches, as it is shown in the figure above. The speed of the magnetic field moving in the air gap is

$$v = \frac{2\tau_\mathrm{p}}{T} = 2\tau_\mathrm{p} f.$$

The effective value of the induced voltage in one conductor is:

$$E_\mathrm{1c} = \frac{\hat{B}_\delta}{\sqrt{2}} l' 2\tau_\mathrm{p} f.$$

Contrary to a transformer, where approximately the same value of magnetic flux density penetrates all the winding turns, Fig 2.11 shows that in AC rotating-field machines, the conductors are subject to the sinusoidal waveform of flux density, and each conductor is in a different value of magnetic flux density. Therefore, an average value of the magnetic flux density is calculated to unify the value of the magnetic flux for all conductors. The average value of the flux density produces the maximum value of the flux penetrating a full-pitch winding:

$$\hat{\Phi} = B_{\delta\mathrm{av}} l' \tau_\mathrm{p}.$$

B_δ is spread over the pole pitch τ_p, and we get for the average value

$$B_{\delta\mathrm{av}} = \frac{2}{\pi}\hat{B}_\delta \Rightarrow \hat{B}_\delta = \frac{\pi}{2} B_{\delta\mathrm{av}}.$$

Now, the effective average value of the voltage induced in a conductor written by means of average magnetic flux density is:

$$E_\mathrm{c} = \frac{\pi}{2\sqrt{2}} B_{\delta\mathrm{av}} l' 2\tau_\mathrm{p} f = \frac{\pi}{\sqrt{2}} \hat{\Phi} f.$$

The frequency f is found by the speed n

$$f = \frac{pn}{60} = \frac{2 \cdot 1500}{60} = 50\,\mathrm{Hz}$$

The information about three conductors in each slot can be used for calculating the number of turns N in series. In one phase, there are $2N$ conductors, and they are embedded in the slots belonging to one phase Q/m. Therefore, the number of conductors in one slot z_Q will be:

$$z_\mathrm{Q} = \frac{2N}{Q/m} = \frac{2Nm}{2pqm} = \frac{N}{pq}.$$

In this case, the number of turns in series in one phase is $N = 3pq = 3 \cdot 2 \cdot 3 = 18$. The effective value of the induced voltage in one slot is $\frac{N}{pq} E_\mathrm{c}$. The number of such slots is $2pq$. The linear sum of the voltages of all conductor belonging to the same phase must be reduced by the winding factor to get the phase voltage $E_\mathrm{ph} = \frac{N}{pq} E_\mathrm{c} q 2 p k_\mathrm{w}$. The final expression for the effective value of the induced voltage in the AC rotating machine is $E_\mathrm{ph} = E_\mathrm{c} \frac{N}{pq} q 2 p k_\mathrm{w1} = \frac{\pi}{\sqrt{2}} \hat{\Phi} f \frac{N}{pq} q 2 p k_\mathrm{w1} = \sqrt{2}\pi f \hat{\Phi} N k_\mathrm{w1}$. In

this example, there is a full-pitch one-layer winding, and therefore $k_p = 1$, and only k_d must be calculated:

$$k_{w1} = k_{d1} = \frac{1}{2q\sin\frac{30^o}{q}} = \frac{1}{2\cdot 3\sin\frac{30^o}{3}} = 0.96$$

The maximum value of the magnetic flux is: $\hat{\Phi} = \frac{2}{\pi}\hat{B}_\delta \tau_p l' = \frac{2}{\pi} 0.8 \cdot 0.236 \cdot 0.5 = 0.060$ Wb, where the pole pitch τ_p is: $\tau_p = \frac{\pi D_s}{2p} = \frac{\pi \cdot 0.3}{4} = 0.236$ m. An effective value of the phase induced voltage is:

$E_{ph} = \sqrt{2}\pi f \hat{\Phi} N k_d = \sqrt{2}\pi \cdot 50 \cdot 0.060 \cdot 18 \cdot 0.96 = 230$ V.

EXAMPLE 2.8: A stator of a four-pole three-phase induction motor has 36 slots, and it is fed by 3×400/230 V, 50 Hz. The diameter of the stator bore is D_s = 15 cm and the length l_{Fe} = 20 cm. A two-layer winding is embedded in the slots. Besides this, there is a one-layer, full-pitch, search coil embedded in two slots. In the no-load condition, a voltage of 11.3 V has been measured at its terminals. Calculate the air gap flux density, if the voltage drop on the impedance of the search coil can be neglected.

SOLUTION: To be able to investigate the air gap flux density, the data of the search coil can be used. This coil is embedded in two electrically opposite slots, and therefore the distribution factor k_d = 1; because it is a full-pitch coil, also the pitch factor k_p = 1, and therefore k_w = 1.

Now, the maximum value of magnetic flux is: $\hat{\Phi} = \frac{U_c}{\sqrt{2}\pi f N_c k_{wc}} = \frac{11.3}{\sqrt{2}\pi \cdot 50 \cdot 4 \cdot 1.0}$ Wb = 0.0127 Wb

The amplitude of the air gap flux density is:

$$\hat{B}_\delta = \frac{\pi}{2} B_{av} = \frac{\pi}{2} \frac{\hat{\Phi}}{\frac{\pi D_s}{2p} l'} = \frac{\pi}{2} \frac{0.0127}{\frac{\pi 0.15}{4} 0.2} \text{T} = 0.847 \text{ T}.$$

2.5 Winding Analysis

The winding analysis starts with the analysis of a single-layer stator winding, in which the number of coils is $Q_s/2$. In the machine design, the following setup is advisable: The periphery of the air gap of the stator bore (diameter D_s) is distributed evenly in all poles, that is, $2p$ of equal parts, which yields the pole pitch τ_p. Figure 2.14 illustrates the configuration of a two-pole slot winding (p = 1).

The pole pitch is evenly distributed in all stator phase windings, that is, in m_s equal parts. Now we obtain a zone distribution τ_{sv}. In Fig. 2.14, the number of stator phases is m_s = 3. The number of zones becomes thus $2pm_s$ = 6. The number of stator slots in a single zone is q_s, which is the number of slots per pole and phase in the stator. By using stator values in the general Eq. (2.5), we obtain

$$q_s = \frac{Q_s}{2pm_s}. \qquad (2.27)$$

If q_s is an integer, the winding is termed an integral slot winding, and if q_s is a fraction, the winding is called a fractional slot winding.

The phase zones are labelled symmetrically to the phase windings, and the directions of currents are determined so that we obtain a number of m_s magnetic axes at the distance of 360º/ m_s from each other. The phase zones are labelled as stated in 2.2. The positive zone of the phase U, that is, a zone where the current of the phase U is flowing away from the observer, is set as an example (Figure 2.14). Now the negative zone of the phase U is at the distance of 180 electrical degrees, in other words, electrically on the opposite side. The conductors of respective zones are connected so that the current flows as desired. This can be carried out for instance as illustrated in the figure below. In the figure, it is assumed that there are three slots in each zone, q_s = 3. The figure shows that the magnetic axis of the phase winding U is to the direction of the arrow drawn in the middle of the illustration. Because this is a three-phase machine, the directions of the currents of the phases V and W have to be such that the magnetic axes of the phases V and W are at the distance of 120° (electrical degrees) from the magnetic axis of the phase U. This can be realized by setting the zones of the V and W phases and the current directions according to Fig. 2.14.

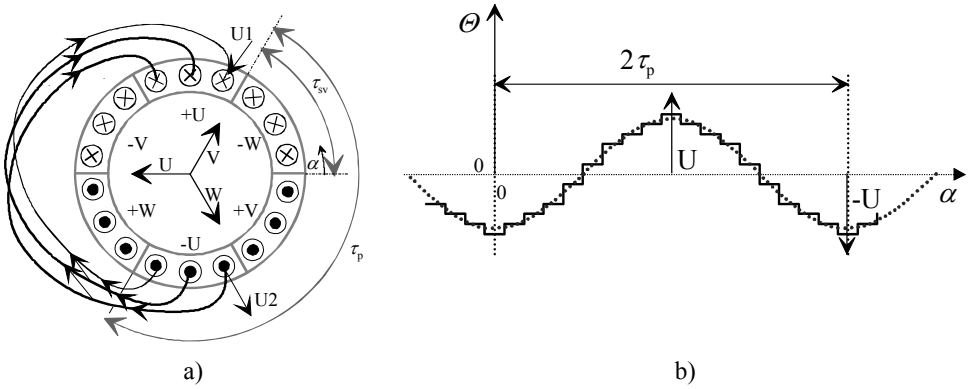

Figure 2.14. a) Three-phase stator diamond winding p = 1, q_s = 3, Q_s = 18. Only the coil end on the side of observation is visible of the U phase winding. The figure also illustrates the positive magnetic axes of the phase windings U, V, and W. The current linkage creates a flux in the direction of the magnetic axis when the current is penetrating the winding at its positive terminal, e.g. U1. The current directions of the figure depict a situation in which the current of the windings V and W is a negative half of the current in the winding U. b) The created current linkage distribution Θ_s is shown at the moment, when its maximum is in the direction of the magnetic axis of the phase U. The small arrows in Fig. 2.14a at the end winding indicate the current directions and the transitions from coil to coil. The same winding will be observed in Fig. 2.23.

The way how the conductors of different zones are connected produces different mechanical winding constructions, but the air gap remains similar irrespective of the mechanical construction. However, the arrangement of connections has a significant influence on the space requirements for the end windings, the amount of copper and the production costs of the winding. The connections also have an effect on certain electric properties, such as the leakage flux of the end windings.

The poly-phase winding in the stator of a rotating-field machine creates a flux wave when a symmetric poly-phase current flows in the winding. A flux wave is created for instance when the current linkage of Fig. 2.14 begins to propagate in the direction of the positive α-axis, and the currents of the poly-phase winding are alternating sinusoidally as a function of time. We have to note, however, that the propagation speeds of the harmonics created by the winding are different from the speed of the fundamental (n_{sv}= ± n_{s1}/v), and therefore the shape of the current linkage curve changes as a function of time. However, the fundamental propagates in the air gap at a speed defined by the fundamental of the current and by the number of pole pairs. Furthermore, the fundamental is usually dominating (when $q \geq 1$), and thus the operation of the machine can be analyzed basically

with the fundamental. For instance in a three-phase winding, time-varying sinusoidal currents with a 120° phase shift in time create a temporally and positionally alternating flux in the windings that are distributed at the distances of 120 electrical degrees. The flux distribution propagates as a wave on the stator surface. (See e.g. Fig. 7.7 illustrating the fundamental $\nu = 1$ of a six-pole and a two-pole machine.)

2.6 Short-Pitching

In a double-layer diamond winding, the slot is divided into an upper and a lower part, and there is one coil side in each half slot. The coil side at the bottom of the slot belongs to the bottom layer of the slot, and the coil side adjacent to the air gap belongs to the upper layer. The number of coils is now the same as the number of slots Q_s of the winding; see Fig. 2.15b.

A double-layer diamond winding is constructed like the single-layer winding. As illustrated in Fig. 2.15, there are two zone rings, the outer illustrating the bottom layer and the inner the upper layer, Fig. 2.15a. The distribution of zones does not have to be identical in the upper and bottom layer. The zone distribution can be shifted by a multiple of the slot pitch. In Fig. 2.15a, a single zone shift equals to a single slot pitch. Figure 2.15b illustrates one of the coils of the phase U. By comparing the width of the coil to the coil span of the winding in Fig. 2.14, we can see that the coil is now one pole pitch narrower; the coil is said to be short pitched. Because of short-pitching, the coil end has become shorter, and the copper consumption is thus reduced. On the other hand, the flux linking the coil decreases somewhat because of short-pitching, and therefore the number of coil turns at the same voltage has to be higher than for a full-pitch winding. The short-pitching of the coil end is of more significance than the increased number of coil turns, and as a result, the consumption of coil material decreases.

Short-pitching also influences the harmonics content of the flux density of the air gap. A correctly short-pitched winding produces a more sinusoidal current linkage distribution than a full-pitch winding. In a salient pole synchronous generator, where the flux density distribution is basically governed by the shape of pole shoes, a short-pitch winding produces a more sinusoidal pole voltage than a full-pitch winding.

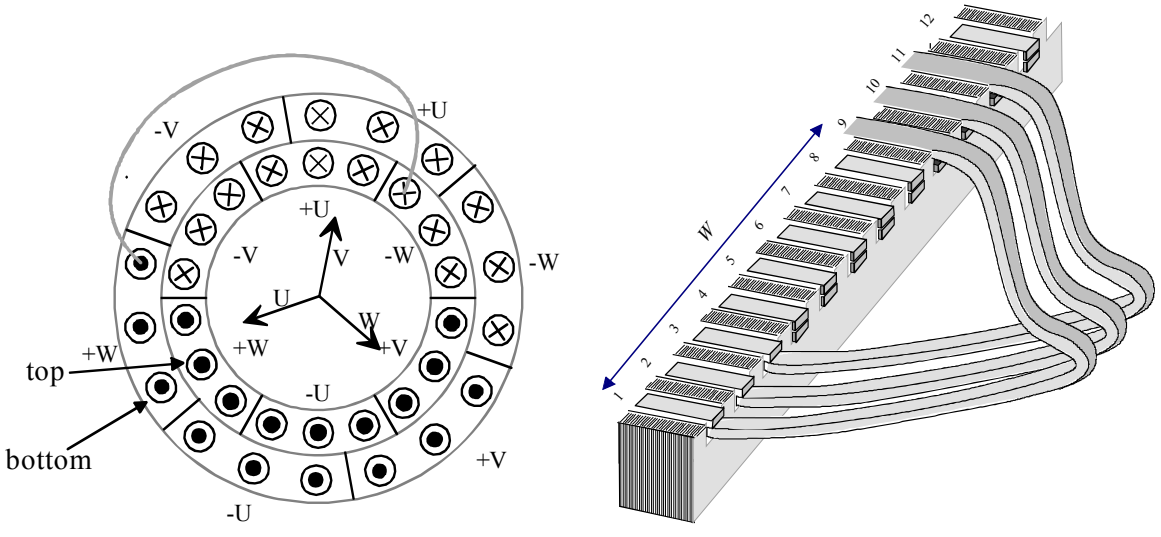

a) b)

Fig. 2.15. a) Three-phase double-layer diamond winding $Q_s = 18$, $q_s = 3$, $p = 1$. One end winding is shown to illustrate the coil span. The winding is created from the previous winding by dividing the slots into upper and bottom layers and by shifting the bottom layers clockwise by a single pole pitch. The magnetic axes of the new short-pitched winding are

also shown. b) A coil end of a double-layer winding produced of preformed copper, coil span W or expressed in numbers of slot pitches y. The coil ends start from the left at the bottom of the slot and continue to the right to the top of the slot.

Figure 2.16 illustrates the basic difference of a short-pitch winding and a full-pitch winding.

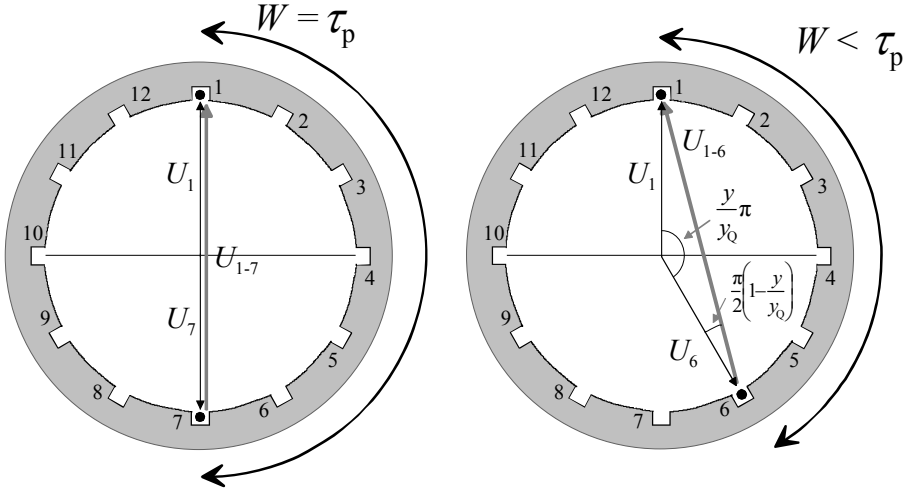

Figure 2.16. Cross-sectional areas of two machines with 12 slots. The basic differences of a) a two-pole full-pitch winding and b) a two-pole short-pitch winding. In the short-pitch winding, the width of a single coil W is less than the pole pitch τ_p or expressed in the number of slots the short pitch y is less than a full pitch y_Q. The voltage $U_{1\text{-}6}$ is lower than $U_{1\text{-}7}$. The short-pitched coil is located on the chord of the periphery, and therefore the winding type is also called a chorded winding. The coil without short-pitching is located on the diameter of the machine.

The short-pitch construction is now investigated in more detail. Short-pitching is commonly created by winding step shortening (Fig. 2.17b), coil side shift in a slot (Fig. 2.17c), and coil side transfer to another zone (Fig. 2.17d). In Fig. 2.17, the zone graphs illustrate the configurations of a full-pitch winding and of the short-pitch windings constructed with the above-mentioned methods. Of these methods, the step shortening can be considered to be created from a full-pitch winding by shifting the upper layer left for a certain number of slot pitches.

Coil side shift in a slot is generated by changing the coil sides of the upper and bottom layers in certain slots of a short pitch winding. For instance if in Fig. 2.17 b, the coil sides of the bottom layer in the slots 8 and 20 are removed to the upper layer, and in the slots 12 and 24, the upper coil sides are shifted to the bottom layer, we get the winding of Fig 2.17c. Now, the width of a coil is again $W = \tau_p$, but because the magnetic voltage of the air gap does not depend on the position of a single coil side, the magnetizing characteristics of the winding remains unchanged. The windings with a coil side shift in a slot and winding step shortening are equal in this respect. The average number of slots per pole and phase for windings with a coil side shift in a slot is

$$q_s = \frac{Q_s}{2pm} = \frac{q_1 + q_2}{2},\ q_1 = q + j;\ \ q_2 = q - j \tag{2.28}$$

where j is the difference of q (the numbers of slots per pole and phase) in different layers. In Fig. 2.17, $j = 1$.

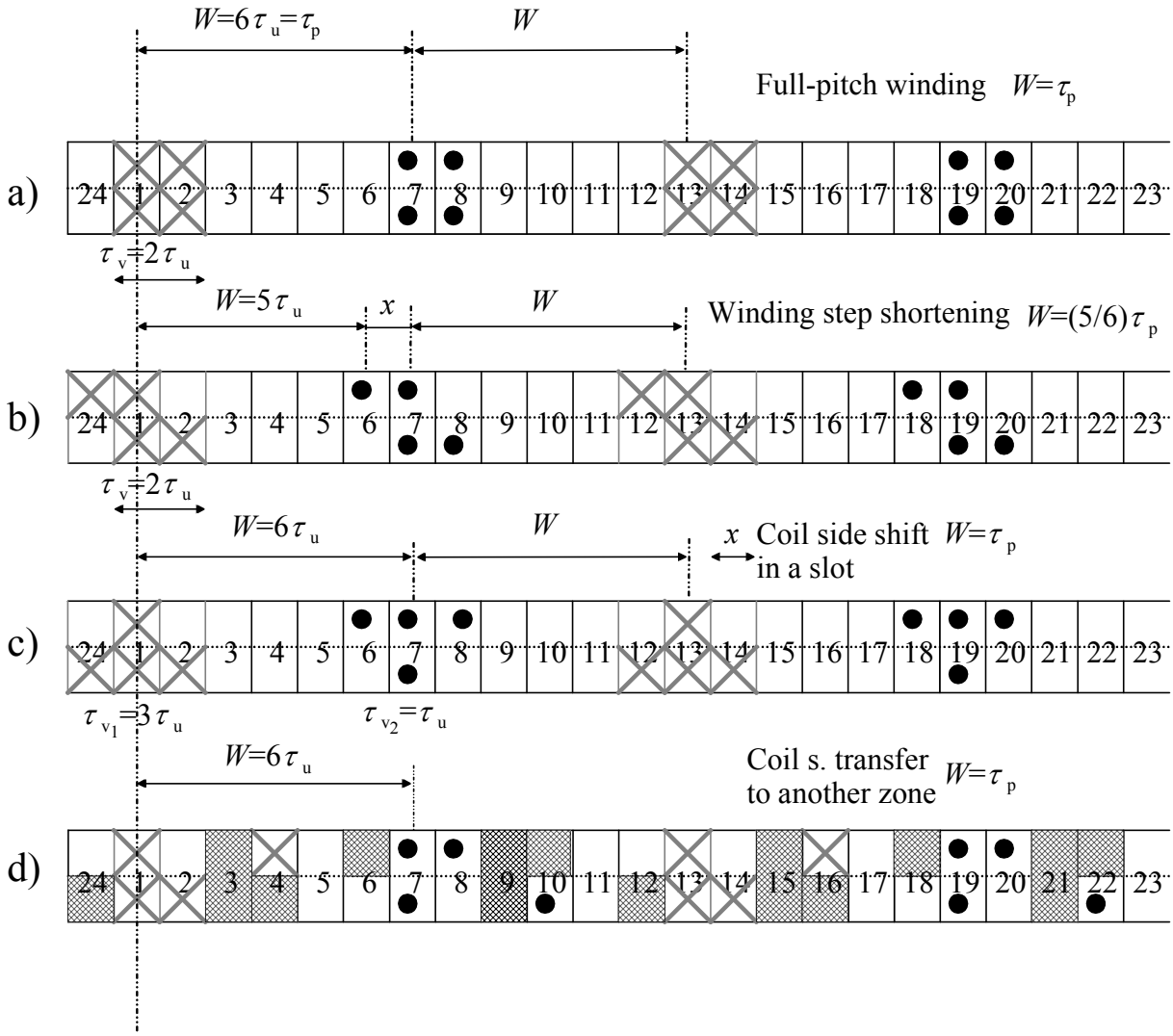

Figure 2.17. Different methods of short-pitching for a double-layer winding; a) full-pitch winding, b) winding step shortening, c) coil side shift in a slot, d) coil side transfer to another zone. $\tau_v \mathrel{\hat{=}}$ zone, $\tau_u \mathrel{\hat{=}}$ slot pitch, $W \mathrel{\hat{=}}$ coil span. $x \mathrel{\hat{=}}$ coil span decrease. In the figure, a cross sign indicates one coil end of the phase U, and the dot indicates the other coil end of the phase U. In the graph for a coil side transfer to another zone, the grid indicates the parts of slots filled with the windings of the phase W.

Coil side transfer to another zone (Fig 2.17d) can be considered to be created from the full-pitch winding of Fig. 2.17a by transferring the side of the upper layers of 2 and 14 to a foreign zone W. There is no general rule for the transfer, but practicality and the purpose of use decide the solution to be selected. The method may be adopted in order to cancel a certain harmonic from the current linkage of the winding.

The above-described methods can also be employed simultaneously. For instance, if we shift the upper layer of the coil with a coil side transfer of Fig. 2.17d left for the distance of one slot pitch, we receive a combination of a winding step shortening and a coil side transfer. This kind of winding is double short pitched, and it can eliminate two harmonics. This kind of short-pitching is often employed in machines where the windings may be rearranged during drive to form another pole number.

When different methods are compared, we have to bear in mind that when considering the connection, a common winding step shortening is always the simplest to realize, and the consumption of copper is often the lowest. A winding step shortening is an advisable method down

to $W = 0.8\tau_p$ without an increase in copper consumption. In short two-pole machines, the ends are relatively long, and therefore it is advisable to use even shorter pitches to make the end winding area shorter. Short-pitchings down to $W = 0.7\tau_p$ are used in two-pole machines with prefabricated coils. The most crucial issue concerning short pitching is, however, how completely we wish to eliminate the harmonics. This is best investigated with winding factors.

The winding factor k_{wv} was already determined with Fig. 2.10 and Eq. (2.16). When the winding is short pitched, and the coil ends are not at a distance of 180 electrical degrees from each other, we can easily understand that short-pitching reduces the winding factor of the fundamental. This is described with a pitch factor k_{pv}. Further, if the number of slots per pole and phase is higher than 1, we can see that in addition to the pitch factor k_{pv}, the distribution factor k_{dv} is required as it was discussed above. Thus, we can consider the winding factor to consist of the pitch factor k_{pv} and the distribution factor k_{dv} and is some cases, of a skewing factor (c.f. Eq. 2.35).

The full pitch can be expressed in radians as π, as a pole pitch τ_p, or in the number of slot pitches y_Q covering the pole pitch. The pitch expressed in the number of slots is y, and now the relative shortening is y / y_Q .Therefore, the angle of the short pitch is $(y / y_Q)\,\pi$. A complement to π, which is the sum of angles in a triangle, is: $\left(\pi - \frac{y}{y_Q}\pi\right) = \pi\left(1 - \frac{y}{y_Q}\right)$.This value will be divided equally to the other two angles as in Fig 2.16b: $\frac{\pi}{2}\left(1 - \frac{y}{y_Q}\right)$. Also the pitch factor is defined as a ratio of the geometric sum of phasors and the sum of the absolute values of the voltage phasors, see Fig.2.16b: The pitch factor is

$$k_p = \frac{U_{total}}{2U_{slot}}. \tag{2.29}$$

When $\cos\left(\frac{\pi}{2}\left(1 - \frac{y}{y_Q}\right)\right)$ is expressed in the triangle analyzed, it will be found that it equals with the pitch factor defined:

$$\cos\left(\frac{\pi}{2}\left(1 - \frac{y}{y_Q}\right)\right) = \frac{U_{total}/2}{U_{slot}} = \frac{U_{total}}{2U_{slot}} = k_p. \tag{2.30}$$

After rearranging the final expression for the pitch factor will be obtained:

$$k_p = \sin\left(\frac{y}{y_Q}\frac{\pi}{2}\right) = \sin\left(\frac{W}{\tau_p}\frac{\pi}{2}\right). \tag{2.31}$$

In a full-pitch winding, the pitch is equal to the pole pitch, $y = y_Q$, $W = \tau_p$ and the pitch factor is $k_p = 1$. If the pitch is less than y_Q, $k_p < 1$.

In a general presentation, the distribution factor k_{dv} and the pitch factor k_{pv} have to be valid also for harmonic frequencies. We may write for the ν^{th} harmonic, the pitch factor k_{pv}, and the distribution factor k_{dv}

$$k_{pv} = \sin\left(\nu\frac{W}{\tau_p}\frac{\pi}{2}\right) = \sin\left(\nu\frac{y}{y_Q}\frac{\pi}{2}\right), \tag{2.32}$$

$$k_{\mathrm{dv}} = \frac{\sin(\nu q \alpha_{\mathrm{u}}/2)}{q\sin(\nu\alpha_{\mathrm{u}}/2)} = \frac{2\sin\left(\nu\dfrac{\pi}{2m}\right)}{\dfrac{Q}{mp}\sin\left(\nu\dfrac{\pi p}{Q}\right)}. \tag{2.33}$$

Here α_{u} is the slot angle, $\alpha_{\mathrm{u}} = p2\pi/Q$.

The skewing factor will be developed in Chapter 4, but it is shown here

$$k_{\mathrm{sqv}} = \frac{\sin\left(\nu\dfrac{s}{\tau_{\mathrm{p}}}\dfrac{\pi}{2}\right)}{\nu\dfrac{s}{\tau_{\mathrm{p}}}\dfrac{\pi}{2}} = \frac{\sin\nu\dfrac{\pi}{2}\dfrac{1}{mq}}{\nu\dfrac{\pi}{2}\dfrac{1}{mq}}. \tag{2.34}$$

Here the skew is measured as s/τ_{p} (c.f. Fig. 2.16).

The winding factor is thus a product of these factors

$$k_{\mathrm{w}\nu} = k_{\mathrm{p}\nu}k_{\mathrm{d}\nu}k_{\mathrm{sk}\nu} = \sin\left(\nu\frac{W}{\tau_{\mathrm{p}}}\frac{\pi}{2}\right)\cdot\frac{2\sin\left(\dfrac{\nu}{m}\dfrac{\pi}{2}\right)}{\dfrac{Q}{mp}\sin\left(\nu\pi\dfrac{p}{Q}\right)}\cdot\frac{\sin\nu\dfrac{\pi}{2}\dfrac{1}{mq}}{\nu\dfrac{\pi}{2}\dfrac{1}{mq}}. \tag{2.35}$$

EXAMPLE 2.9: Calculate a winding factor for the two-layer winding Q = 24, 2p = 4, m = 3, y = 5, (see Fig 2.17 b). There is no skewing, i.e. $k_{\mathrm{sk}\nu} = 1$.

SOLUTION: The number of slots per phase per pole is $q = \dfrac{Q}{2pm} = \dfrac{24}{4\cdot 3} = 2$ .The distribution factor for the three-phase winding is $k_{\mathrm{d1}} = \dfrac{1}{2q\sin\dfrac{30}{q}} = \dfrac{1}{2\cdot 2\sin\dfrac{30}{2}} = 0.966$. The number of slots per pole, or in the other words, the pole pitch expressed in the number of slots: $y_{\mathrm{Q}} = \dfrac{Q}{2p} = \dfrac{24}{4} = 6$. If the pitch is 5 slots, it means that it is a short pitch, and it is necessary to calculate the pitch factor:

$k_{\mathrm{p1}} = \sin\left(\dfrac{y}{y_{\mathrm{Q}}}\dfrac{\pi}{2}\right) = \sin\left(\dfrac{5}{6}\dfrac{\pi}{2}\right) = 0.966$. The winding factor is:

$k_{\mathrm{w1}} = k_{\mathrm{d1}}k_{\mathrm{p1}}k_{\mathrm{sk}\nu} = 0.966\cdot 0.966\cdot 1 = 0.933$.

EXAMPLE 2.10: A two-pole alternator has on the stator a three-phase two-layer winding embedded in 72 slots, two conductors in each slot, with a short pitch of 29/36. The diameter of the stator bore is D_{s} = 0.85 m, the effective length of the stack is l' = 1.75 m. Calculate the fundamental component of the induced voltage in one phase of the stator winding, if the amplitude of the fundamental component of the air gap flux density is $\hat{B}_{1\delta}$ = 0.92 T and the speed of rotation is 3000 min^{-1}.

SOLUTION: The effective value of the induced phase voltage will be calculated from the expression $E_{1\mathrm{ph}} = \sqrt{2}\pi f \hat{\Phi}_1 N_\mathrm{s} k_{1\mathrm{w}}$ at the frequency of $f = \frac{pn}{60} = \frac{1 \cdot 3000}{60} = 50\,\mathrm{Hz}$. The pole pitch is $\tau_\mathrm{p} = \frac{\pi D_\mathrm{s}}{2p} = \frac{\pi \cdot 0.85\mathrm{m}}{2} = 1.335$ m. The maximum value of the magnetic flux is $\hat{\Phi}_1 = \frac{2}{\pi}\hat{B}_{1\delta}\tau_\mathrm{p} l' = \frac{2}{\pi} 0.92\mathrm{T} \cdot 1.335\mathrm{m} \cdot 1.75\mathrm{m} = 1.368$ Wb. The number of slots per pole and phase is $q_\mathrm{s} = \frac{Q_\mathrm{s}}{2pm} = \frac{72}{2 \cdot 3} = 12$. The number of turns in series N_s will be determined from the number of conductors in the slot: $z_\mathrm{Q} = \frac{N}{pq} = 2 \Rightarrow N = 2pq = 2 \cdot 1 \cdot 12 = 24$. There is a two-layer distributed short-pitch winding, and therefore both the distribution and pitch factors must be calculated (c.f. Eq. 2.26):

$k_{\mathrm{d}1} = \frac{1}{2q_\mathrm{s} \sin\frac{\pi/6}{q_\mathrm{s}}} = \frac{1}{2 \cdot 12 \sin\frac{\pi/6}{12}} = 0.955$, $k_{\mathrm{p}1} = \sin\left(\frac{y}{y_\mathrm{Q}}\frac{\pi}{2}\right) = \sin\left(\frac{29}{36}\frac{\pi}{2}\right) = 0.953$, because the full pitch is $y_Q = \frac{Q}{2p} = \frac{72}{2} = 36$. The winding factor yields $k_{\mathrm{w}1} = k_{\mathrm{d}1} k_{\mathrm{p}1} = 0.955 \cdot 0.953 = 0.91$ and the induced phase voltage of the stator is: $E_\mathrm{ph} = \sqrt{2}\pi f \hat{\Phi}_1 N_\mathrm{s} k_\mathrm{w} = \sqrt{2}\pi \cdot 50 \frac{1}{\mathrm{s}} 1.368\mathrm{Vs} \cdot 24 \cdot 0.91 = 6637\,\mathrm{V}$.

On the other hand, as it was shown previously, the winding constructed with the coil side shift in a slot in Fig. 2.17c proved to have an identical current linkage as the winding step shortening 2.17b, and therefore also its winding factor has to be same. The distribution factor k_dv is calculated with an average number of slots per pole and phase $q = 2$, and thus the pitch factor k_pv has to be the same as above, although no actual winding step shortening has been performed. For coil side shift in a slot, Eq. (2.32) is not valid as such for the calculation of pitch factor (because $\sin(\nu\pi/2) = 1$).

When comparing magnetically equivalent windings of Fig. 2.17 that apply winding step shortening and coil side shift in a slot, it is shown that an equivalent reduction x of the coil span for a winding with coil side shift is

$$x = \tau_\mathrm{p} - W = \frac{1}{2}(q_1 - q_2)\tau_\mathrm{u}. \tag{2.36}$$

The substitution of slot pitch $\tau_\mathrm{u} = 2p\tau_\mathrm{p}/Q$ in the equation yields

$$\frac{W}{\tau_\mathrm{p}} = 1 - \frac{p}{Q}(q_1 - q_2). \tag{2.37}$$

In other words, if the number of slots per pole and phase of the different layers of coil side shift are q_1 and q_2, the winding corresponds to the winding step shortening in the ratio of W/τ_p. By substituting (2.37) in Eq. (2.32) we obtain a pitch factor k_pwv of the coil side shift in a slot

$$k_{\mathrm{pw}\nu} = \sin\left\{\nu\left[1 - \frac{p}{Q}(q_1 - q_2)\right]\frac{\pi}{2}\right\}. \tag{2.38}$$

In the case of the coil side shift of Fig. 2.17c, $q_1 = 3$ and $q_2 = 1$. We may assume the winding to be a four-pole construction as a whole ($p = 2$, $Q_s = 24$). In the figure, a basic winding is constructed of the conductors of the first twelve slots (the complete winding may comprise an undefined number of sets of twelve-slot windings in series), and thus we obtain for the fundamental winding factor

$$k_{\mathrm{pw1}} = \sin\left\{\left[1 - \frac{2}{24}(3-1)\right]\frac{\pi}{2}\right\} = \sin\left(\frac{5}{6}\frac{\pi}{2}\right) = 0.966.$$

Which is the same result of Eq. (2.32) in the case of a winding step shortening of Fig. 2.17b.

Because we may often apply both the winding step shortening and coil side transfer in a different zone in the same winding, the winding factor has to be rewritten

$$k_{\mathrm{w}\nu} = k_{\mathrm{d}\nu} k_{\mathrm{pw}\nu} k_{\mathrm{p}\nu}. \tag{2.39}$$

With this kind of a doubly short-pitched winding, we may eliminate two harmonics, as stated earlier. The elimination of harmonics implies that we select a double-short pitched winding for which for instance $k_{\mathrm{pw5}} = 0$ and $k_{\mathrm{p7}} = 0$. Now we can eliminate the undesirable fifth and seventh harmonics. However, the fundamental winding factor will get smaller. The distribution factor k_{dv} is now calculated with the average number of slots per pole and phase $q = (q_1 + q_2)/2$.

When analyzing complicated short-pitch arrangements, it is often difficult to find a universal equation for the winding factor. In that case, a voltage phasor diagram can be employed, as mentioned earlier in the discussion of Fig. 2.10. Next, the coil side transfer to another zone of Fig. 2.17 is discussed.

Figure 2.18a depicts the fundamental voltage phasor diagram of the winding with coil side transfer to another zone in Fig. 2.17, assuming that there are $Q = 24$ slots and $2p = 4$ poles. The slot angle is now $\alpha_u = 30$ electrical degrees, and thus the phase shift of the emf is 30°. Figure 2.18b depicts the phasors of the phase U in a polygon according to the Fig. 2.17d. The resultant and its ratio to the sum of the absolute values of the phasors is the fundamental winding factor. By drawing also the resultants of the windings V and W from point 0, we obtain an illustration of the symmetry of a three-phase machine. The other harmonics (ordinal ν) are treated equally, but the phase shift angle of the phasors is now $\nu\alpha_u$.

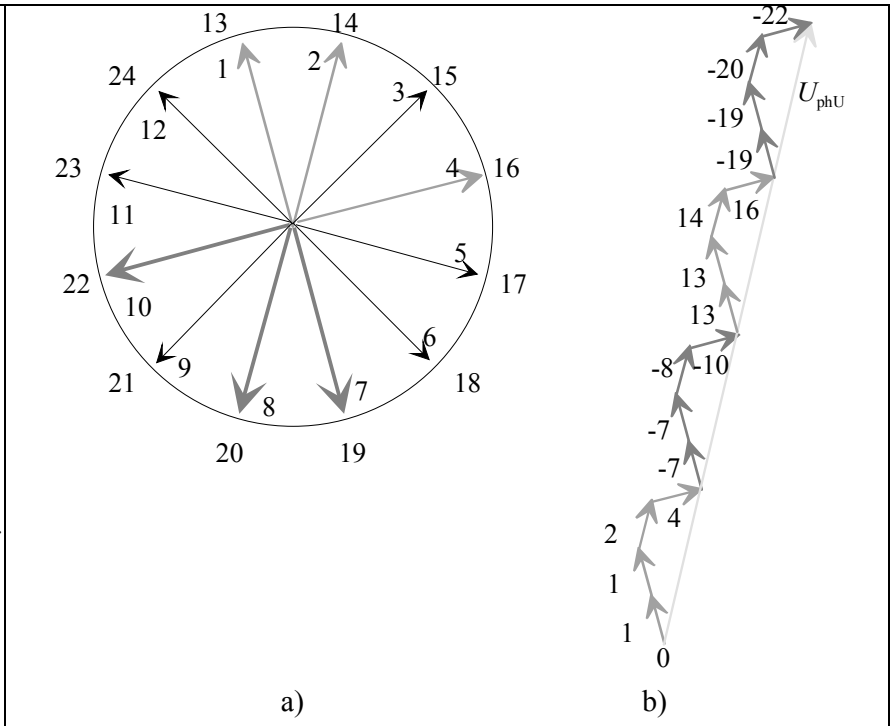

Figure 2.18. Voltage phasor diagram of a four-pole winding with a coil side transfer (Fig. 2.17d) and b) the sum of slot voltage phasors of a single phase. Note that the voltage phasor diagram for a four-pole machine (p = 2) is doubled, because it is drawn in electrical degrees. The parts of the figure are in different scales. In the voltage phasor diagram, there are in principle two layers (one for the bottom layer and another for the top layer), but only one of them is illustrated here. Now two consequent phasors, e.g. 2 and 14, when placed one after another, form a single radius of the voltage phasor diagram. The winding factor is thus defined with the voltage phasor diagram by comparing the geometrical sum to the sum of absolute values.

2.7 Current Linkage of a Slot Winding

Current linkage of a slot winding refers to a function $\Theta = f(\alpha)$, created by the winding and its currents to the equivalent air gap of the machine. The winding of Fig. 2.8 and its current linkage in the air gap are investigated at a time when $i_W = i_V = -½i_U$, Fig. 2.9. The curve function in the figure is drawn at time t = 0. The phasors of the phase currents rotate at an angular speed ω, and thus after a time $2\pi/(3\omega) = 1/(3f)$ the current of the phase V has reached its positive peak, and the function of current linkage has shifted three slot pitches to the right. After a time $2/(3f)$, the shift is six slot pitches and so on. The curve function shifts constantly to the direction $+\alpha$. To be exact, the curve waveform is of the form presented in the figure only at times $t = c/(3f)$, when the factor c is of the values c = 0, 1, 2, 3, ... As the time elapses, the waveform proceeds constantly. The Fourier analysis of the waveform, however, produces harmonics that remain constant.

Figure 2.19 illustrates the current linkage $\Theta(\alpha)$ produced by a single coil at a single pole pitch. A flux that passes through the air gap at an angle γ returns at an angle $\beta = \pi - \gamma$. In the case of a non-full-pitch winding, the current linkage is distributed in the ratio of the permeances of the paths. This gives us a pair of equations

$$z_Q i = \Theta_\gamma + \Theta_\beta;\ \frac{\Theta_\gamma}{\Theta_\beta} = \frac{\beta}{\gamma}, \tag{2.40}$$

from which we obtain two constant values for the current linkage waveform $\Theta(\alpha)$

$$\Theta_\gamma = \frac{\beta}{\pi} z_Q i;\ \Theta_\beta = \frac{\gamma}{\pi} z_Q i\ . \tag{2.41}$$

The Fourier series of the function $\Theta(\alpha)$ of a single coil is

$$\Theta(\alpha) = \hat{\Theta}_1 \cos\alpha + \hat{\Theta}_3 \cos 3\alpha + \hat{\Theta}_5 \cos 5\alpha + ... + \hat{\Theta}_\nu \cos \nu\alpha + ... \tag{2.42}$$

The magnitude of the νth term of the series is obtained from the equation by substituting the function of the current linkage waveform for a single coil

$$\hat{\Theta}_\nu = \frac{2}{\pi}\int_0^\pi \Theta(\alpha)\cos(\nu\alpha)\mathrm{d}\alpha = \frac{2}{\nu\pi} z_\mathrm{Q} i \sin\left(\frac{\nu\gamma}{2}\right). \tag{2.43}$$

As $\gamma / W = 2\pi/2\tau_\mathrm{p}$, and hence $\gamma/2 = (W/\tau_\mathrm{p})\cdot(\pi/2)$ the last factor of Eq. (2.43)

$$\sin\left(\frac{\nu\gamma}{2}\right) = \sin\left(\nu\frac{W}{\tau_\mathrm{p}}\frac{\pi}{2}\right) = k_{\mathrm{p}\nu} \tag{2.44}$$

is the pitch factor of the harmonic ν for the coil observed. For the fundamental $\nu = 1$, we obtain $k_{\mathrm{p}1}$. We can thus see that the fundamental is just a special case of the general harmonic ν. While the electrical angle of the fundamental is α, the corresponding angle for the harmonic ν is always $\nu\alpha$. If now $\nu\gamma/2$ is a multiple of the angle 2π, the pitch factor becomes $k_{\mathrm{p}\nu} = 0$. Thus, the winding does not produce such harmonics, neither are voltages induced to the winding by the influence of possible flux components at this distribution. However, voltages are induced to the coil sides, but in the whole coil these voltages compensate each other. Thus, with a suitable short-pitching, it is possible to eliminate harmful harmonics.

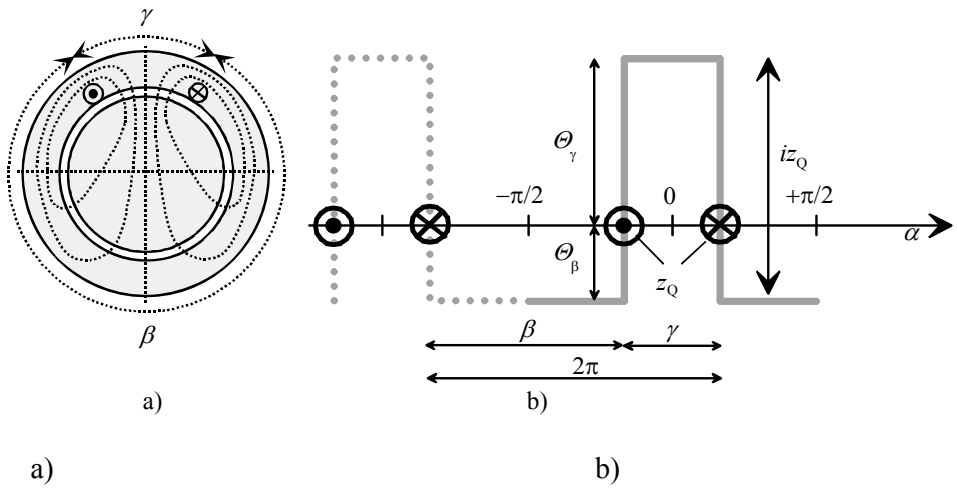

a) b)

Figure 2.19. a) Currents and schematic flux lines of a short-pitch coil in a two-pole system. b) Two wavelengths of the current linkage created by a single, narrow coil.

In Fig. 2.20, there are several coils 1 ... q in a single pole of a slot winding. The current linkage of each coil is $z_\mathrm{Q}i$. The coil angle (in electrical degrees) for the harmonic ν of the narrowest coil is $\nu\gamma$, the next being $\nu(\gamma + 2\alpha_\mathrm{u})$ and the broadest $\nu(\gamma + 2(q - 1)\alpha_\mathrm{u})$. For an arbitrary coil g, the current linkage is according to Eq. (2.43)

$$\Theta_{\mathrm{v}g} = \frac{2}{\nu\pi} z_\mathrm{Q} i \sin\left[\nu\left(\frac{\gamma}{2} + (q-1)\alpha_\mathrm{u}\right)\right]. \tag{2.45}$$

When all the harmonics of the same ordinal generated by all coils of one phase are summed, we obtain per pole

$$\Theta_{\nu\mathrm{tot}} = \sum_{g=1}^{q} \Theta_{\nu g} = \frac{2}{\nu\pi} q z_{\mathrm{Q}} i \sum_{g=1}^{q} k_{\mathrm{w}\nu} = \\ = \frac{2}{\nu\pi} z_{\mathrm{Q}} i \left\{ \sin\frac{\nu\gamma_1}{2} + \sin\nu\left(\frac{\gamma_1}{2} + \alpha_{\mathrm{u}}\right) + \ldots + \sin\nu\left(\frac{\gamma_1}{2} + (q-1)\alpha_{\mathrm{u}}\right) \right\} . \tag{2.46}$$

The sum $k_{\mathrm{w}\nu}$ in brackets can be calculated for instance with the geometrical figure of Figs. 2.20 and 2.12. The line segment $\overline{AC}$ is written as

$$\overline{AC} = 2r \sin\frac{\nu q \alpha_{\mathrm{u}}}{2} . \tag{2.47}$$

The arithmetical sum of unit segments is

$$q\overline{AB} = q 2r \sin\frac{\nu\alpha_{\mathrm{u}}}{2} \tag{2.48}$$

and we may find for the harmonic ν

$$k_{\mathrm{d}\nu} = \frac{\overline{AC}}{q\overline{\mathrm{AB}}} = \frac{\sin\frac{\nu q \alpha_{\mathrm{u}}}{2}}{q \sin\frac{\nu\alpha_{\mathrm{u}}}{2}} . \tag{2.49}$$

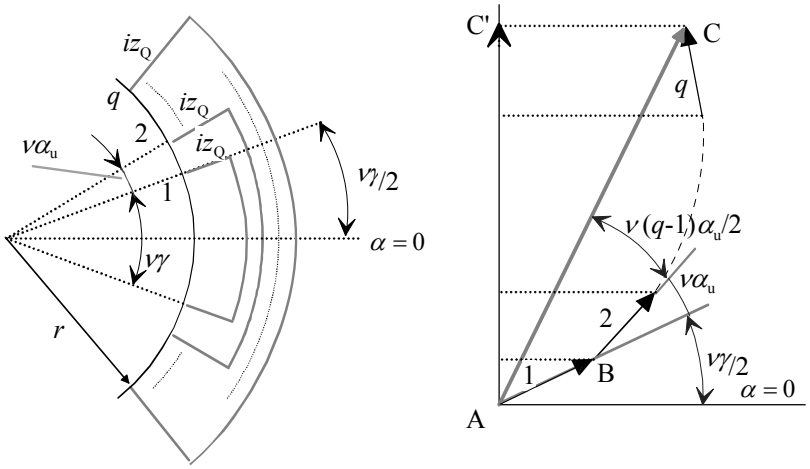

Figure 2.20. Concentric coils of a single pole; the calculation of winding factor for a harmonic ν.

This equals to the distribution factor of Eq. (2.33). Now, we see that the line segment $\overline{AC} = qk_{\mathrm{dv}}$. We use Fig 2.12 a again: The angle BAC is obtained from Fig. 2.12 as a difference of the angles OAB and OAC. It is $\nu(q-1)\alpha_{\mathrm{u}}/2$. The projection $\overline{AC'}$ is thus

$$\overline{AC'} = \overline{AC} \sin\frac{\nu\left(\gamma + (q-1)\alpha_{\mathrm{u}}\right)}{2} = \overline{AC} k_{\mathrm{p}\nu} . \tag{2.50}$$

Here we have a pitch factor influencing the harmonic ν, because in Fig. 2.20, $\nu[\gamma + (q-1)\alpha_u]$ is the average coil width angle. Eq. (2.46) is now reduced

$$\Theta_{\nu tot} = \frac{2}{\pi}\frac{k_{w\nu}}{\nu} q z_Q i , \tag{2.51}$$

where

$$k_{w\nu} = k_{p\nu} k_{d\nu} . \tag{2.52}$$

This is the winding factor of the harmonic ν. This is an important observation. The winding factor was originally found for the calculation of the induced voltages. Now we understand that the same distribution and pitch factors also affect the current linkage harmonic production. By substituting the harmonic current linkage Θ_ν in Eq. (2.42) with the current linkage $\Theta_{\nu tot}$, we obtain the harmonic ν generated by the current linkage of q coils

$$\Theta_\nu = \Theta_{\nu tot} \cos \nu\alpha . \tag{2.53}$$

This is valid for a single phase coil. The harmonic ν created by a poly-phase winding is calculated by summing all the harmonics created by different phases. By its nature, the pitch factor is zero, if $\nu\alpha_u = \pm c2\pi$ (since $\sin(\nu q \alpha_u / 2) = \sin(\pm c\pi q) = 0$) (i.e., the coil sides are in the same magnetic potential), when the factor c = 0, 1, 2, 3, 4... It allows thereby only the harmonics

$$\nu \neq c\frac{2\pi}{\alpha_u} . \tag{2.54}$$

The slot angle and the phase number are interrelated

$$q\alpha_u = \frac{\pi}{m} . \tag{2.55}$$

The distribution factor is zero, if $\nu = \pm c2m$. The winding thus produces harmonics

$$\nu = +1 \pm 2cm . \tag{2.56}$$

EXAMPLE 2.11: Calculate which ordinals of the harmonics can be created by a three-phase winding.

SOLUTION: A symmetrical three-phase winding may create harmonics calculated based on Eq. (2.56), by inserting m = 3. These are listed in Table 2.2.

Table 2.2. Ordinals of the harmonics created by a three-phase winding (m = 3).

c	0	1	2	3	4	5	6	7...	
ν	+1	+7	+13	+19	+25	+31	+37	+43...	positive sequence
	-	–5	–11	–17	–23	–29	–35	–41...	negative sequence

We see that ν = –1, and all even harmonics and harmonics divisible by three are missing. In other words, a symmetrical poly-phase winding does not produce for instance a harmonic propagating to an opposite direction at the fundamental frequency. Instead, a single-phase winding m = 1 creates

also a harmonic, the ordinal of which is $\nu = -1$. This is a particularly harmful harmonic, and impedes the operation of single-phase machines. For instance a single-phase induction motor, because of the field rotating to negative direction, does not start without assistance because the positive and negative sequence fields are equally strong.

EXAMPLE 2.12: Calculate the pitch and distribution factors for $\nu = 1, 5, 7$ if a chorded stator of an AC machine has 18 slots per pole and the first coil is embedded in the slots 1 and 16. Calculate also the relative harmonic current linkages.

SOLUTION: The full pitch would be $y_Q = 18$ and a full-pitch coil should be embedded in the slots 1 and 19. If the coil is located in the slots 1 and 16, the coil pitch is shorted to $y = 15$. Therefore, the pitch factor for the fundamental will be:

$k_{p1} = \sin\frac{W}{\tau_p}\frac{\pi}{2} = \sin\frac{y}{y_Q}\frac{\pi}{2} = \sin\frac{15}{18}\frac{\pi}{2} = 0.966$, and correspondingly for the fifth and seventh harmonics:

$$k_{p5} = \sin\left(\nu\frac{y}{y_Q}\frac{\pi}{2}\right) = \sin\left(-5\frac{15}{18}\frac{\pi}{2}\right) = -0.259\,,\ k_{p7} = \sin\left(\nu\frac{y}{y_Q}\frac{\pi}{2}\right) = \sin\left(7\frac{15}{18}\frac{\pi}{2}\right) = 0.259$$

The number of slots per pole and phase is $q = 18/3 = 6$ and the slot angle is $\alpha_u = \pi/18$. Now, the distribution factor is

$$k_{d\nu} = \frac{\sin\frac{\nu q\alpha_u}{2}}{q\sin\frac{\nu\alpha_u}{2}},\ k_{d1} = \frac{\sin\frac{1\cdot 6\pi/18}{2}}{6\sin\frac{1\pi/18}{2}} = 0.956,\ k_{d-5} = \frac{\sin\frac{-5\cdot 6\pi/18}{2}}{6\sin\frac{-5\pi/18}{2}} = -0.197,$$

$$k_{d7} = \frac{\sin\frac{7\cdot 6\pi/18}{2}}{6\sin\frac{7\pi/18}{2}} = -0.145.$$

$$k_{w1} = k_{d1}k_{p1} = 0.956\cdot 0.966 = 0.923\,,\ k_{w-5} = k_{d-5}k_{p-5} = -0.197\cdot(-0.259) = 0.051$$

$$k_{w7} = k_{d7}k_{p7} = -0.145\cdot 0.259 = -0.038$$

The winding creates current linkages $\Theta_{\nu tot} = \frac{2}{\pi}\frac{k_{w\nu}}{\nu}qz_Q i$. Calculating $\frac{k_{w\nu}}{\nu}$ for the harmonics 1, −5, 7

$$\frac{k_{w1}}{1} = 0.923\,,\ \frac{k_{w-5}}{-5} = \frac{0.051}{-5} = 0.01\,,\ \frac{k_{w7}}{7} = \frac{-0.038}{7} = 0.0054\,.$$

Here we can see that because of the chorded winding, the current linkages of the fifth and seventh harmonics will be reduced to 1.1% and 0.58 % of the fundamental, as the fundamental is also reduced to 92.3 % of the full sum of the absolute values of slot voltages.

EXAMPLE 2.13: A rotating magnetic flux created by a three-phase 50 Hz, 600 min^{-1} alternator has a spatial distribution of magnetic flux density given by the expression:

$B = \hat{B}_1\sin\vartheta + \hat{B}_3\sin 3\vartheta + \hat{B}_5\sin 5\vartheta = 0.9\sin\vartheta + 0.25\sin 3\vartheta + 0.18\sin 5\vartheta$ [T].

The alternator has 180 slots, the winding is wound with two layers, and each coil has three turns with the span of 15 slots. The armature diameter is 135 cm and the effective length of the iron core 0.50 m. Write the expression for the instantaneous value of the induced voltage in one phase of the winding. Calculate the effective value of phase voltage and also the line-to-line voltage of the machine.

SOLUTION: The number of pole pairs is given by the speed and the frequency:

$f = \frac{p\,n}{60} \Rightarrow p = \frac{60\,f}{n} = \frac{60 \cdot 50}{600} = 5$, and the number of poles is 10. The area of one pole is:

$\tau_\mathrm{p} l' = \frac{\pi D}{2p} l' = \frac{\pi 1.35}{10} 0.50 = 0.212\ \mathrm{m}^2$.

From the expression for the instantaneous value of the magnetic flux density, we may derive $\hat{B}_1 = 0.9$ T, $\hat{B}_3 = 0.25$ T and $\hat{B}_5 = 0.18$ T. The fundamental of the magnetic flux on the τ_p is

$\hat{\Phi}_1 = \frac{2}{\pi} \hat{B}_1 \tau_\mathrm{p} l' = \frac{2}{\pi} \cdot 0.9\mathrm{T} \cdot 0.212\mathrm{m}^2 = 0.1214$ Vs. To be able to calculate the induced voltage, it is necessary to make a preliminary calculation of some parameters:

The number of slots per pole and phase is $q = \frac{Q}{2\,p\,m} = \frac{180}{10 \cdot 3} = 6$,

The angle between the voltages of adjacent slots $\alpha_\mathrm{u} = \frac{p\,2\pi}{Q} = \frac{\pi}{18}$,

The distribution and pitch factors for each harmonics:

$$k_{\mathrm{d}1} = \frac{\sin\left(q\frac{\alpha_\mathrm{u}}{2}\right)}{q\sin\left(\frac{\alpha_\mathrm{u}}{2}\right)} = \frac{\sin\left(6 \cdot \frac{\pi}{36}\right)}{6\sin\left(\frac{\pi}{36}\right)} = 0.956,\ k_{\mathrm{d}3} = \frac{\sin\left(3 \cdot 6 \cdot \frac{\pi}{36}\right)}{6\sin\left(3 \cdot \frac{\pi}{36}\right)} = 0.643,\ k_{\mathrm{d}5} = \frac{\sin\left(5 \cdot 6 \cdot \frac{\pi}{36}\right)}{6\sin\left(5 \cdot \frac{\pi}{36}\right)} = 0.197$$

The number of slots per pole is $Q_\mathrm{p} = \frac{180}{10} = 18$, which would be a full pitch. The coil span is 15 slots, which means the chorded pitch y = 15, and the pitch factors are:

$$k_{\mathrm{p}1} = \sin\left(\frac{y}{y_\mathrm{Q}}\frac{\pi}{2}\right) = \sin\left(\frac{15}{18}\frac{\pi}{2}\right) = 0.966,\ k_{\mathrm{p}3} = \sin\left(3\frac{y}{y_\mathrm{Q}}\frac{\pi}{2}\right) = \sin\left(3 \cdot \frac{15}{18}\frac{\pi}{2}\right) = -0.707$$

$k_{\mathrm{p}5} = \sin\left(5\frac{y}{y_\mathrm{Q}}\frac{\pi}{2}\right) = \sin\left(5 \cdot \frac{15}{18}\frac{\pi}{2}\right) = 0.259$, which results in the following winding factors:

$k_{\mathrm{w}1} = k_{\mathrm{d}1} \cdot k_{\mathrm{p}1} = 0.955 \cdot 0.966 = 0.9234$, $k_{\mathrm{w}3} = 0.643 \cdot (-0.707) = -0.4546$, $k_{\mathrm{w}5} = 0.197 \cdot 0.259 = 0.051$.

Now, it is possible to calculate the effective values of the induced voltages of the harmonics. The phase number of turns is determined as follows: the total number of coils in a 180-slot machine in a two-layer winding is 180. It means that the number of coils per phase is $180/3 = 60$, each coil has three turns, and therefore $N = 60 \times 3 = 180$.

$E_1 = \sqrt{2}\pi f \hat{\Phi}_1 N k_{\mathrm{w}1} = \sqrt{2}\pi \cdot 50\frac{1}{\mathrm{s}} \cdot 0.1214\mathrm{Vs} \cdot 180 \cdot 0.9234 = 4482\ \mathrm{V}$.

The induced voltage of harmonics can be written similarly as follows:

$$E_\nu = \sqrt{2}\pi f_\nu \hat{\Phi}_\nu N k_{\mathrm{w}\nu} = \sqrt{2}\pi f_\nu \frac{2}{\pi} \hat{B}_\nu \tau_{\mathrm{p}\nu} N k_{\mathrm{w}\nu} = \sqrt{2}\pi \nu f_1 \frac{2}{\pi} \hat{B}_\nu \frac{\tau_{\mathrm{p}1}}{\nu} N k_{\mathrm{w}\nu} = \sqrt{2}\pi f_1 \frac{2}{\pi} \hat{B}_\nu \tau_{\mathrm{p}1} N k_{\mathrm{w}\nu}$$

The ratio of the ν^{th} harmonic and fundamental is $\frac{E_\nu}{E_1} = \frac{\sqrt{2}\pi f_1 \frac{2}{\pi}\hat{B}_\nu \tau_{\text{p1}} N k_{\text{wv}}}{\sqrt{2}\pi f_1 \frac{2}{\pi}\hat{B}_1 \tau_{\text{p1}} N k_{\text{w1}}} = \frac{\hat{B}_\nu k_{\text{wv}}}{\hat{B}_1 k_{\text{w1}}}$ results for E_ν:

$$E_3 = \frac{\hat{B}_3 k_{\text{w3}}}{\hat{B}_1 k_{\text{w1}}} E_1 = \frac{0.25 \cdot (-0.4546)}{0.9 \cdot 0.9225} 4482\text{V} = -612.9 \text{ V},$$

$$E_5 = \frac{\hat{B}_5 k_{\text{w5}}}{\hat{B}_1 k_{\text{w1}}} E_1 = \frac{0.18 \cdot 0.051}{0.9 \cdot 0.9225} 4482\text{V} = 49.5\text{V}.$$

Finally, the expression for the instantaneous value of the induced voltage is:

$$e(t) = \hat{E}_1 \sin \omega t + \hat{E}_3 \sin 3\omega t + \hat{E}_5 \sin 5\omega t = \sqrt{2}E_1 \sin \omega t + \sqrt{2}E_3 \sin 3\omega t + \sqrt{2}E_5 \sin 5\omega t$$

$$e(t) = \sqrt{2} \cdot 4482 \sin \omega t - \sqrt{2} \cdot 612.9 \sin 3\omega t + \sqrt{2} \cdot 49.5 \sin 5\omega t = 6338.5 \sin \omega t - 866.77 \sin 3\omega t + 70 \sin 5\omega t$$

The total value of the effective phase voltage is:

$E_{\text{ph}} = \sqrt{E_1^2 + E_3^2 + E_5^2} = \sqrt{4482^2 + 612.9^2 + 49.5^2}\text{V} = 4524\text{ V}$, and its line-to-line voltage is

$E = \sqrt{3}\sqrt{E_1^2 + E_5^2} = \sqrt{3}\sqrt{4482^2 + 49.5^2}\text{V} = 7763.58\text{ V}$. The third harmonic component does not appear in the line-to-line voltage, which will be demonstrated later on.

EXAMPLE 2.14: Calculate the winding factors and per unit magnitudes of the current linkage for ν = 1, 3, –5 if Q = 24, m = 3, q = 2, $W/\tau_{\text{p}} = \frac{y}{y_{\text{Q}}} = 5/6$.

SOLUTION: The winding factor is used to derive the per unit magnitude of the current linkage. In Fig. 2.21, we have a current linkage distribution of the phase U of a short-pitch winding (Q = 24, m = 3, q = 2, $2p$ = 4, $W/\tau_{\text{p}} = \frac{y}{y_{\text{Q}}} = 5/6$), as well as its fundamental and the third harmonic at time t = 0, when $i_{\text{U}} = \hat{i}$. The total maximum height of the current linkage of a pole pair is at that moment $qz_{\text{Q}}\hat{i}$. A half of the magnetic circuit (involving a single air gap) is influenced by a half of this current linkage. The winding factors for the fundamental and lowest harmonics and the amplitudes of the current linkages according to Eq. (2.51), (2.52) and Example 2.13 are:

$\nu = 1$	$k_{\text{w1}} = k_{\text{p1}}k_{\text{d1}} = 0.965 \cdot 0.965 = 0{,}931$	$\hat{\Theta}_1 = 1.185\ \Theta_{\text{max}}$
$\nu = 3$	$k_{\text{w3}} = k_{\text{p3}}k_{\text{d3}} = -0.707 \cdot 0.707 = -0{,}5$	$\hat{\Theta}_3 = -0.212\ \Theta_{\text{max}}$
$\nu = -5$	$k_{\text{w5}} = k_{\text{p}-5}k_{\text{d}-5} = -0.258 \cdot 0.258 = -0.067$	$\hat{\Theta}_{-5} = -0.017\ \Theta_{\text{max}}$

The negative signs for the third and fifth harmonic amplitudes mean that, if starting at the same phase, the third and fifth harmonics will have a negative peak value as the fundamental is in its positive peak, see Fig. 2.21 and 2.22.

For instance, the fundamental is calculated with (2.51); see also (2.15)

$$\hat{\Theta}_1 = \frac{2}{\pi}\frac{k_{\text{w}\nu}}{\nu} qz_{\text{Q}} i = \frac{2}{\pi}\frac{0.931}{1} 2z_{\text{Q}} i = 1.185 z_{\text{Q}} i$$

Only the fundamental and the third harmonic are illustrated in Fig. 2.21.

The amplitude of harmonics is often expressed as a percentage of the fundamental. In this case, the amplitude of the third harmonic is 17.8 % (0.212./1.185) of the amplitude of the fundamental. However, this is not necessarily harmful in a three-phase machine, because in the harmonic current linkage created by the windings together, the third harmonic is compensated. The situation is illustrated in Fig. 2.22, where the currents $i_U = 1$ and $i_V = i_W = -½$ flow in the winding of Fig. 2.21. In salient pole machines, the third harmonic may, however, cause circulating currents in delta connection, and therefore the star connection in the armature is preferred.

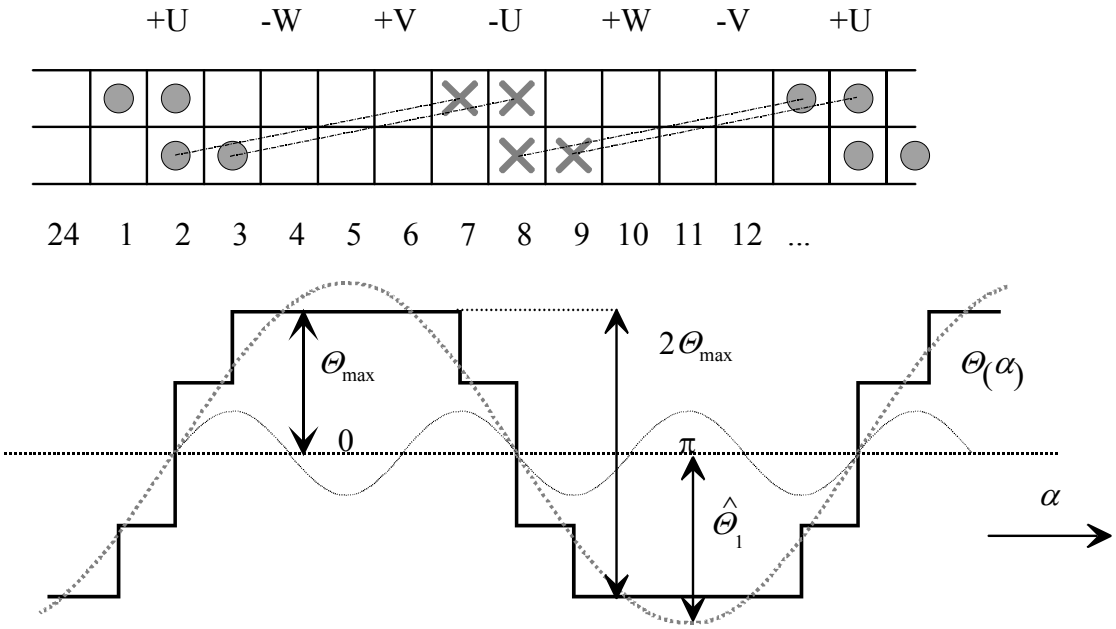

Figure 2.21. Short-pitch winding ($Q_s = 24$, $p = 2$, $m = 3$, $q_s = 2$) and the analysis of its current linkage distribution of the phase U. The distribution includes a notable amount of the third harmonic. In the figure, the fundamental and third harmonic are illustrated with dashed lines.

In single- and two-phase machines, the number of slots is preferably selected higher than in three-phase machines, because in these coils, at certain instants only a single phase coil alone creates the whole current linkage of the winding. In such a case, the winding alone should produce as sinusoidal current linkage as possible. In single- and double-phase windings, it is sometimes necessary to fit a different number of conductors in the slots to make the stepped line $\Theta(\alpha)$ approach sinusoidal form.

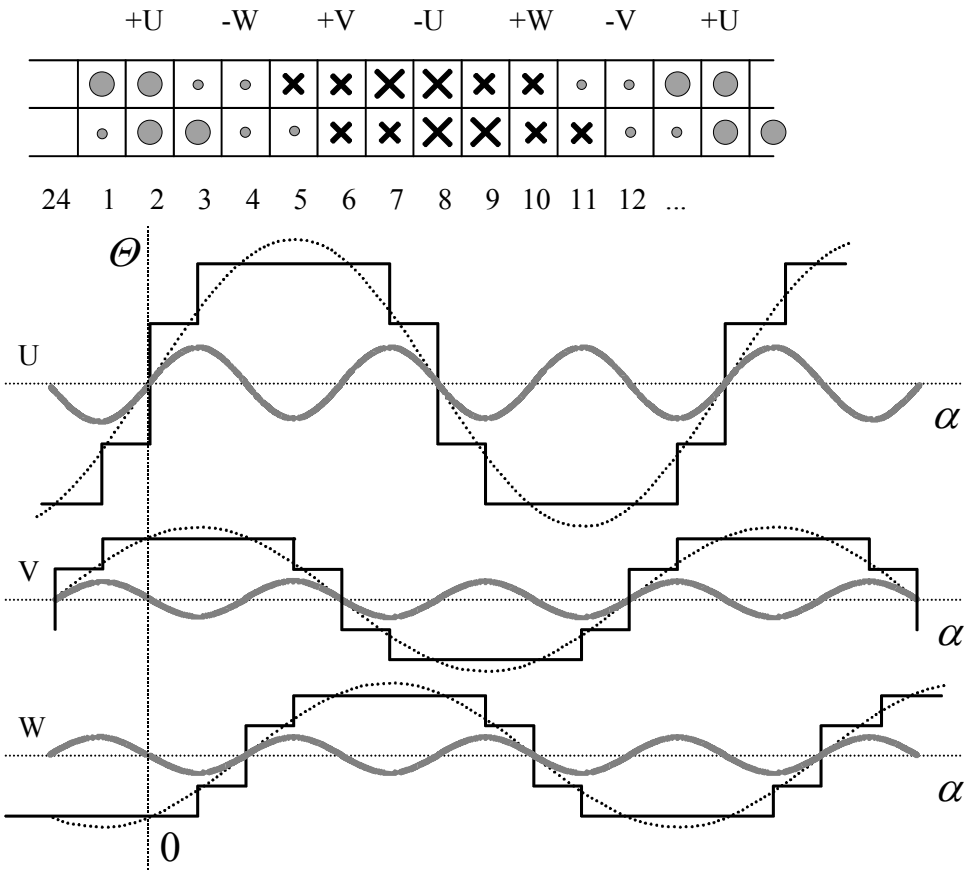

Figure 2.22. Compensation of the third harmonic in a three-phase winding. There are currents $i_U = -2i_V = -2i_W$ flowing in the winding. We see that when we sum the third harmonics of the phases V and W with the harmonic of the phase U, the harmonics compensate each other.

A poly-phase winding thus produces harmonics, the ordinals of which are calculated with Eq. (2.56). When the stator is fed at an angular frequency ω_s, the angular speed of the harmonic ν with respect to stator is

$$\omega_{\nu s} = \frac{\omega_s}{\nu}. \tag{2.57}$$

The situation is illustrated in Fig. 2.23, which shows that the shape of the harmonic current linkage changes as the harmonic propagates in the air gap. The deformation of the harmonic indicates the fact that harmonic amplitudes propagate at different speeds and in different directions. A harmonic according to Eq. (2.57) induces the voltage of the fundamental frequency to the stator winding. The ordinal of the harmonic indicates how many wavelengths of a harmonic are fitted to a distance $2\tau_p$ of a single pole pair of the fundamental. This yields the number of pole pairs and the pole pitch of a harmonic

$$p_\nu = \nu p, \tag{2.58}$$

$$\tau_{p\nu} = \frac{\tau_p}{\nu}. \tag{2.59}$$

The amplitude of the ν^{th} harmonic is determined with the ordinal from the amplitude of the current linkage of the fundamental, and it is calculated in relation of the winding factors

$$\hat{\Theta}_\nu = \hat{\Theta}_1 \frac{k_{w\nu}}{\nu k_{w1}}. \tag{2.60}$$

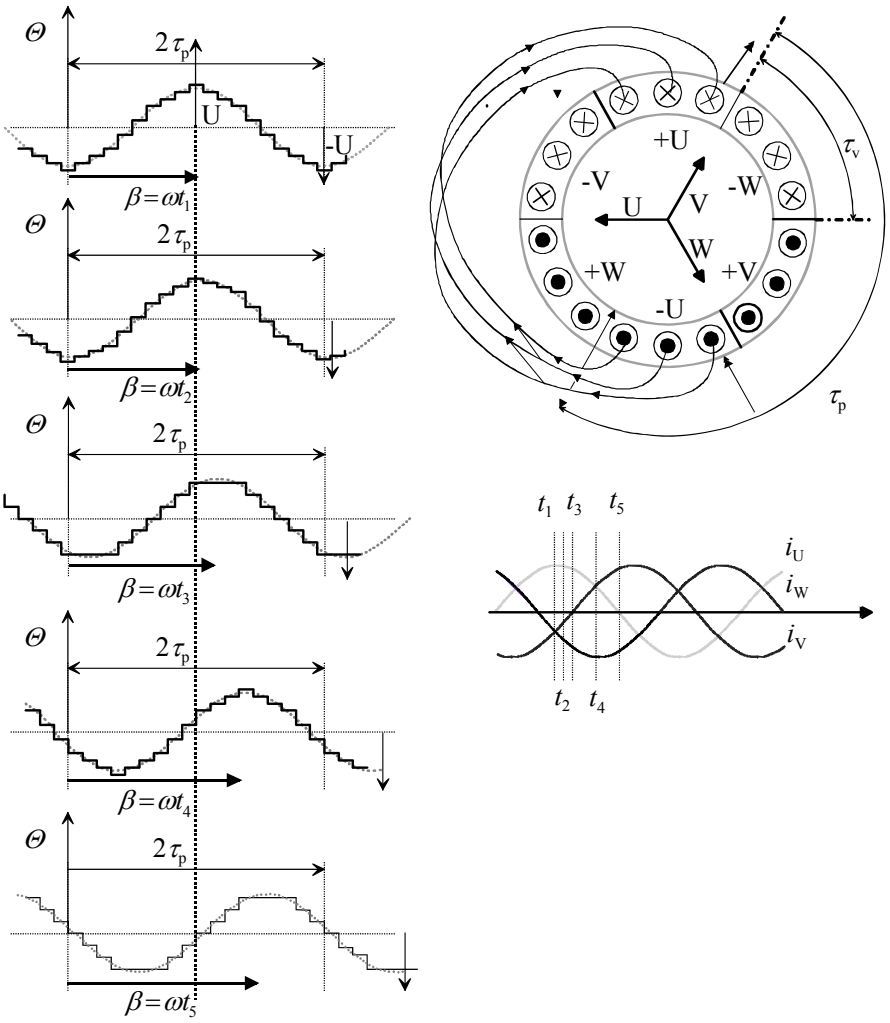

Figure 2.23. Propagation of a harmonic current linkage and the deformations caused by harmonics. If there is a current flowing only in the stator winding, we are able to set the peak of the air gap flux density at β. The flux propagates but the magnetic axis of the winding U remains stable.

The winding factor of the harmonic ν can be determined with Eqs. (2.32) and (2.33) by multiplying the pitch factor $k_{p\nu}$ and the distribution factor $k_{d\nu}$.

$$k_{w\nu} = k_{p\nu} k_{d\nu} = \frac{2\sin\left(\nu \frac{W}{\tau_p}\frac{\pi}{2}\right)\sin\left(\frac{\nu}{m}\frac{\pi}{2}\right)}{\frac{Q}{mp}\sin\left(\nu\pi\frac{p}{Q}\right)}. \tag{2.61}$$

Compared with the angular velocity ω_{1s} of the fundamental component, a harmonic current linkage wave propagates in the air gap at a fractional angular velocity ω_{1s}/ν. The synchronous speed of the harmonic ν is at the same very angular speed ω_{1s}/ν. If a motor is running at about synchronous speed, the rotor is travelling much faster than the harmonic wave. If we have an asynchronously

running motor with a per-unit slip $s = (\omega_s - p\Omega_r)/\omega_s$, ($\omega_s$ is the stator angular frequency and Ω_r is the rotor mechanical angular rotating frequency), the slip of the rotor with respect to the ν^{th} stator harmonic

$$s_\nu = 1 - \nu(1 - s). \tag{2.62}$$

The angular frequency of the ν^{th} harmonic in the rotor is thus

$$\omega_{\nu r} = \omega_s(1 - \nu(1 - s)). \tag{2.63}$$

If we have a synchronous machine running with the slip $s = 0$, we immediately observe from Eq. (2.62) and (2.63) that the angular frequency created by the fundamental component of the flux density of the stator winding is zero in the rotor co-ordinate. However, harmonic current linkage waves pass the rotor at different speeds. If the shape of the pole shoe is such that the rotor produces flux density harmonics, they propagate at the speed of the rotor and thereby generate pulsating torques with the stator harmonics travelling at different speeds. This is a problem particularly in low-speed permanent magnet synchronous motors, in which the rotor magnetizing often produces a quadratic flux density and the number of slots in the stator is small, for instance $q = 1$ or even lower, the amplitudes of the stator harmonics being thus notably high.

2.8 Poly-Phase Fractional Slot Windings

If the number of slots per pole and phase q of a winding is a fraction, the winding is called a fractional slot winding. The windings of this type are either concentric or diamond windings with one or two layers. Some advantages of fractional slot windings when compared with integer slot windings are:

- great freedom of choice with respect to the number of slots
- opportunity to reach a suitable magnetic flux density with the given dimensions
- multiple alternatives for short-pitching
- if the number of slots is predetermined, the fractional slot winding can be applied to a wider range of numbers of poles than the integral slot winding
- segment structures of large machines are better controlled by using fractional slot windings
- opportunity to improve the voltage waveform of a generator by removing certain harmonics

The greatest disadvantage of fractional slot windings is subharmonics, when the denominator of q (slots per pole and phase) is $n \neq 2$

$$q = \frac{Q}{2pm} = \frac{z}{n}. \tag{2.64}$$

Now, q is reduced so that the numerator and the denominator are smallest possible integers: the numerator being z and the denominator n. If the denominator n is an odd number, the winding is said to be a first-grade winding, and when n is an even number, the winding is of the second grade. The most reliable fractional slot winding is constructed by selecting $n = 2$. An especially interesting winding of this type can be designed for fractional slot permanent magnet machines by selecting $q = ½$.

In integral slot windings, the base winding is of the length of two pole pitches (the distance of the fundamental wavelength), whereas in the case of fractional slot windings, a distance of several fundamental wavelengths has to be travelled before the phasor of a voltage phasor diagram meets the same exact point of the waveform again. The difference of an integral slot and fractional slot winding is illustrated in Fig. 2.24.

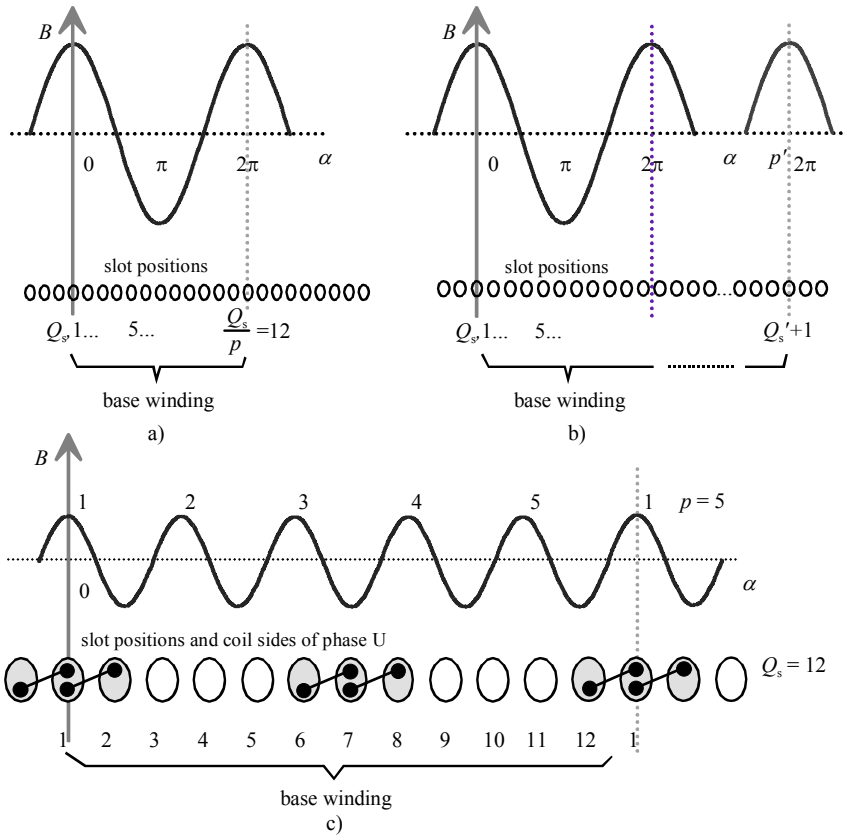

Figure 2.24. Basic differences of a) an integral slot stator winding and b) a fractional slot winding. The number of stator slots is Q_s. In an integral slot winding, the length of the base winding is Q_s/p slots (a: 12 slots, $q_s = 2$), but in a fractional slot winding, the division is not equal (b: $q_s < 2$). In the observed integer slot winding, the base winding length is $Q_s = 12$ and after that, the magnetic conditions for the slots repeat themselves equally; observe the slots 1 and 13. In the fractional slot winding, the base winding is notably longer and contains Q_s' slots. Figure c illustrates an example of a fractional slot winding with $Q_s = 12$ and $p = 5$. Such a winding may be used in concentrated wound permanent magnet fractional slot machines, where $q = 0.4$. In a two-layer system, each of the stator phases carries four coils. The coil sides are located in the slots 12–1, 1–2, 6–7, and 7–8.

In a fractional slot winding, we have to proceed the distance of p' pole pairs before a coil side of the same phase meets exactly the peak value of the flux density again. Then, we need a number of Q_s' phasors of the voltage phasor diagram, pointing at different directions. Now, we can write

$$Q_s' = p' \frac{Q_s}{p}, \quad Q_s' < Q_s, \qquad p > p'. \tag{2.65}$$

Here the voltage phasors $Q_s' + 1$, $2Q_s' + 1$, $3Q_s' + 1$ and $(t\text{-}1)Q_s' + 1$ are in the same position in the voltage phasor diagram as the voltage phasor of the slot 1. In this position, the cycle of the voltage phasor diagram is always started again. Either a new periphery is drawn, or more slot numbers are added to the phasors of the initial diagram. In the numbering of a voltage phasor diagram, each layer of the diagram has to be circled p' times. Thus, t layers are created to the voltage phasor diagram. In other words, in each electrical machine, there are t electrically equal slot sequences, the slot number of which is $Q_s' = Q_s/t$ and the number of pole pairs $p' = p/t$. To determine t, we have to find the

smallest integers Q_s' and p'. t is thus the largest common divider of Q_s and p. If $Q_s/(2pm) \in \mathbf{N}$ ($\mathbf{N}$ is a set of integers, $\mathbf{N}_{even}$ is a set of even integers, and $\mathbf{N}_{odd}$ is a set of odd integers), we have an integral slot winding, and $t = p$, $Q_s' = Q_s/p$ and $p' = p/p = 1$. Table 2.3 shows some parameters of a voltage phasor diagram. To generalize the representation, the subscript 's' is left out in the following.

Table 2.3. Parameters of voltage phasor diagrams.

t	the largest common divider of Q and p, the number of phasors of a single radius, the number of layers of a voltage phasor diagram
$Q' = Q/t$	the number of radii, or the number of phasors of a single turn in a voltage phasor diagram. (the number of slots in a base winding)
$p' = p/t$	the number of revolutions around a single layer when numbering a voltage phasor diagram
$(p/t) - 1$	the phasors skipped in the numbering of the voltage phasor diagram

If the number of radii in the voltage phasor diagram is $Q' = Q/t$, the angle of adjacent radii, that is, the phasor angle α_z is written

$$\alpha_z = \frac{2\pi}{Q} t . \tag{2.66}$$

The slot angle α_u is correspondingly a multiple of the phasor angle α_z

$$\alpha_u = \frac{p}{t}\alpha_z = p'\alpha_z . \tag{2.67}$$

When $p = t$, we obtain $\alpha_u = \alpha_z$, and the numbering of the voltage phasor diagram proceeds continuously. If $p > t$, $\alpha_u > \alpha_z$, a number of $(p/t) - 1$ phasors have to be skipped in the numbering of slots. In that case, a single layer of a voltage phasor diagram has to be circled (p/t) times when numbering the slots. When considering the voltage phasor diagrams of harmonics ν, we see that the slot angle of the ν th harmonic is $\nu\alpha_u$. Also the phasor angle is $\nu\alpha_z$. The voltage phasor diagram of the ν th harmonic differs from the voltage phasor diagram of the fundamental with respect to the angles, which are ν-fold.

EXAMPLE 2.15: Create voltage phasor diagrams for two different fractional slot windings: a) $Q = 27$ and $p = 3$, b) $Q = 30$, $p = 4$.

SOLUTION: a) $Q = 27$, $p = 3$, $Q/p = 9 \in \mathbf{N}$, $q_s = 1.5$, $t = p = 3$, $Q' = 9$, $p' = 1$, $\alpha_u = \alpha_z = 40°$.

There are, hence, nine radii in the voltage phasor diagram, each having three phasors. Because $\alpha_u = \alpha_z$, no phasors are skipped in the numbering, Fig. 2.25a.

b) $Q = 30$, $p = 4$, $Q/p = 7.5 \notin \mathbf{N}$, $q_s = 1.25$, $t = 2 \neq p$, $Q' = 15$, $p' = 2$, $Z = Q/t = 30/2 = 15$, $\alpha_z = 360°/15 = 24°$, $\alpha_u = 2\alpha_z = 2\times 24° = 48°$, $(p/t) - 1 = 1$.

In this case, there are 15 radii in the voltage phasor diagram, each having two phasors. Because $\alpha_u = 2\alpha_z$, the number of phasors skipped will be $[(p/t) - 1 = 1]$. Both of the layers of the voltage phasor diagram have to be circled twice in order to number all the phasors, Fig. 2.25b.

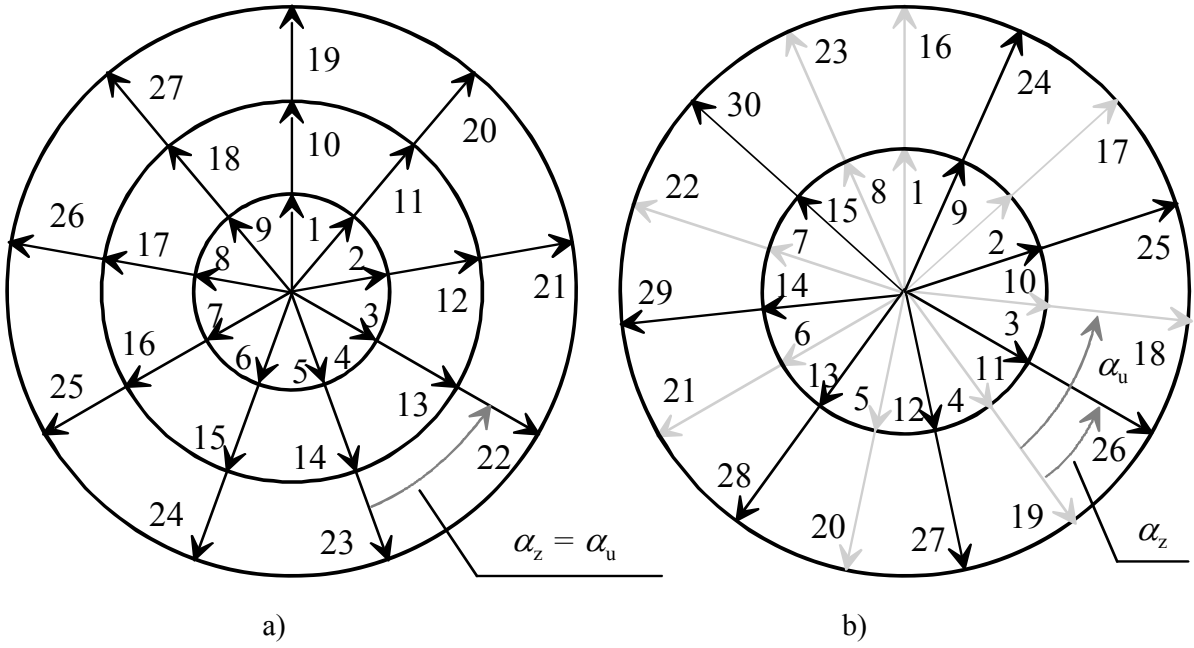

Figure 2.25. Voltage phasor diagrams for two different fractional slot windings. Left, the numbering is continuous, whereas on the right, certain phasors are skipped. a) $Q = 27$, $p = 3$, $t = 3$, $Q' = 9$, $p' = 1$ $\alpha_u = \alpha_z = 40°$; b) $Q = 30$, $p = 4$, $t = 2$, $Q' = 15$, $p' = 2$ $\alpha_u = 2\alpha_z = 48°$; α_u is the angle between voltages in the slots in electrical degrees and the angle α_z is the angle between two adjacent phasors in electrical degrees.

2.9 Phase Systems and Zones of Windings

Phase systems

Generally speaking, windings may involve single or multiple phases, the most common case being a three-phase winding, which has been discussed here also. However, various other winding constructions are possible, as illustrated in Table 2.4.

On a single magnetic axis of an electrical machine, there may be located only one axis of a single phase winding. If another phase winding is placed on the same axis, no genuine poly-phase system is created, because both windings produce parallel fluxes. Therefore, each phase system that involves an even number of phases is reduced to involve only a half of the original number of phases m' as illustrated in Table 2.4. If the reduction produces a system with an odd number of phases, we obtain a radially symmetric poly-phase system, also known as a **normal system**.

If the reduction produces a system with an even number of phases, the result is called a **reduced system**. In this sense, an ordinary two-phase system is a reduced four-phase system, as illustrated in Table 2.4. For an m-phase normal system, the phase angle is

$$\alpha_{ph} = 2\pi/m. \tag{2.68}$$

Correspondingly for a reduced system, the phase angle is

$$\alpha_{ph} = \pi/m. \tag{2.69}$$

For example in a three-phase system, $\alpha_{ph3} = 2\pi/3$ and for a two-phase system, $\alpha_{ph2} = \pi/2$.

If there is even a single odd number as a multiplicand of the phase number in the reduced system, a radial-symmetric winding can be constructed again by turning the direction of the suitable phasors by 180 electrical degrees in the system, as shown in Table 2.4 for a six-phase system (6 = 2×3). With this kind of a system, a non-loaded star point is created exactly like in a normal system. In a normal reduced system, the star point is loaded, and thus for instance a star point of a reduced two-phase machine requires a conductor of its own, which is not required in a normal system. Without a neutral conductor, a reduced two-phase system becomes a single-phase system, because the windings cannot operate independently, but the same current that produces the current linkage is always flowing in them, and together they form only a single magnetic axis. An ordinary three-phase system also becomes a single-phase system for instance if the voltage supply of one phase ceases for some reason.

Table 2.4. Phase systems of the windings of electrical machines. The fourth column introduces radially symmetric winding alternatives.

Number of phases m	**Non-reduced winding systems have separate windings for positive and negative magnetic axes**	**Reduced system: loaded star point needs a neutral line unless radial-symmetric (e.g.** $m = 6$**)**	**Normal system: non-loaded star point and no neutral line, unless** $m = 1$
1	 $m' = 2$	-	
2	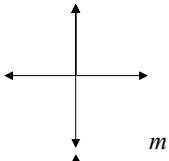 $m' = 4$		-
3	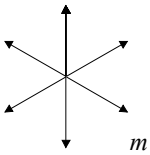 $m' = 6$	-	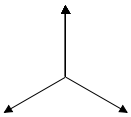
4	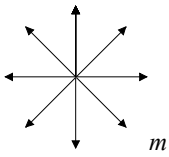 $m' = 8$	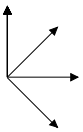	-
5	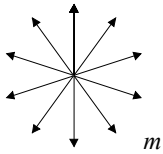 $m' = 10$	-	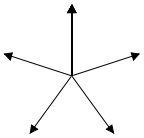
6	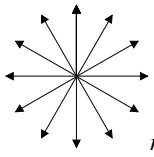 $m' = 12$	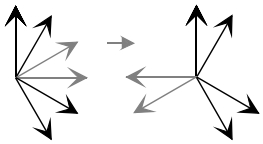	-
… 12	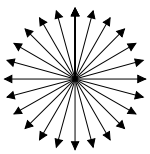 $m' = 24$	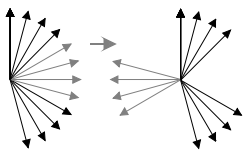	-

Reading instructions for Table 2.4

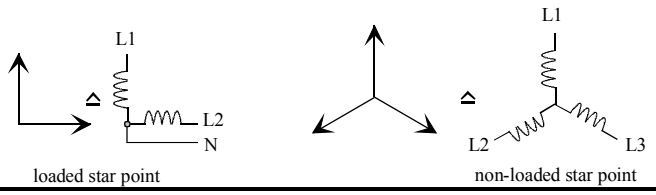

Of the winding systems in Table 2.4, the three-phase normal system is dominant in industrial applications. Five- and seven-phase windings have been suggested for frequency converter use to increase the system output power at a low voltage. Six-phase motors are used in large synchronous motor drives. In some larger high-speed applications, six-phase windings are also useful. In practice, all phase systems divisible by three are practical in inverter supplies. Each of the three-phase partial systems is supplied by its own three-phase frequency converter having a temporal phase shift $2\pi/m'$, in a 12-phase system e.g. $\pi/12$. For example a 12-phase system is supplied with four three-phase converters having a $\pi/12$ temporal phase shift.

Single-phase windings may be used in single-phase synchronous generators and also in small induction motors. In the case of a single-phase-supplied induction motor, the motor, however, needs starting assistance, which is often realized as an auxiliary winding with a phase shift of $\pi/2$. In such a case, the winding arrangement starts to resemble the two-phase reduced winding system, but since the windings are usually not similar, the machine is not purely a two-phase machine

Zones of Windings

In double-layer windings, both layers have separate zones; an upper-layer zone and a bottom-layer zone, Fig. 2.26. This double number of zones means also a double number of coil groups when compared with single-layer windings. In double-layer windings, one coil side is always located in the upper layer, and the other in the bottom layer. In short-pitched double-layer windings, the upper layer is shifted with respect to the bottom layer, as it is shown in Figs. 2.15 and 2.17. The span of the zones can be varied between the upper and bottom layer, as shown in Fig. 2.17 (zone variation). With double-layer windings, we can easily apply systems with a double zone span, which usually occur only in machines, where the windings may be rearranged during the drive to produce another number of poles. In fractional slot windings, zones of varying spans are possible. This kind of zone variation is called natural zone variation.

In a single-layer winding, each coil requires two slots. For each slot, there is now one half of a coil. In double-layer windings, there are two coil sides in each slot, and thus, in principle, there is one coil per slot. A total number of coils z_c is thereby

$$\text{for single-layer windings: } z_c = \frac{Q}{2}. \tag{2.70}$$

$$\text{for double-layer windings: } z_c = Q. \tag{2.71}$$

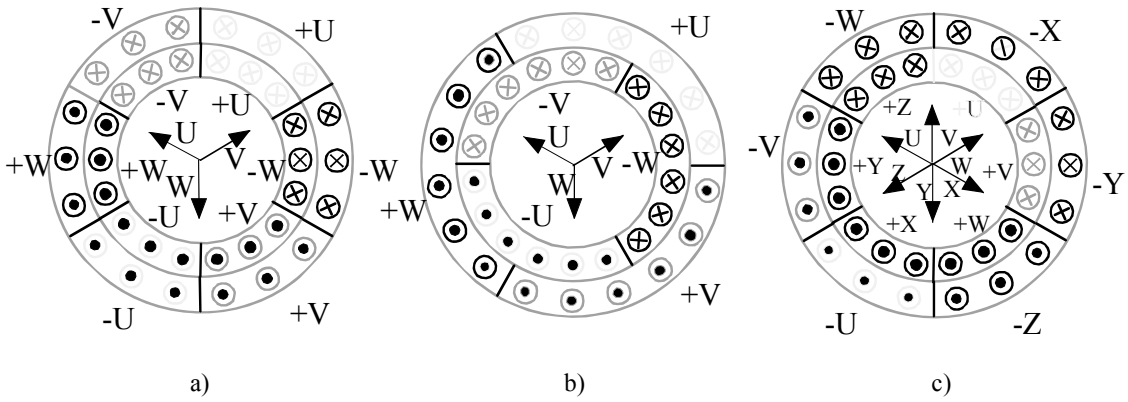

Figure 2.26. Zone formation of double-layer windings, $m = 3$, $p = 1$. a) a normal zone span b) a double zone span, c) the zone distribution of a six-phase radial-symmetric winding with a double zone span. The tails and heads of the arrows correspond to a situation in which there are currents $I_U = -2I_V = -2I_W$ flowing in the windings. The winding in Fig. 2.26a corresponds to a single-layer winding, which is obtained by unifying the winding layers by removing the insulation layer between the layers.

The single-layer windings and double-layer windings with double-width zones form m coil groups per pole pair. Double-layer windings with a normal zone span form $2m$ coil groups per pole pair. The total numbers of coil groups are thus pm and $2pm$ respectively. Table 2.5 lists some of the core parameters of phase windings.

Table 2.5. Phase winding parameters

Winding	**Number of coils** z_c	**Number of groups of coil**	**Average zone span**	**Average zone angle** α_{zav}
Single-layer	$Q/2$	pm	τ_p/m	π/m
Double-layer, normal zone span	Q	$2pm$	τ_p/m	π/m
Double-layer, double zone span	Q	pm	$2\tau_p/m$	$2\pi/m$

2.10 Symmetry Conditions

A winding is said to be symmetrical, if it, when fed from a symmetrical supply, creates a rotating magnetic field. Both of the following symmetry conditions must be fulfilled.

a) *The first condition of symmetry*: Normally, the number of coils per phase winding has to be an integer:

$$\text{For single-layer windings: } \frac{Q}{2m} = pq \in \mathbf{N}. \tag{2.72}$$

$$\text{For double-layer windings: } \frac{Q}{m} = 2pq \in \mathbf{N}. \tag{2.73}$$

The first condition is met easier by double-layer windings than by single-layer windings, thanks to a wider range of alternative constructions.

b) *The second condition of symmetry*: In poly-phase machines, the angle α_{ph} between the phase windings has to be an integral multiple of the angle α_z. Therefore for normal systems, we can write

$$\frac{\alpha_{\mathrm{ph}}}{\alpha_{\mathrm{z}}} = \frac{2\pi Q}{m 2\pi t} = \frac{Q}{mt} \in \mathbf{N} \ , \tag{2.74}$$

and for reduced systems

$$\frac{\alpha_{\mathrm{ph}}}{\alpha_{\mathrm{z}}} = \frac{\pi Q}{m 2\pi t} = \frac{Q}{2mt} \in \mathbf{N} \ . \tag{2.75}$$

Let us now consider how the symmetry conditions are met with integral slot windings. The first condition is always met, since p and q are integers. The number of slots in integral slot windings is $Q = 2pqm$. Now the largest common divider t of Q and p is always p. When we substitute $p = t$ to the second symmetry condition, we can see that it is always met, since

$$\frac{Q}{mt} = \frac{Q}{mp} = 2q \in \mathbf{N} \ . \tag{2.76}$$

Integral slot windings are thus symmetrical. Because $t = p$, also $\alpha_{\mathrm{u}} = \alpha_{\mathrm{z}}$, and hence the numbering of the voltage phasor diagram of the integral slot winding is always consecutive, as can be seen for instance in Figures 2.10 and 2.18.

Symmetrical Fractional Slot Windings

Fractional slot windings are not necessarily symmetrical. A successful fulfilment of symmetry requirements starts with the correct selection of the initial parameters of the winding. First, we have to select q (slots per pole and phase) so that the fraction presenting the number of slots

$$q = \frac{z}{n} \tag{2.77}$$

is indivisible. Here the denominator n is a quantity typical of fractional slot windings.

a) *The first condition of symmetry*: For single-layer windings (Eq. 2.72), it is required that in the equation

$$\frac{Q}{2m} = pq = p\frac{z}{n}, \qquad \frac{p}{n} \in \mathbf{N}. \tag{2.78}$$

Here z and n constitute an indivisible fraction, and thus <u>p and n have to be evenly divisible</u>. We see that when designing a winding, with the pole pair number p usually as an initial condition, we can select only certain integer values for n. Correspondingly, for double-layer windings (Eq. 2.73), the first condition of symmetry requires that in the equation

$$\frac{Q}{m} = 2pq = 2p\frac{z}{n}, \qquad \frac{2p}{n} \in \mathbf{N}. \tag{2.79}$$

When comparing Eq. (2.78) with Eq. (2.79), we can see that we achieve a wider range of alternative solutions for fractional slot windings by applying a double-layer winding than a single-layer winding. For instance for a two-pole machine $p = 1$, a single-layer winding can be constructed only when $n = 1$, which leads to an integral slot winding. On the other hand, a fractional slot winding, for which $n = 2$ and $p = 1$, can be constructed as a double-layer winding.

b) *The second condition of symmetry*: To meet the second condition of symmetry (Eq. 2.74), the largest common divider t of Q and n has to be defined. This divider can be determined from the following equation:

$$Q = 2pqm = 2mz\frac{p}{n} \text{ and } p = n\frac{p}{n}.$$

According to Eq. (2.78), $p/n \in \mathbf{N}$, and thus this ratio is a divider of both Q and p. Because z is indivisible by n, the other dividers of Q and p can be included only in the figures $2m$ and n. These dividers are denoted generally with c, and thus

$$t = c\frac{p}{n}. \tag{2.80}$$

Now the second condition of symmetry can be rewritten for normal poly-phase windings in a form that is in harmony with Eq. (2.74)

$$\frac{Q}{mt} = \frac{2mz\dfrac{p}{n}}{mc\dfrac{p}{n}} = \frac{2z}{c} \in \mathbf{N}\ . \tag{2.81}$$

The divider c of n cannot be a divider of z. The only possible values for c are $c = 1$ or $c = 2$.

For normal poly-phase systems, m is an odd integer. For reduced poly-phase systems, according to Eq. (2.75), it is written

$$\frac{Q}{2mt} = \frac{2mz\dfrac{p}{n}}{2mc\dfrac{p}{n}} = \frac{z}{c} \in \mathbf{N}\ . \tag{2.82}$$

For c, this allows only the value $c = 1$.

As shown in Table 2.4, for normal poly-phase windings, the phase number m has to be an odd integer. The divider $c = 2$ of $2m$ and n cannot be a divider of m. For reduced poly-phase systems, m is an even integer, and thus the only possibility is $c = 1$. The second condition of symmetry can now be written simply in the form: n and m cannot have a common divider $n/m \notin \mathbf{N}$. If $m = 3$, n cannot be divisible by three, and the second condition of symmetry reads:

$$\frac{n}{3} \notin \mathbf{N}. \tag{2.83}$$

The conditions (2.78) and (2.83) automatically determine that if p includes only the figure three as its factor ($p = 3, 9, 27, ...$), a single-layer fractional slot winding cannot be constructed at all.

Table 2.6 lists the symmetry conditions of fractional slot windings.

Table 2.6. Conditions of symmetry for fractional slot windings.

Number of slots per pole and phase $q = z/n$, where z and n cannot be mutually divisible

Type of winding, number of phases	Condition of symmetry
Single-layer windings	$p/n \in \mathbf{N}$
Double-layer windings	$2p/n \in \mathbf{N}$
Two-phase $m = 2$	$n/m \notin \mathbf{N} \rightarrow n/2 \notin \mathbf{N}$
Three-phase $m = 3$	$n/m \notin \mathbf{N} \rightarrow n/3 \notin \mathbf{N}$

As shown, it is not always possible to construct a symmetrical fractional slot winding for certain numbers of pole pairs. However, if some of the slots are left without a winding, a fractional slot winding can be carried out. In practice, only three phase windings are realized with empty slots.

Free slots Q_o have to be distributed on the periphery of the machine so that the phase windings become symmetrical. The number of free slots has thus to be divisible by three, and the angle between the corresponding free slots has to be 120°. The first condition of symmetry is now written as:

$$\frac{Q - Q_o}{6} \in \mathbf{N}. \tag{2.84}$$

The second condition of symmetry is

$$\frac{Q}{3t} \in \mathbf{N}. \tag{2.85}$$

Furthermore, it is also required that

$$\frac{Q_o}{3} \in \mathbf{N}_{odd}. \tag{2.86}$$

Usually, the number of free slots is selected to be three, because this enables the construction of a winding, but does not leave a considerable amount of the volume of the machine without utilization. For normal zone-width windings with free slots, the average number of slots of a coil group is obtained from the equation

$$Q_{av} = \frac{Q - Q_o}{2pm} = \frac{Q}{2pm} - \frac{Q_o}{2pm} = q - \frac{Q_o}{2pm}. \tag{2.87}$$

2.11 Base Windings

It was shown previously that in fractional slot windings, a certain coil side of a phase winding occurs at the same position with the air gap flux always after $p' = p/t$ pole pairs, if the largest common divider t of Q and p is larger than one. In that case, there are t electrically equal slot sequences containing Q' slots in the armature, each of which includes a single layer of the voltage phasor diagram. Now it is worth considering whether it is possible to connect a system of t equal sequences of slots containing a winding as t equal independent winding sections. This is possible when all the slots Q' of the slot sequence of all t electrically equal slot groups meet the first condition of symmetry. The second condition of symmetry does not have to be shown.

If Q'/m is an even number, both a single-layer and a double-layer winding can be constructed in Q' slots. If Q'/m is an odd number, only a double-layer winding is possible in Q' slots. When constructing a single-layer winding, q has to be an integer. Thus, two slot pitches of t with $2Q'$ slots altogether are required for a smallest independent symmetrical single-layer winding. The smallest independent symmetrical section of a winding is called a base winding. When a winding consists of several base windings, the current and voltage of which are due to geometrical reasons always of the same phase and magnitude, it is possible to connect these basic windings in series and in parallel to form a complete winding. Depending on the number of Q'/m, that is, whether it is an even or odd number, the windings are defined either as first- or second-grade windings.

Table 2.7 lists some of the parameters of base windings.

Table 2.7. Some parameters of fractional slot base windings.

	Base winding of first grade	**Base winding of second grade**	
Parameter q	$q = z/n$		
Denominator n	$n \in \mathbf{N}_{\text{odd}}$	$n \in \mathbf{N}_{\text{even}}$	
Parameter Q'/m	$\frac{Q'}{m} \in \mathbf{N}_{\text{even}}$	$\frac{Q'}{m} \in \mathbf{N}_{\text{odd}}$	
Parameter Q/tm	$\frac{Q}{tm} \in \mathbf{N}_{\text{even}}$	$\frac{Q}{tm} \in \mathbf{N}_{\text{odd}}$	
Divider t, the largest common divider of Q and p	$t = \frac{p}{n}$	$t = \frac{2p}{n}$	
Slot angle α_u expressed with voltage phasor angle α_z	$\alpha_u = n\alpha_z = n\frac{2\pi}{Q}t$	$\alpha_u = \frac{n}{2}\alpha_z = n\frac{\pi}{Q}t$	
Type of winding	single-layer windings double-layer windings	single-layer windings	double-layer windings
Number of slots Q^* of a base winding	$Q^* = \frac{Q}{t}$	$Q^* = 2\frac{Q}{t}$	$Q^* = \frac{Q}{t}$
Number of pole pairs p^* of a base winding	$p^* = \frac{p}{t} = n$	$p^* = 2\frac{p}{t} = n$	$p^* = \frac{p}{t} = \frac{n}{2}$
Number of layers t^* in a voltage phasor diagram for a base winding	$t^* = 1$	$t^* = 2$	$t^* = 1$

The asterix * indicates the values of the base winding.

2.11.1 First-Grade Fractional Slot Base Windings

In first-grade base windings,

$$\frac{Q'}{m} = \frac{Q}{mt} \in \mathbf{N}_{\text{even}}. \tag{2.88}$$

There are Q^* slots in a first-grade base winding, and the following is valid for the parameters of the winding:

$$Q^* = \frac{Q}{t}, p^* = \frac{p}{t} = n, t^* = 1. \tag{2.89}$$

The both conditions of symmetry (2.72)–(2.75) are met under these conditions.

2.11.2 Second-Grade Fractional Slot Base Windings

A precondition of the second-grade base windings is that

$$\frac{Q'}{m} = \frac{Q}{mt} \in \mathbf{N}_{\text{odd}} . \tag{2.90}$$

According to Eqs. (2.81) and (2.82), Eq. (2.90) is valid for normal poly-phase windings, when $c = 2$ only for the even values of n. Thus we obtain $t = 2p/n$ and $\alpha_u = n\alpha_z/2$. The first condition of symmetry is met with the base windings of the second grade only when $Q^* = 2Q'$. Only now we obtain

$$\frac{Q^*}{2m} = \frac{Q'}{m} = \frac{Q}{mt} \in \mathbf{N} . \tag{2.91}$$

The second-grade single-layer base winding comprises thus two consequent t^{th} parts of a total winding. Their parameters are written as

$$Q^* = 2\frac{Q}{t}, p^* = 2\frac{p}{t} = n, t^* = 2 . \tag{2.92}$$

With these values, also the second condition of symmetry is met, since

$$\frac{Q^*}{mt^*} = \frac{2Q'}{2m} = \frac{Q}{mt} \in \mathbf{N} . \tag{2.93}$$

The second-grade double-layer base winding meets the first condition of symmetry immediately when the number of slots is $Q^* = Q'$. Hence

$$\frac{Q^*}{m} = \frac{Q'}{m} = \frac{Q}{mt} \in \mathbf{N} . \tag{2.94}$$

The parameters are now

$$Q^* = \frac{Q}{t}, p^* = \frac{p}{t} = \frac{n}{2}, t^* = 1 . \tag{2.95}$$

The second condition of symmetry is now also met.

2.11.3 Integral Slot Base Windings

For integral slot windings, $t = p$. Hence, we obtain for normal poly-phase systems

$$\frac{Q}{mt} = \frac{Q}{mp} = 2q \in \mathbf{N}_{\text{even}} . \tag{2.96}$$

For a base winding of the first grade, we may write

$$Q^* = \frac{Q}{p},\ p^* = \frac{p}{p} = 1,\ t^* = 1. \tag{2.97}$$

Since also the integral slot windings of reduced poly-phase systems form base windings of the first grade, we can see that all integral slot windings are of the first grade, and that integral slot base windings comprise only a single pole pair. The design of integral slot windings is therefore fairly easy. As we can see in Fig. 2.17, the winding construction is repeated without changes always after one pole pair. Thus, to create a complete integral slot winding, we connect a sufficient number of base windings with a single pole pair either in series or in parallel.

EXAMPLE 2.16: Create a voltage phasor diagram of a single-layer integral slot winding, for which $Q = 36$, $p = 2$, $m = 3$.

SOLUTION: The number of slots per pole and phase is

$$q = \frac{Q}{2pm} = 3.$$

A zone distribution, Fig. 2.27, and a voltage phasor diagram, Fig. 2.28 are constructed for the winding.

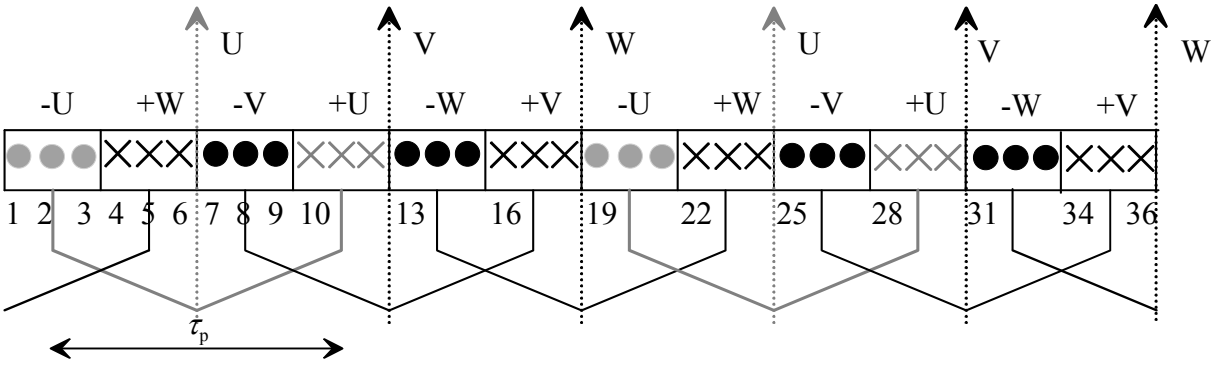

Figure 2.27. Zone distribution for a single-layer winding. $Q = 36$, $p = 2$, $m = 3$, $q = 3$.

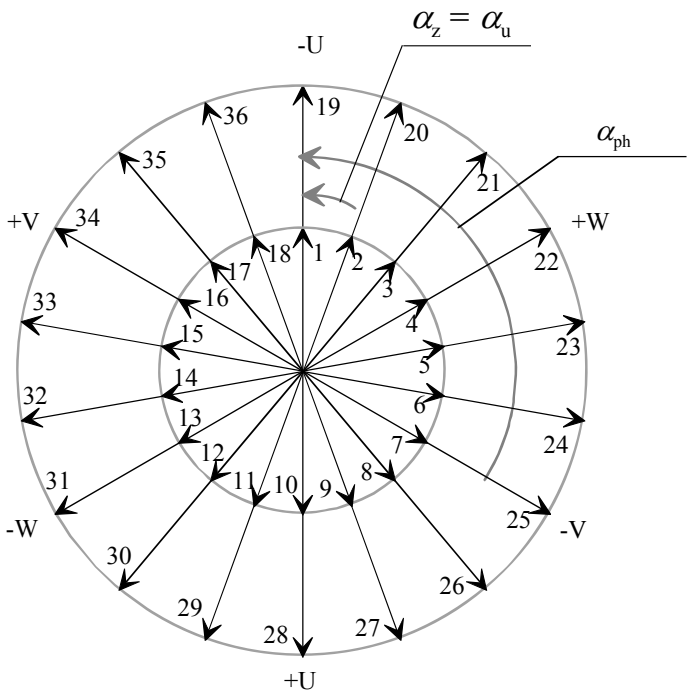

Figure 2.28. Complete voltage phasor diagram for a single-layer winding. $p = 2$, $m = 3$, $Q = 36$, $q = 3$, $t = 2$, $Q' = 18$, $\alpha_z = \alpha_u = 20°$. The second layer of the voltage phasor diagram repeats the first layer and it may, hence, be omitted. The base winding length is 18 slots.

A double-layer integral slot winding is now easily constructed by selecting different phasors of the voltage phasor diagram of Fig. 2.28 for instance for the upper layer. This way, we can immediately calculate the influence of different short-pitchings. The voltage phasor diagram of Fig. 2.28 is applicable to the definition of the winding factors of the short-pitched coils of Fig. 2.15. Only the zones labelled in the figure will change place. Figure 2.28 is directly applicable to a full-pitch winding of Fig. 2.14.

2.12 Fractional Slot Windings

2.12.1 Single-Layer Fractional Slot Windings

Fractional slot windings with extremely small fractions are popular in brushless DC machines and permanent magnet synchronous machines (PMSM). Machines operating with sinusoidal voltages and currents are regarded as synchronous machines even though their air gap flux density might be rectangular. Figure 2.29 depicts the differences between single-layer and double-layer windings in a case where the permanent magnet rotor has four poles and $q = ½$.

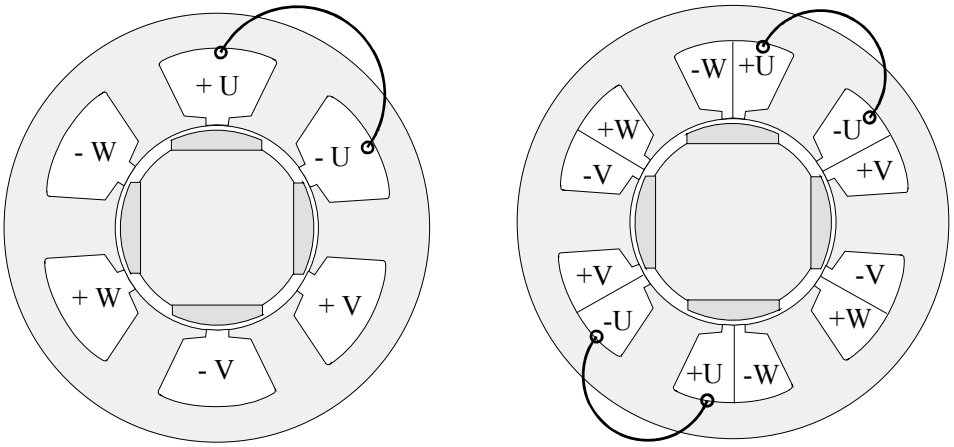

Figure 2.29. Comparison of a single-layer and a double-layer fractional slot winding with concentrated coils. $Q_s = 6$, $m = 3$, $p = 2$, $q = ½$.

When the number of slots per pole and phase q of a fractional slot machine is larger than one, the coil groups of the winding have to be of the desired slot number q in average. In principle, the zone distribution of the single-layer fractional slot windings is carried out either based on the voltage phasor diagram or the zone diagram. The use of a voltage phasor diagram has often proved to lead to an uneconomical distribution of coil groups, and therefore it is usually advisable to apply a zone diagram in the zone distribution. The average slot number per pole and per phase of a fractional slot winding is hence q, which is a fraction that gives the average number of slots per pole and phase q_{av}. This kind of an average number of slots can naturally be realized only by varying the number of slots in different zones. The number of slots in a single zone is denoted by q_k. Now

$$q_k \neq q_{av} = q \notin \mathbf{N}. \tag{2.98}$$

q_{av} has thus to be an average of the different values of q_k. Now we write

$$q = g + \frac{z'}{n}, \tag{2.99}$$

where g is an integer, and the quotient is indivisible so that $z' < n$. Now we have an average number of slots per pole and phase $q = q_{av}$, when the width of z zones in n coil groups is set $g + 1$ and the width of $n - z$ zones is g.

$$q_{av} = \frac{1}{n}\sum_{k=1}^{n} q_k = \frac{z'(g+1) + (n-z')g}{n} = g + \frac{z'}{n} = q. \tag{2.100}$$

The divergences from a totally symmetrical winding are at smallest when the same number of slots per pole and phase occurs in consequent coil groups as seldom as possible. The best fractional slot winding is found with $n = 2$, when the number of slots per pole and phase varies constantly when travelling from one zone to another. To fulfil Eq. (2.100), at least n groups of coil are required. Now we obtain the required number of coils

$$q_{av} nm = qp * m = \frac{Q*}{2}. \tag{2.101}$$

This number corresponds to the size of a single-layer base winding. Now we have shown again that a base winding is the smallest independent winding for single-layer windings. When the second

condition of symmetry for fractional slot windings is considered, it makes no difference how the windings are distributed in the slots (n zones, q_k coil sides in each), if only the desired average q_{av} is reached (e.g. 1 + 2 + 1 + 1 + 2 gives an average of $1\ ^2/_5$). The nm coil groups of a base winding have to be distributed to m phase windings so that each phase gets n single values of q_k (a local number of slots), in the same order in each phase. The coil numbers of consequent coil groups run through the single values of q_k n times in m equal cycles. This way, a cycle of coil groups is generated.

The first column of Table 2.8 shows m consequently numbered cycles of coil groups. The second column consists of nm coil groups in running order. The third column lists n single values of q_k m times in running order. Because the consequent coil groups belong to consequent phases, we get a corresponding running phase cycle in the fourth column. During a single cycle, the adjacent, fifth column goes through all the phases U, V, W, … m of the machine. The sixth column repeats the numbers of coil groups.

Table 2.8. Order of coil groups for symmetrical single-layer fractional slot windings.

Cycle of coil groups 1…m	Number of coil group. This column runs m times from 1 to n (the divider of the fraction $q = z/n$)	Local number of slots per pole and phase (equals local number of slots per pole and phase q_k)	Phase cycle, All the phases are introduced once	Phases from 1 to m (for a three-phase system we have U, V, W)	Number of coil group
1	1	Q_1	1	U	1
1	2	Q_2	1	V	2
1	3	Q_3	1	W	3
1	|	|	1	|	|
1	K	q_k	1	m	m
1	|	|	2	U	m+1
1	|	|	2	V	m+2
1	|	|	2	W	m+3
1	N	q_n	2	|	|
2	n+1	Q_1	2	|	|
2	n+2	|	2	|	|
2	|	|		|	|
2	$n+k$	q_k		|	|
	|	|		|	|
	Dn	q_n		|	|
d+1	dn+1	Q_1	c	|	|
	|	|	c	|	|
	|	|	C	m	Cm
	$dn+k$	q_k	c+1	U	cm+1
	|	|		V	|
	|	|		W	|
m	(m-1)n+k	q_k		|	|
m	|	|		|	|
m	|	|		|	|
m	|	|		|	|
m	|	|		|	|
m	mn	q_n	N	m	Nm

EXAMPLE 2.17: Compare two single-layer windings, an integral slot winding and a fractional slot winding, having the same number of poles. The parameters for the integral slot winding are: $Q = 36$, $p = 2$, $m = 3$, $q = 3$ and for the single-layer fractional slot winding $Q = 30$, $p = 2$, $m = 3$, $q = 2½$.

SOLUTION: For the fractional slot winding, $q_{\mathrm{av}} = \frac{1}{n}\sum_{k=1}^{n} q_{\mathrm{k}} = \frac{z'(g+1)+(n-z')g}{n} = g + \frac{z'}{n} = q$. We see that in this case $g = 2$, $z' = 1$, $n = 2$. Now, a group of coils with $z' = 1$ is obtained, in which there are $q_1 = g + 1 = 3$ coils, and another $n - z' = 1$ group of coils with $q_2 = g = 2$ coils. As $p = p^* = n = 2$, we have here a base winding with three ($m = 3$) cycles of coil groups of both the coil numbers q_1 and q_2. They occur in $n = 2$ cycles of three phases. In Table 2.9, example of Table 2.8 is applied to Fig. 2.30. For the fractional slot winding $q = z/n = 5/2$.

Table 2.9. Example of Table 2.8 applied to Fig. 2.30. For the fractional slot winding $q = z/n = 5/2$.

Cycle of coil groups	Number of coil group	Number of coils (q_{k})	Phase cycle	Phase	Number of coil group
1	1	$3 = q_1$	1	U	1
1	2 (= n)	$2 = q_2$	1	V	2
2	2+1 = 3	3	1	W	3
2	2+2 = 4	2	2	U	4
3 (= m)	(2+2)+1 = 5	3	2	V	5
3 (= m)	(2+2)+2 = 6 = nm = 2·3	2	2	W	6 = nm

The above table can be presented simply as:

q_{k}	3	2	3	2	3	2
phase	U	V	W	U	V	W

Each phase is comprised of a single coil group with two coils, and one coil group with three coils. Figure 2.30 compares the above integral slot winding and a fractional slot winding.

Fractional slot windings create more harmonics than integral slot windings. By dividing the ordinal number ν of the harmonics of a fractional slot winding by the number of pole pairs p^*, we obtain

$$\nu' = \frac{\nu}{p^*}. \tag{2.102}$$

In integral slot windings, such relative ordinal numbers of the harmonics are the following odd integers: $\nu' = 1, 3, 5, 7, 9, \ldots$ For fractional slot windings, when $\nu = 1, 2, 3, 4, 5, \ldots$ the relative ordinal number gets the values $\nu' = 1/p^*$, $\nu' = 2/p^*$, $\nu' = 3/p^*$, ... in other words, values for which $\nu' < 1$; $\nu' \notin \mathbf{N}$ and $\nu' \in \mathbf{N}_{\mathrm{even}}$. The lowest harmonic created by an integral slot winding is the fundamental ($\nu' = 1$), but a fractional slot winding can produce also subharmonics ($\nu' < 1$). There occur also harmonics, the ordinal number of which is a fraction or an even integer. These harmonics cause additional forces, unintended torques and losses. These additional harmonics are the stronger, the greater is the zone variation, in other words, the divergence of the current linkage distribution from the respective distribution of an integral slot winding. In poly-phase windings, not all the integer harmonics are present. For instance, of the spectrum of three-phase windings, those harmonics are absent, the ordinal number of which is divisible by three, because $\alpha_{\mathrm{str},\nu} = \alpha_{\mathrm{str},1} = \nu 360°/m = \nu 120°$, and thus, because of the displacement angle of the phase windings $\alpha_{\mathrm{str}} = 120°$, they do not create a voltage between different phases.

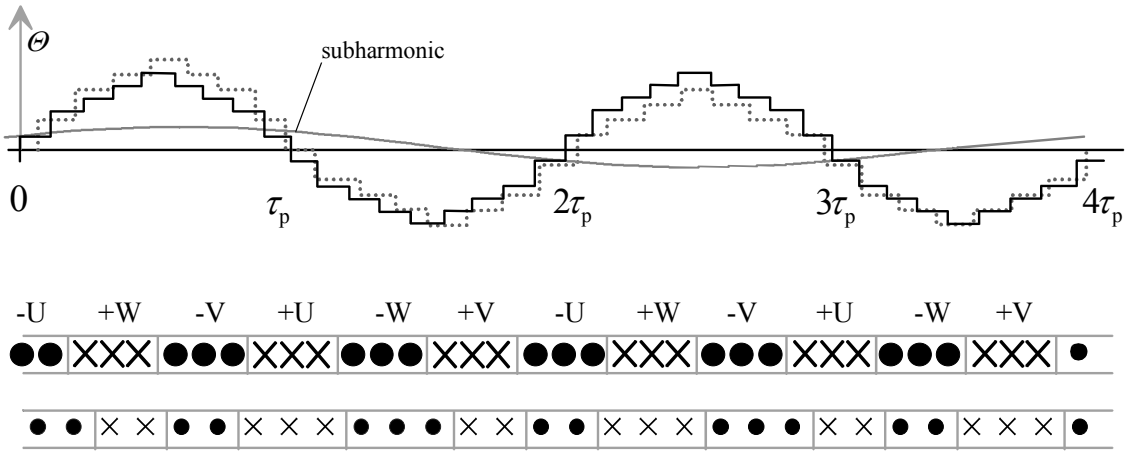

Figure 2.30. Zone diagrams and current linkage distributions of two different windings (q = 3, q = 2½). The integral slot winding is fully symmetrical, but the current linkage distribution of the fractional slot winding (dotted line) differs somewhat from the distribution of the integral slot winding (continuous line). The current linkage clearly contains a sub-harmonic, which has a double pole pitch compared with the fundamental.

EXAMPLE 2.18: Design a single-layer fractional slot winding of the first grade, for which Q = 168, p = 20, m = 3. What is the winding factor of the fundamental?

SOLUTION: The number of slots per pole and phase is

$$q = \frac{168}{2 \cdot 20 \cdot 3} = 1\frac{2}{5},$$

We have a fractional slot winding with n = 5 as a divider. The conditions of symmetry (Table 2.6) $p/n = 20/5 = 4 \in \mathbf{N}$ and $n/3 = 5/3 \notin \mathbf{N}$ are met. According to Table 2.7, when n is an odd number $n = 5 \in \mathbf{N}_{\text{odd}}$, a first-grade fractional slot winding is created. When $t = p/n = 4$, its parameters are

$$Q^* = Q/t = 168/4 = 42, \qquad p^* = n = 5; \qquad t^* = 1.$$

The diagram of coil groups, according to Eq. (2.101), $q_{\text{av}} nm = qp^* m = \dfrac{Q^*}{2}$ consists of $p^*m = nm = 5 \cdot 3 = 15$ groups of coils. The coil groups and the phase order are selected according to Table 2.8

q_k	2	1	2	1	1	2	1	2	1	1	2	1	2	1	1
phase	U	V	W	U	V	W	U	V	W	U	V	W	U	V	W

m = 3 cycles of coil groups with n = 5 consequent numbers of coils q_k, yield a symmetrical distribution of coil groups for single phase coils

q_k	q_1	q_2	q_3	q_4	q_5	q_1	q_2	q_3	q_4	q_5	q_1	q_2	q_3	q_4	q_5
phase U	2			1			1			1			2		
phase V		1			1			2			2			1	
phase W			2			2			1			1			1

In each phase, there is one group of coils q_n. The average number of slots per pole and phase q_{av} of the coil group is written according to Eq. (2.100) using the local q_k value order of phase U

$$\frac{1}{5}\sum_{k=1}^{5} q_{\mathrm{k}} = \frac{1}{5}(2+1+1+1+2) = 1\frac{2}{5} = q\,.$$

We now obtain a coil group diagram according to Fig. 2.31 and a winding phasor diagram according to Fig. 2.32.

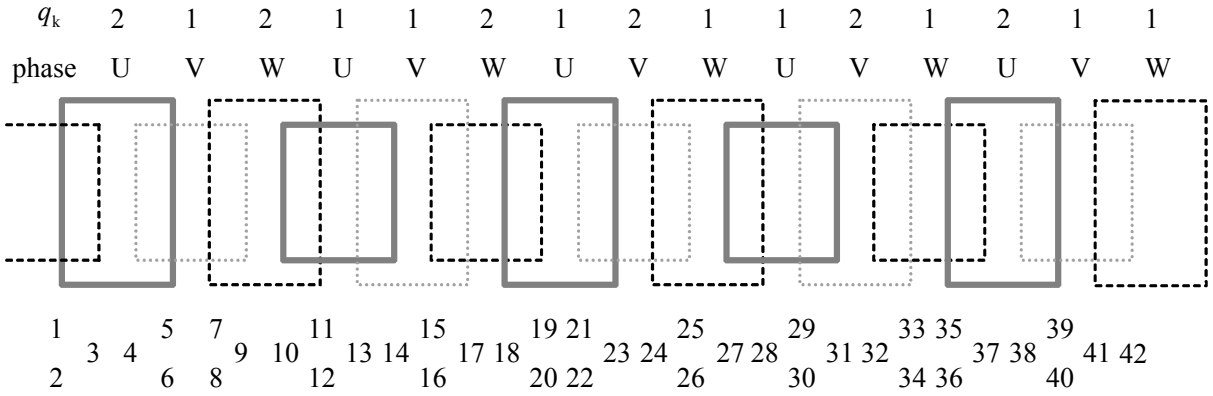

Figure 2.31. Coil group diagram of single-layer fractional slot winding. $Q^* = Q/t = 168/4 = 42$, $p^* = n = 5$; $t^* = 1$.

When calculating the winding factor for the winding, the following parameters are obtained for the voltage phasor diagram:

Number of layers in the voltage phasor diagram	$t^* = 1$
Number of radii	$Q' = Q^*/t^* = 42$
Slot angle	$\alpha_u = 360°p^*/Q^* = 360°\cdot 5/42 = 42^6/_7°$
Phasor angle	$\alpha_z = 360°t^*/Q^* = 360°\cdot 1/42 = 8^4/_7°$
Number of phasors skipped in the numbering	$(p^*/t^*) - 1 = 5 - 1 = 4$.
Number of phasors for one phase	$Z = Q'/m = 42/3 = 14$

The voltage phasor diagram is illustrated in Fig. 2.32.

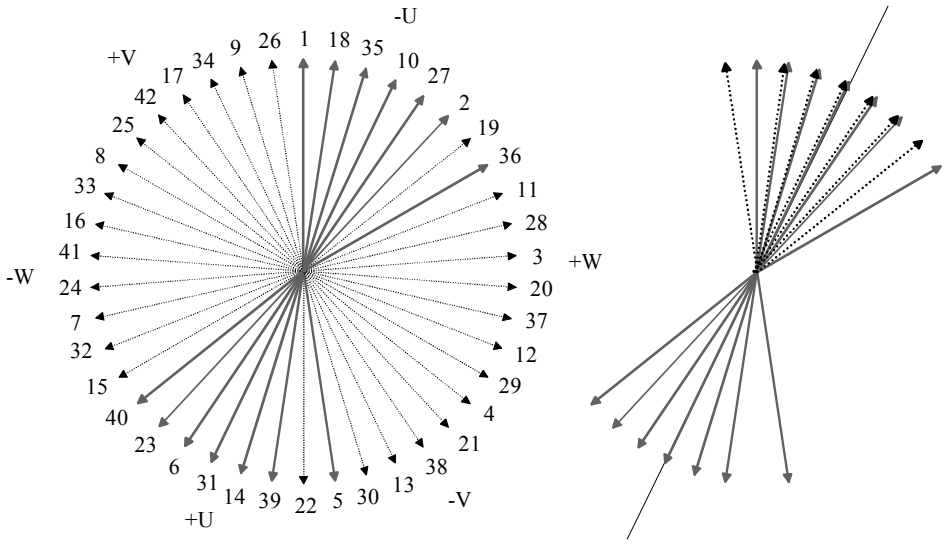

a) b)

Figure 2.32 a) Voltage phasor diagram of a first-grade single-layer base winding. $p^* = 5$, $m = 3$ $Q' = Q^* = 42$, $q = 1^2/_5$, $t^* = 1$, $\alpha_u = 5\alpha_z = 42^6/_7°$, $\alpha_z = 8^4/_7°$ The phasors of the phase U are illustrated with a continuous line, b) the phasors of phase U turned to form a bunch of phasors for the winding factor calculation and the symmetry line.

The winding factor may now be calculated using Eq. (2.16) $k_{wv} = \dfrac{\sin\dfrac{\nu\pi}{2}}{Z}\sum_{\rho=1}^{Z}\cos\alpha_\rho$

The number of phasors $Z = 14$ for one phase and the angle between the phasors in the bunch is $\alpha_z = 8^4/_7°$. The fundamental winding factor is found after having determined the angles α_ρ between the phasors and the symmetry line, hence

$$k_{w1} = \frac{\left(\cos\left(4\cdot 8\,{}^4\!/_7°\right)+\cos\left(3\cdot 8\,{}^4\!/_7°\right)+2\cos\left(2\cdot 8\,{}^4\!/_7°\right)+2\cos\left(8\,{}^4\!/_7°\right)+1\right)\cdot 2}{14} = 0.945$$

As a result of the winding design based on the zone distribution given above, we have a winding in which, according to the voltage phasor diagram, certain coil sides are transferred to the zone of the neighbour phase. By exchanging the phasors 19–36, 5–22, and 8–33 we would also receive a functioning winding but there would be less similar coils than in the winding construction presented above. This kind of a winding would lead to a technically inferior solution, in which undivided and divided coil groups would occur side by side. Such winding solutions are favourable, in which the variation of coil arrangements is kept to a minimum. This way, the best shape of the end winding is achieved.

EXAMPLE 2.19: Is it possible to design a winding with a) $Q = 72$, $p = 5$, $m = 3$, b) $Q = 36$, $p = 7$, $m = 3$, c) $Q = 42$, $p = 3$, $m = 3$?

SOLUTION: a) Using Table 2.6, we check the conditions of symmetry for fractional slot windings. The number of slots per pole and phase is $q = z/n = 72/(2\cdot5\cdot3) = 2^2/_5$. $z = 12$ and $n = 5$, which are not mutually divisible. As $p/n = 5/5 = 1 \in \mathbf{N}$ a single-layer winding should be made and as $n/m = 5/3 \notin \mathbf{N}$ the symmetry conditions are OK. And as $n \in \mathbf{N}_{odd}$ we will consider a first-grade base winding as follows:

$Q^* = 72$, $p^* = 5$, $m = 3$, $q = 2^2/_5$.

q_k	3	2	2	2	3	3	2	2	2	3	3	2	2	2	3
phase	U	V	W	U	V	W	U	V	W	U	V	W	U	V	W

$q_{av} = \frac{1}{5}(3+2+2+2+3) = 2\frac{2}{5} = q$. This is a feasible winding.

SOLUTION: b) The number of slots per pole and phase is $q = z/n = 36/(2\cdot7\cdot3) = {}^6\!/_7$. $z = 6$ and $n = 7$, which are not mutually divisible. As $p/n = 7/7 = 1 \in \mathbf{N}$ a single layer winding can be made, and as $n/m = 7/3 \notin \mathbf{N}$ the symmetry conditions are OK. And as $n \in \mathbf{N}_{odd}$ we will consider a first-grade base winding as follows:

$Q^* = 36$, $p^* = 7$, $m = 3$, $q = {}^6\!/_7$.

q_k	1	1	1	0	1	1	1	1	1	1	0	1	1	1	1	1	1	0	1	1	1
phase	U	V	W	U	V	W	U	V	W	U	V	W	U	V	W	U	V	W	U	V	W

$q_{av} = \frac{1}{7}(1+1+1+0+1+1+1) = \frac{6}{7}$.

The number of slots per pole and phase can thus also be smaller than one $q < 1$. In such a case, there occur coil groups with no coils. These non-existent coil groups are naturally evenly distributed in all phases.

SOLUTION: c) The number of slots per pole and phase is $q = z/n = 42/(2\cdot3\cdot3) = 2\ ^1/_3$. $z = 7$ and $n = 3$, which are mutually divisible, the condition $n/3 \notin \mathbf{N}$ is not met, and the winding is not symmetric. If we, despite the non symmetrical nature, considered a first-grade base winding, we should get a result as follows:

$$Q^* = 42, \qquad p^* = 3, \qquad m = 3, \qquad q = 2\,^1/_3.$$

q_k	2	2	3	2	2	3	2	2	3
phase	U	V	W	U	V	W	U	V	W

We can see that all coil groups with two coils now belong to the phase W. Such a winding is not functional.

EXAMPLE 2.20: Create a winding with $Q = 60$, $p = 8$, $m = 3$.

SOLUTION: The number of slots per pole and phase is $q = 60/(2\cdot8\cdot3) = 1\,^1/_4$. $z = 5$, $n = 4$. The largest common divider of Q and p is $t = 2p/n = 16/4 = 4$. As t also indicates the number of layers in the phasor diagram we get $Q' = Q/t = 60/4 = 15$ which is the number of radii in the phasor diagram in one layer. $Q'/m = 15/3 = 5 \in \mathbf{N}_{odd}$. The conditions of symmetry $p/n = 8/4 = 2 \in \mathbf{N}$ and $n/3 = 4/3 \notin \mathbf{N}$ are met. Because $n = 4 \in \mathbf{N}_{even}$, we have according to the parameters in Table 2.7 a second-grade single-layer fractional slot winding. We get the base winding parameters

$$Q^* = 2Q/t = 2\cdot60/4 = 30, \qquad p^* = n = 4, \qquad t^* = 2$$

The second-grade single-layer fractional slot windings are designed like the first-grade windings. However, the voltage phasor diagram is now doubled. The coil group diagram of the base winding comprises $p^*\cdot m = n\cdot m = 4\cdot3 = 12$ coil groups. The coil group phase diagram is selected as follows:

q_k	2	1	1	1	2	1	1	1	2	1	1	1
phase	U	V	W	U	V	W	U	V	W	U	V	W

A coil group diagram for a base winding corresponding to this case is illustrated in Fig. 2.33.

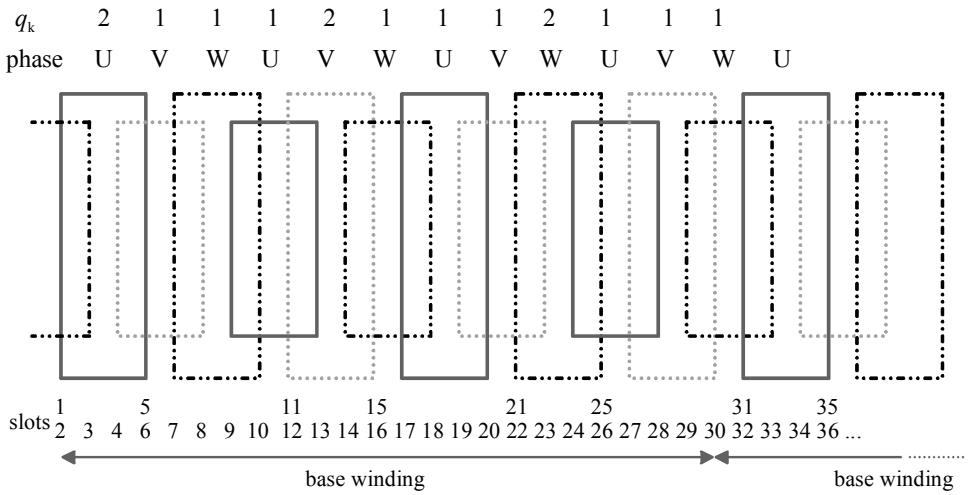

Figure 2.33. Coil group diagram of a base winding for a single-layer fractional slot winding $p = 8$, $m = 3$, $Q = 60$, $q = 1^1/_4$.

A voltage phasor diagram for the base winding is illustrated in Fig. 2.34.

Number of layers in the voltage vector diagram	$t^* = 2$ (second-grade winding)
Number of radii	$Q' = Q^*/t^* = 30/2 = 15$
Slot angle	$\alpha_u = 360° p^*/Q^* = 360° \cdot 4/30 = 48°$
Phasor angle	$\alpha_z = 360° t^*/Q^* = 360° \cdot 2/30 = 24°$
Number of phasors skipped in the numbering	$(p^*/t^*) - 1 = 4/2 - 1 = 1$.

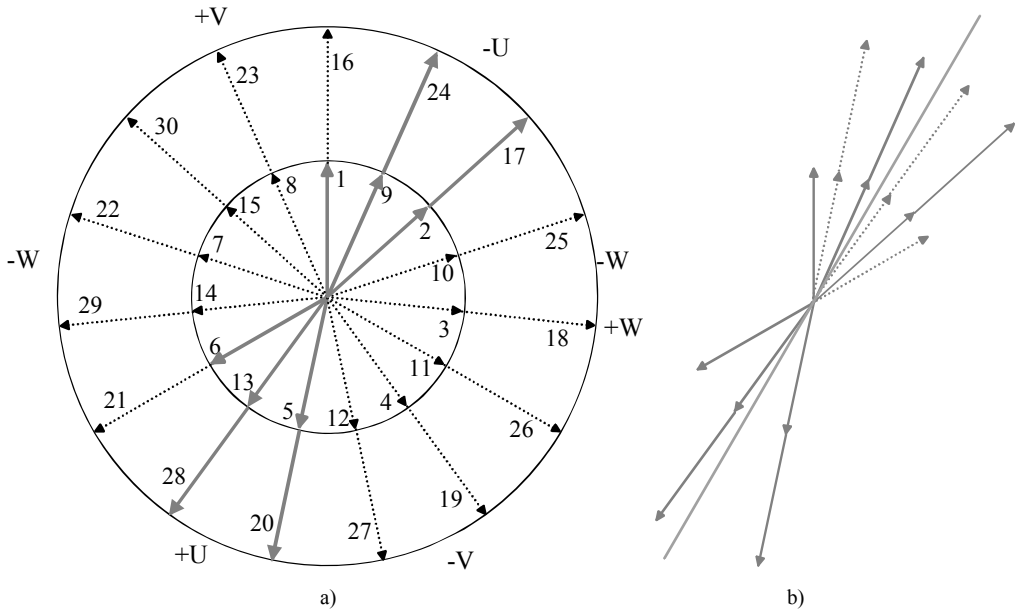

Figure 2.34 a). Voltage phasor diagram of the base winding $p^* = 4$, $Q^* = 30$, $t^* = 2$, $Q' = 15$, $\alpha_u = 2\alpha_z = 48°$ of a single-layer fractional slot winding $p = 12$, $m = 3$, $Q = 60$, $q = 1^1/_4$. The phasors belonging to the phase U are illustrated with a continuous line. b) The phasors of the phase U turned for calculating the winding factor and for illustrating a symmetrical bunch of phasors.

The number of phasors $Z = 10$ for one phase and the angle between the phasors in the bunch is $\alpha_z = 24°$. After having found the angles α_ρ with respect to the symmetry line the fundamental winding factor may be calculated using Eq. (2.16)

$$k_{w1} = \frac{\left(2\cos(6°) + 2\cos(6° + 12°) + \cos(6° + 24°)\right) \cdot 2}{10} = 0.951 .$$

2.12.2 Double-Layer Fractional Slot Windings

In double-layer windings, one of the coil sides of each coil is in the upper layer of the slot, and the other coil side is in the bottom layer. The coils are all of equal span. Consequently, when the positions of the left coil sides are defined, also the right sides will be defined. Here double-layer fractional slot windings differ from single-layer windings. Let us now assume that the left coil sides are positioned in the upper layer. For these coil sides of the upper layer, a voltage phasor diagram of a double-layer winding is valid. Contrary to the voltage phasor diagram illustrated in Fig. 2.34, there is only one layer in the voltage phasor diagram of the double-layer fractional slot winding. Therefore, the design of a symmetrical double-layer fractional slot winding is fairly straightforward

with a voltage phasor diagram of a base winding. Now, symmetrically distributed closed bunches of phasors are composed of the phasors of single phases. This phasor order produces the minimum divergence when compared with the current linkage distribution of the integral slot winding.

First, we investigate first-grade double-layer fractional slot windings. It is possible to divide the phasors of such a winding into bunches of equal size, in other words, into zones of equal width.

EXAMPLE 2.21: Design the winding previously constructed as a single-layer winding $Q = 168$, $p = 20$, $m = 3$, $q = 1^2/_5$ now as a double layer winding.

SOLUTION: We have a fractional slot winding for which the divider $n = 5$. The conditions of symmetry (Table 2.6) $p/n = 20/5 = 4 \in \mathbf{N}$ and $n/3 = 5/3 \notin \mathbf{N}$ are met. According to Table 2.7, if n is an odd number $n = 5 \in \mathbf{N}_{\text{odd}}$, a first-grade fractional slot winding is created. The parameters of the voltage phasor diagram of such a winding are:

Number of layers in the voltage phasor diagram	$t^* = 1$
Number of pole pairs in the base winding	$p^* = 5$
Number of radii	$Q' = Q^*/t^* = 42$
Slot angle	$\alpha_u = 360°p^*/Q^* = 360°\cdot 5/42 = 42^6/_7°$
Phasor angle	$\alpha_z = 360°t^*/Q^* = 360°\cdot 1/42 = 8^4/_7°$
Number of phasors skipped in the numbering	$(p^*/t^*) - 1 = 5 - 1 = 4$.

Since $t^* = 1$, the number of radii Q' is the same as the number of phasors Q^*, and we obtain $Q^*/m = 42/3 = 14$ phasors for each phase, which then are divided into negative Z^- and positive Z^+ phasors. The number of phasors per phase in the first-grade base winding is $Q^*/m = Q/mt \in \mathbf{N}_{\text{even}}$. In normal cases, there is no zone variation, and the phasors are evenly divided into positive and negative phasors. In the example case, the number of phasors of both types is seven, $Z^- = Z^+ = 7$. By employing a normal zone order -U, +W, -V, +U, -W, +V we are able to divide the voltage phasor diagram into zones with seven phasors in each, Fig. 2.35.

When the voltage phasor diagram is ready, the upper layer of the winding is set. The positions of the coil sides in the bottom layer are defined when an appropriate coil span is selected. For fractional slot windings, it is not possible to construct a full-pitch winding, because $q \notin \mathbf{N}$. For a winding in question, the full-pitch coil span y_Q of a full-pitch winding would be y in slot pitches

$$y = y_Q = mq = 3 \cdot 1\frac{2}{5} = 4\frac{1}{5} \notin \mathbf{N},$$

which is not possible in practice because the step has, of course, to be an integer number of slot pitches.

Now the coil span may be decreased by $y_v = 1/5$. The coil span thus becomes an integer, which enables the construction of the winding.

$$y = mq - y_v = 3 \cdot 1\frac{2}{5} - \frac{1}{5} = 4 \in \mathbf{N}.$$

Double-layer fractional slot windings are thus short-pitched windings.

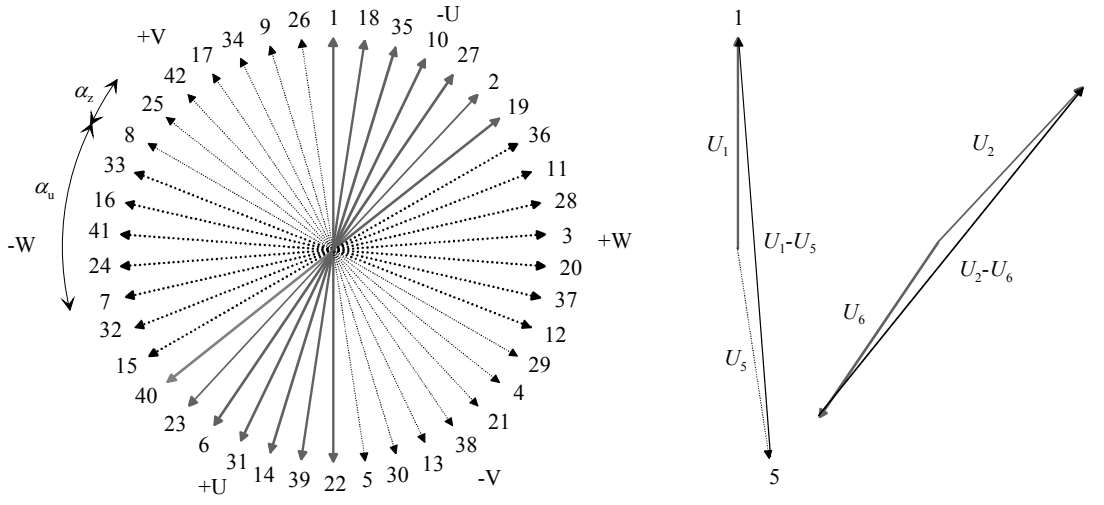

a) b)

Figure 2.35 a) Voltage phasor diagram of a first-grade double-layer base winding $p^* = 5$, $m = 3$, $Q' = Q^* = 42$, $q^* = 1^2/_5$, $t^* = 1$, $\alpha_u = 5\alpha_z = 42^6/_7°$, $\alpha_z = 8^4/_7°$, b) A couple of examples of coil voltages in the phase U.

When constructing a two-layer fractional slot winding, there are two coil sides in each slot. Hence, we have as many coils as slots in the winding. In this example, we first locate the U-phase bottom coil side in slot 1. The other coil side is placed according to the coil span of $y = 4$ at a distance of four slots in the upper part of slot 5. Similarly, coils run from 2 to 6. The coils to be formed are 1–5, 18–22, 35–39, 10–14, 27–31, 2–6, and 19–23. Starting from the +U zone, we have coils 22–26, 39–1, 14–18, 31–35, 6–10, 23–27, and 40–2. Now, six coil groups with one coil in each and four coil groups with two coils in each are created in each phase. The average is

$$q = \frac{1}{10}\left(6 \cdot 1 + 4 \cdot 2\right) = \frac{14}{10} = 1\frac{2}{5}.$$

A section of the base winding of the constructed winding is illustrated in Fig. 2.36.

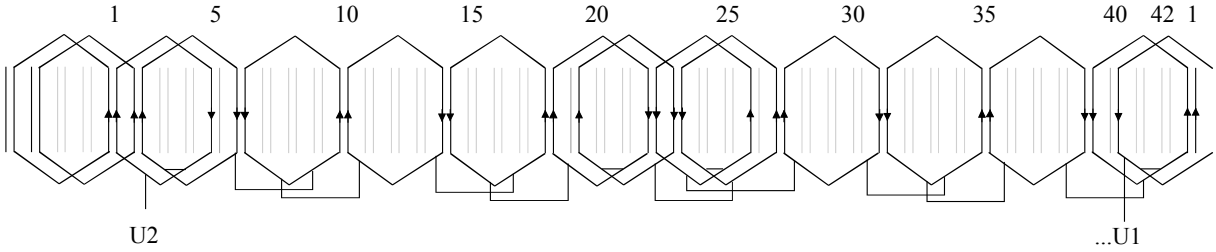

Figure 2.36. Base winding of a fractional slot winding. $p = 20$, $m = 3$, $Q = 168$, $q = 1^2/_5$. The U1 end of the base winding is placed in the slot 40.

Next, a configuration of a second-grade double-layer fractional slot winding is investigated. Because now $Q'/m = Q^*/m = Q/mt \in \mathbf{N}_{\text{odd}}$, a division $Z^- = Z^+$ is not possible. In other words, all the zones of the voltage phasor diagram are not equal. The voltage phasor diagram can nevertheless be constructed so that phasors of neighbour zones are not located inside the zones of each other.

EXAMPLE 2.22: Create a second-grade double-layer fractional slot winding with $Q = 30$, $p = 4$, $m = 3$.

SOLUTION: The number of slots per pole per phase is written

$$q = \frac{30}{2 \cdot 2 \cdot 3} = 2\text{½}.$$

As $n = 2 \in \mathbf{N}_{\text{even}}$, we have a second-grade double-layer fractional slot winding. Because $t = 2p/n = 2$, its parameters are:

$Q^* = Q/t = 30/2 = 15,$
$p^* = n/2 = 2/2 = 1,$
$t^* = 1.$

This winding shows that a base winding of a second-grade double-layer fractional slot winding can only be of the length of one pole pair. The parameters of the voltage phasor diagram are:

Number of layers in the voltage phasor diagram	$t^* = 1 = p^*$
Number of radii	$Q' = Q^*/t^* = 15$
Slot angle	$\alpha_u = 360°p^*/Q^* = 360°/15 = 24°$
Phasor angle	$\alpha_z = 360°t^*/Q^* = 360°/21 = 24°$
Number of phasors skipped in the numbering	$(p^*/t^*) - 1 = 0.$

For each phase, we obtain $Q'/m = Q^*/m = 15/3 = 5$ phasors. This does not allow an equal number of negative and positive phasors. If a natural zone variation is employed, we have to set either $Z^+ = Z^- + 1$ or $Z^+ = Z^- - 1$. In the latter case, we obtain $Z^- = 3$ and $Z^+ = 2$. With the known zone variation, electrical zones are created in the voltage phasor diagram, for which the number of phasors varies: $Z^- = 3$ phasors of zone -U, $Z^+ = 2$ phasors of zone +W, $Z^- = 3$ phasors of zone –V, and so on, Fig. 2.37.

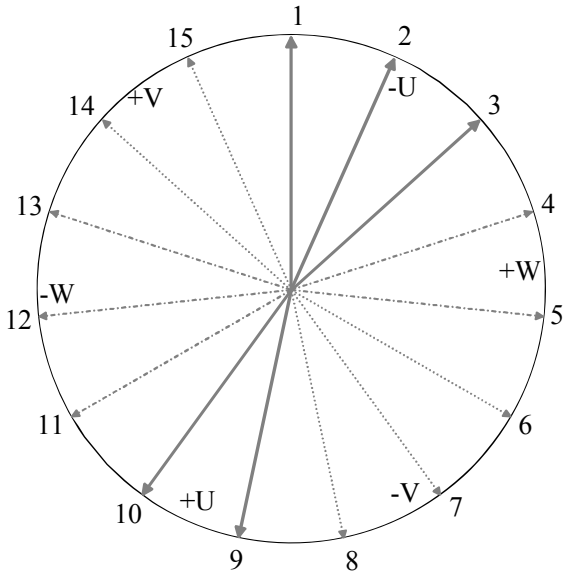

Figure 2.37. Voltage phasor diagram of a second-grade double-layer fractional slot winding. $p^* = 1$, $m = 3$, $q = 2\text{½}$, $Q' = Q^*/t^* = 15$, $\alpha_u = 360°p^*/Q^* = 360°/15 = 24°$, $\alpha_z = 360°t^*/Q^* = 360°/15 = 24°$, $(p^*/t^*) - 1 = 0$.

When the coil span is decreased by $y_v = \text{½}$, the coil span becomes an integer

$$y = mq - y_v = 10\text{½} - \text{½} = 10.$$

The winding diagram of Fig. 2.38 shows that all the positive coil groups consist of three coils, and all the negative coil groups comprise two coils, which yields an average of $q = 2\text{½}$. Since all negative and all positive coil groups are comprised of an equal number of coils, respectively, the

winding can be constructed as a wave winding. A wave is created that passes through the winding three times in one direction and two times in the opposite direction. The waves are connected in series to create a complete phase winding.

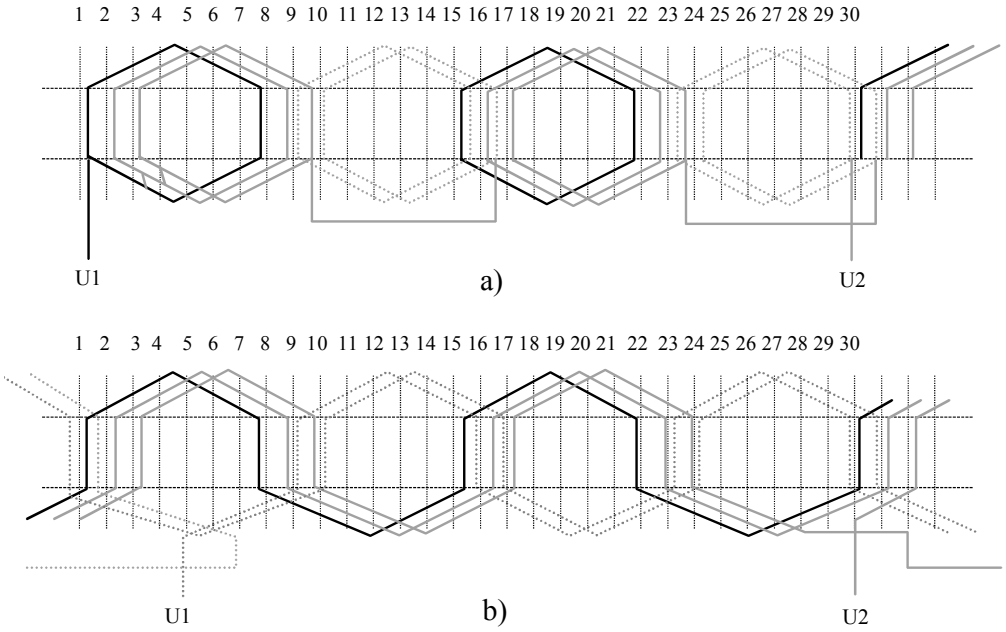

Figure 2.38. Winding diagram of a double-layer fractional slot winding. $p = 2$, $m = 3$, $Q = 30$ $q = 2½$. a) lap winding, b) wave winding. To simplify the illustration, only a single phase is shown.

EXAMPLE 2.23: Create a fractional slot winding for the three phase machine, where the number of slots is 12, and the number of rotor poles is 10, Fig. 2.39.

SOLUTION: The number of slots per pole and phase is $q = 12/(3\cdot 10) = 2/5 = z/n = 0.4$. Hence, $n = 5$. We should thereby find a base winding of the first kind. According to Table 2.6, $p/n \in \mathbf{N}$. In this case $5/5 \in \mathbf{N}$. In a three-phase machine $n/m \notin \mathbf{N} \rightarrow n/3 \notin \mathbf{N}$. Now $5/3 \notin \mathbf{N}$ and the symmetry conditions are met. Let us next consider Table 2.7 parameters. The largest common divider of Q and p is $t = p/n = 5/5 = 1$, $Q/tm = 12/(1\cdot 3) = 4$ which is an even number. The slot angle in the voltage phasor diagram is

$$\alpha_u = n\alpha_z = n\frac{2\pi}{Q}t, \qquad \alpha_u = 5\alpha_z = 5\frac{2\pi}{12}1 = \frac{5\pi}{6}$$

The number slots in the base windings is $Q/t = 12$ and the number of pole pairs in the base winding is $p/t = n = 5$. The winding may be realized either as a single- or double-layer winding, and in this case, a double-layer winding is found. In drawing the voltage phasor diagram, the number of phasors skipped in the numbering is $(p^*/t^*) - 1 = ((p/t)/t^*) - 1 = ((5/1)/1) - 1 = 4$.

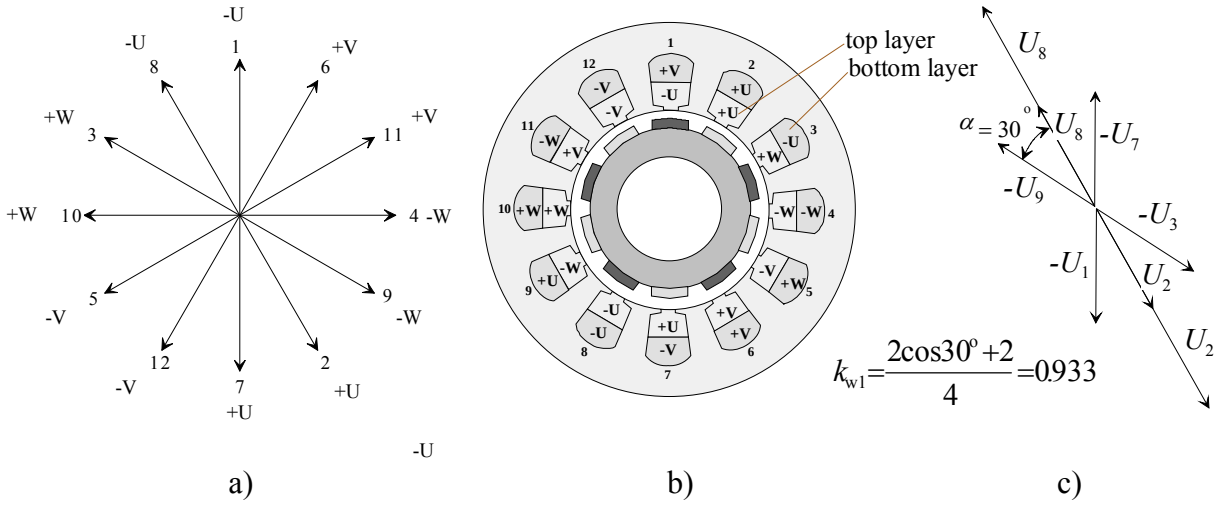

Figure 2.39. a) Phasors of a 12-slot 10-pole machine, b) the double-layer winding of a 12-slot 10-pole machine, c) the phasors of the phase U for the calculation of the winding factor.

First, 12 phasors are drawn (a number of Q', when $Q' = Q^*/t^*$). The phasor number 1 is positioned to point straight upwards, and the next phasor, number 2, is located at an electrical angle of $360 \cdot p/Q$ from the first phasor, in this case $360 \cdot 5/12 = 150$ degrees. The phasor number 3 is, again, located at an angle of 150 degrees from the phasor 2 etc. The first coil 1–2 (–U, +U) will be located on the top layer of the slot 1 and on the bottom layer of the slot 2. The other coil (+U, –U) 2 – 3 will be located on the top layer of the slot 2 and on the bottom layer of the slot 3. The phase coils are set in the order U, –V, W, –U, V, –W. In the example, a single phase zone comprises four slots, and thus a single winding zone includes two positive and two negative slots.

Based on the voltage phasor diagram of 2.39a and the winding construction of 2.39b, the fundamental winding factor of the machine can be solved, Fig. 2.39c. First, the polarity of the coils of phase U in Fig. 2.39b are checked and the respective phasors are drawn. In the slots 1, 2, and 3, there are four coil sides of the phase U in total, and the number of phasors will thus be four. Now, the angles between the phasors and their cosines are calculated. This yields a winding factor of 0.933.

EXAMPLE 2.24: Create a fractional slot winding for the three-phase machine, in which the number of slots is 21, and the number of rotor poles is 22, Fig. 2.40.

SOLUTION: The number of slots per pole and phase is thus only $q = 21/66 = z/n = 7/22 = 0.318$. As $n \in \mathbf{N}_{\text{even}}$, we have a fractional slot winding of the second grade. Although a winding of this kind meets the symmetry conditions, it is not an ideal construction, because in the winding, all the coils of a single phase are located in the same side of the machine. Such a coil system may produce harmful unbalanced magnetic forces in the machine.

Figure 2.40a. 21 phasors are drawn (a number of Q', when $Q' = Q^*/t^*$). The phasor number 1 is placed at the top and the next phasor at the distance of $360 \cdot p/Q$ from it. In this example, the distance is thus $360 \cdot 11/21 = 188.6$ degrees. The phasor number 2 is thus set at an angle of 188.6 degrees from the phasor 1. The procedure is repeated with the phasors 3, 4, ... etc. The phase coils are set in the order –W, U, -V, W, -U, V. Here a single phase consists of seven slots, and therefore we cannot place an equal number of positive and negative coils in one phase. In one phase, there are four positive and three negative slots. Note that we are now generating just the top winding layer, and when also the bottom winding is inserted, we have an equal number of positive and negative coils.

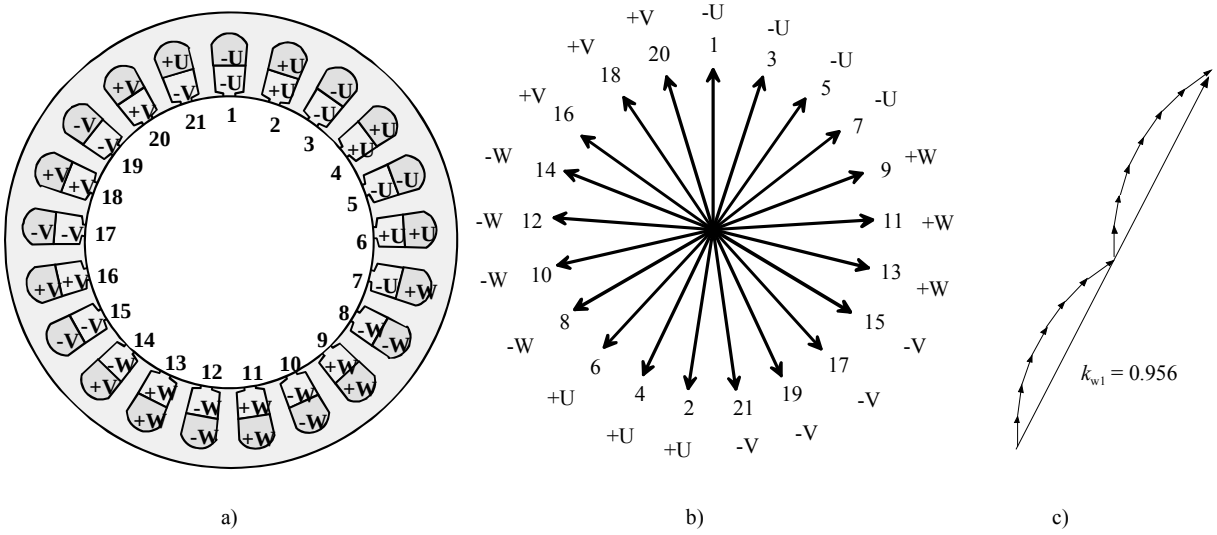

Figure 2.40. a) The winding of a 21-slot 22-pole machine, b) Phasors of a 21-slot 22-pole machine, and c) The phasors of the phase U for the calculation of the winding factor.

Figure 2.40 b. The coils are inserted in the bottom layer of the slots in Fig. 2.40 b) according to the phasors of Fig. 2.40 a). The phasor number 1 of Fig. 2.40 a) is –U, and it is located in the top layer of the slot 1. Correspondingly, the phasor 2, +U, is mounted in the top layer of the slot 2. The bottom winding of the machine repeats the order of the top winding. When the top coil sides are transferred by a distance of one slot forward and the ± sign of each is changed, a suitable bottom layer is obtained. The first coil of the phase U will be located in the bottom of the slot 21 and on the surface of the slot 1, and so on.

Table 2.10 introduces some parameters of double-layer fractional slot windings, when the number of slots $q \leq 0.5$ (Salminen 2004).

Table 2.10 Winding factors k_{w1} of the fundamental and numbers of slots per pole and phase q for double-layer three-phase fractional slot concentrated windings ($q \leq 0.5$). The boldface figures are the highest values in each column. Reproduced by permission of Pia Salminen.

Q_s		Number of poles 2p 4	6	8	10	12	14	16	20	22	24	26
6	k_{w1}	**0.866**	**	**0.866**	0.5	**	0.5	0.866	0.866	0.5	**	0.5
	q	0.5		0.25	0.2		0.143	0.125	0.1	0.091		0.077
9	k_{w1}		**0.866**	*	*	**0.866**	0.617	0.328	0.328	0.617	**0.866**	0.945
	q		0.5	0.375	0.3	0.25	0.214	0.188	0.15	0.136	0.125	0.115
12	k_{w1}			**0.866**	**0.933**	**	**0.933**	0.866	0.5	0.25	**	0.25
	q			0.5	0.4		0.286	0.25	0.2	0.182		0.154
15	k_{w1}				0.866	**	*	*	0.866	0.711	**	0.39
	q				0.5		0.357	0.313	0.25	0.227		0.192
18	k_{w1}					**0.866**	0.902	**0.945**	**0.945**	0.902	**0.866**	0.74
	q					0.5	0.429	0.375	0.3	0.273	0.25	0.231
21	k_{w1}						0.866	0.89	*	*	**	0.89
	q						0.5	0.438	0.35	0.318		0.269
24	k_{w1}							0.866	0.933	**0.949**	**	**0.949**
	q							0.5	0.4	0.364		0.308

* not recommended as single base winding because of unbalanced magnetic pull

** not recommended, because the denominator n ($q = z/n$) is an integral multiple of the number of phases m.

2.13 Single- and Two-Phase Windings

The above three-phase windings are the most common rotating-field windings employed in poly-phase machines. Double- and single-phase windings, windings permitting a varying number of poles, and naturally also commutator windings are common in machine construction. Of commutator AC machines, nowadays only single-phase supplied series-connected commutator machines occur for instance as motors of electric tools. Poly-phase commutator AC machines will eventually disappear as the power electronics enables an easy rotation speed control of different motor types.

Since there is no two-phase supply network, two-phase windings occur mainly as auxiliary and main windings of machines supplied from a single-phase network. In some special cases, for instance small auxiliary automotive drives such as fan drives, two-phase motors are also used in power electronic supply. A two-phase winding can also be constructed on the rotor of low-power slip-ring asynchronous motors. As known, a two-phase system is the simplest possible winding that produces a rotating field, and it is therefore most applicable to rotating-field machines. In a two-phase supply, however, there exist time instants when the current of either of the windings is zero. This means that each of the windings should alone be capable of creating as sinusoidal a supply as possible to achieve low harmonic content in the air gap and low losses in the rotor. This makes the design of high-efficiency two-phase winding machines more demanding than three-phase machines.

The design of a two-phase winding is based on the principles already discussed in the design of three-phase windings. However, we must always bear in mind that in the case of a reduced poly-phase system, when constructing the zone distribution, the signs of the zones do not vary in the way they do in a three-phase system, but the zone distribution will be -U, -V, +U, +V. In a single-phase asynchronous machine, the number of coils of the main winding is usually higher than the number of coils of the auxiliary winding.

EXAMPLE 2.25: Create a 5/6 short-pitched double-layer two-phase winding of a small electrical machine, $Q = 12$, $p = 1$, $m = 2$, $q = 3$.

SOLUTION: The required winding is illustrated in Fig. 2.41, where the rules mentioned above are applied.

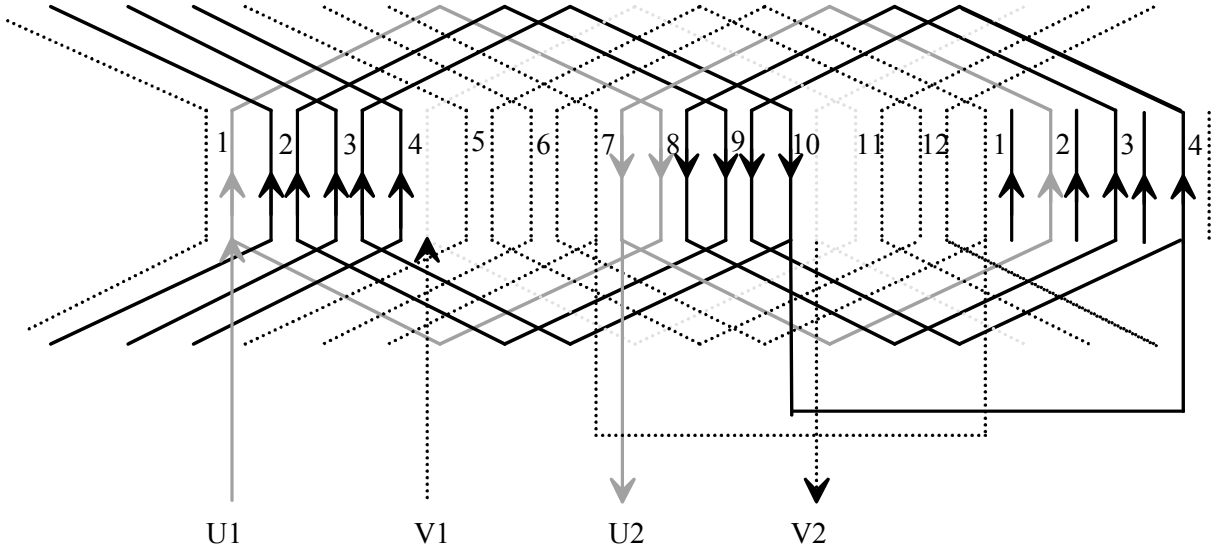

Figure 2.41. Symmetrical 5/6 short-pitched double-layer two-phase winding, $Q = 12$, $p = 1$, $m = 2$, $q = 3$.

When considering a single-phase winding, we must bear in mind that it does not, as a stationary winding, produce a rotating field, but a pulsating field. A pulsating field can be presented as a sum of two fields rotating in opposite directions. The armature reaction of a single-phase machine has thus a field component rotating against the rotor. In synchronous machines, this component can be damped with the damper windings of the rotor. However, the damper winding copper losses are significant. In single-phase squirrel cage induction motors, the rotor also creates extra losses when damping the negative-sequence field.

Also the magnetizing windings of the rotors of non-salient pole machines belong to the group of single-phase windings, as exemplified at the beginning of the chapter. If a single-phase winding is installed on the rotating part of the machine it, of course, creates a rotating field in the air gap of the machine contrary to the pulsating field of a single-phase stator winding.

Large single-phase machines are rare, but for instance in Germany, single-phase synchronous machines are used to feed the supply network of 16 $^2/_3$ Hz electric locomotives. Since there is only one phase in such a machine, there are only two zones per pole pair, and the construction of an integral slot winding is usually relatively simple. In these machines, damper windings have to cancel the negative sequence field. This, however, obviously is problematic because lots of losses are generated in the damper.

The core principle also in designing single-phase windings is to aim at as sinusoidal distribution of the current linkage as possible. This is even more important in the single-phase windings than in the three-phase windings, the current linkage distribution of which is by nature closer to ideal. The current linkage distribution of a single-phase winding can be made to resemble the current linkage distribution of a three-phase winding instantaneously in a position where a current of one phase of a three-phase winding is zero. At that instant, a third of the slots of the machine are in principle currentless. The current linkage distribution of a single-phase machine can best be made to approach a sinusoidal distribution when a third of the slots are left without conductors, and a different number of turns of coil are inserted in each slot. The magnetizing winding of a non-salient pole machine of Fig. 2.3 is illustrated as an example of such a winding.

EXAMPLE 2.26: Create various kinds of zone distributions to approach a sinusoidal current linkage distribution for a single-phase winding with $m = 1$, $p = 1$, $Q = 24$, $q = 12$.

SOLUTION: Figure 2.42 depicts various methods to produce a current linkage waveform with a single-phase winding.

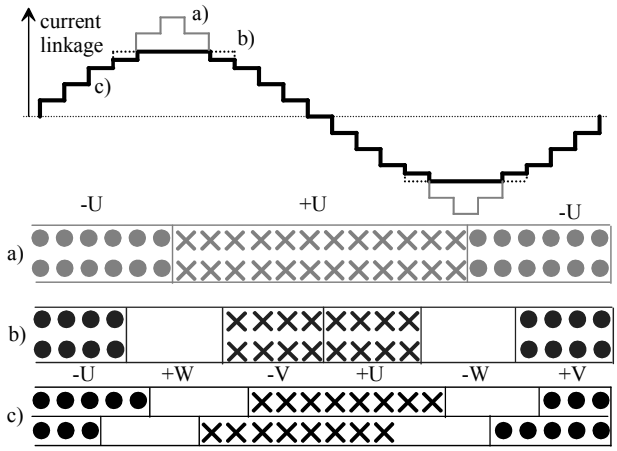

Figure 2.42. Zone diagram of a single-phase winding $p = 1$, $Q = 24$, $q = 12$, and current linkage distributions produced by different zone distributions. a) A single-phase winding covering all slots. b) A $^2/_3$ winding, with the zones of a corresponding three-phase winding. The three phase zones +W and -W are left without conductors. The distribution of

the current linkage is better than in the case a). c) A $^{2}/_{3}$ short-pitched winding, producing a current linkage distribution closer to an ideal (dark stepped line).

2.14 Windings Permitting a Varying Number of Poles

Here, windings permitting a variable pole number refer to such single- or poly-phase windings that can be connected via terminals to a varying number of poles. Windings of this type occur typically in asynchronous machines, when the rotation speed of the machine has to be varied in a certain ratio. The most common example of such machines is a two-speed motor. The most common connection for this kind of an arrangement is a Lindström-Dahlander connection that enables the alteration of the pole number of a three-phase machine in the proportion of 1 to 2. Figure 2.43 illustrates the winding diagram of a single phase of a 24-slot machine. It can be arranged as a double-layer diamond winding, which is a typical Dahlander winding. Now the smaller number of pole pairs is denoted p' and the higher p'', where $p'' = 2p'$. The winding is divided into two sections U_1–U_2 and U_3–U_4, both of which consist of two coil groups with the higher number of poles.

The Dahlander winding is normally realized for the higher pole pair number as a double-layer double zone width winding. The number of coil groups per phase is equal to p'', which is always an even number. Deriving a double-layer integral slot full-pitch (short-pitch or fractional slot Dahlander windings are not possible at all) Dahlander winding starts with creating mp'' negative zones with a double width. All the negative zones –U, -V, -W are located in the top layer and all the positive zones in the bottom layers of slots.

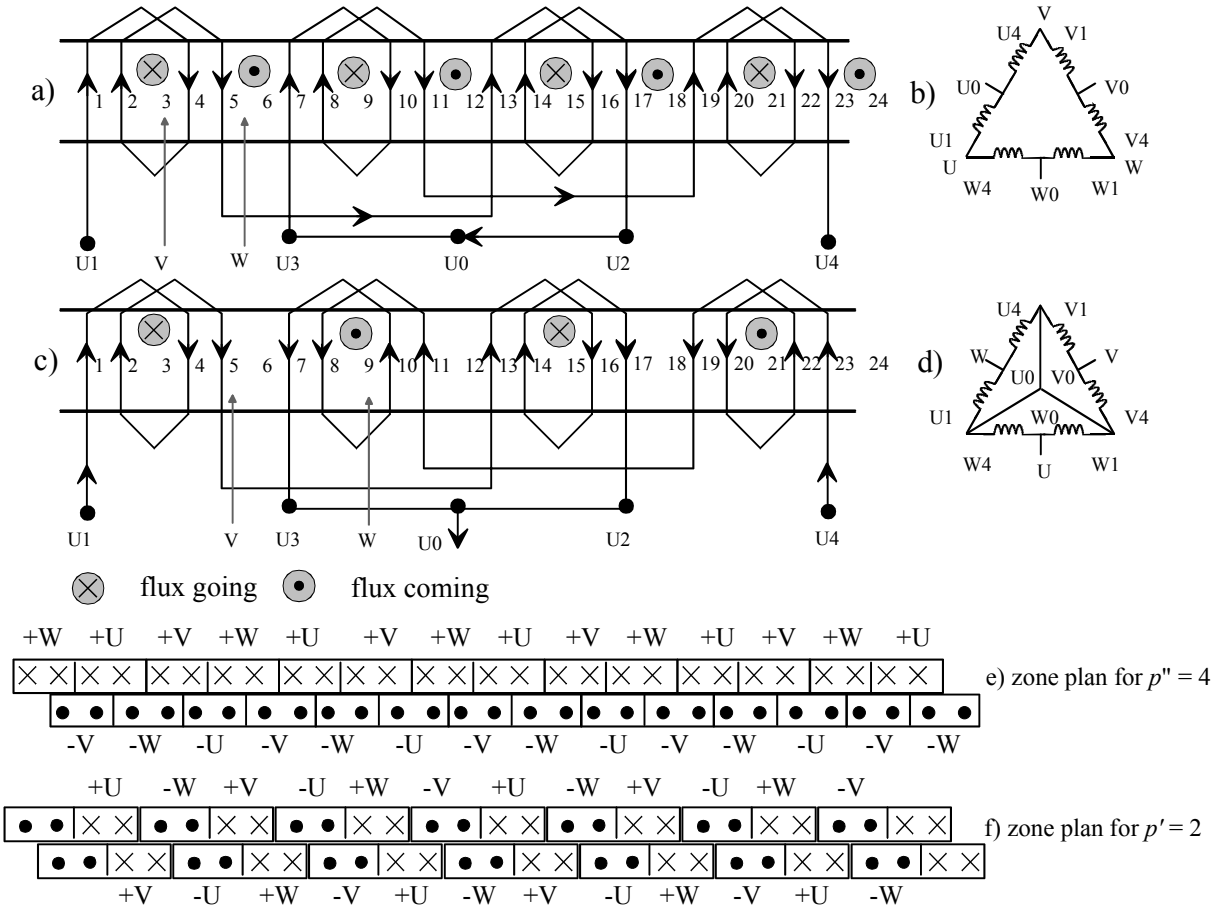

Figure 2.43. Principle of a Dahlander winding. The upper connection a) produces eight poles and the lower c) four poles. The number of poles is shown by the flux arrowheads and tails b) and d) equivalent connections. When also the number of the coil turns of the phase varies inversely proportional to the speed, the winding can be supplied with the same voltage at both speeds. Network connections are U, V, and W. The figure illustrates only a winding of one phase. In Fig. 2.43d between U1 and U4 there is the connection W, between W4 and W1 there is U, and between V1 and V4 there is V to keep the same direction of rotation, e) and f) zone plans for p'' = 4 and p' = 2.

The phase U is followed by the winding V at a distance of 120°. For a number of pole pairs p'' = 4, the winding V has to be placed at a distance

$$\frac{Q}{3p''}\tau_{\mathrm{u}} = \frac{24}{3\cdot 4}\tau_{\mathrm{u}} = 2\tau_{\mathrm{u}}$$

from the winding U. The winding V starts thus from the slot 3 in the same way as the winding U starts from the slot 1. The winding W starts then from the slot 5. When considering the pole pair number p' = 2, we can see that the winding V is placed at a distance

$$\frac{Q}{3p'}\tau_{\mathrm{u}} = \frac{24}{3\cdot 2}\tau_{\mathrm{u}} = 4\tau_{\mathrm{u}}$$

from the winding U and starts thus from the slot 5, and the winding W from the slot 9. External connections have to be arranged to meet these requirements. At simplest, the shift of the above-mentioned pole pair from one winding to another is carried out according to the right-hand circuit diagrams. To keep the machine rotating to the same direction, the phases U, V, and W have to be connected according to the illustration.

There is also another method to create windings with two different pole numbers. Pole-Amplitude-Modulation (PAM) is a method with which even other ratios than 1:2 may be found. PAM is based on the following trigonometric equation

$$\sin p_{\mathrm{b}}\alpha \sin p_{\mathrm{m}}\alpha = \frac{1}{2}\left(\cos\left(p_{\mathrm{b}} - p_{\mathrm{m}}\right)\alpha - \cos\left(p_{\mathrm{b}} + p_{\mathrm{m}}\right)\alpha\right). \qquad (2.103)$$

The current linkage is produced as a function of the angle α running in the perimeter of the air gap. A phase winding might be realized with a base pole pair number p_{b} and a modulating pole pair number p_{m}. In practice, this means that if for instance p_{b} = 4 and p_{m} = 1, the PAM method produces pole pairs 4 – 1 or 4 + 1. The winding must be created so that one of the harmonics is damped and the other dominates.

2.15 Commutator Windings

A characteristic of poly-phase windings is that the phase windings are, in principle, galvanically separated. The phase windings are connected via terminals to each other, in star or in a polygon. The armature winding of commutator machines does not start nor ends at terminals. The winding is comprised of turns of conductor soldered as a continuum and wound in the slots of the rotor so that the sum of induced voltages is always zero in the continuum. This is possible if the sum of slot voltages is zero. All the coil sides of such a winding can be connected in series to form a continuum without causing a current flow in the closed ring as a result of the voltages in the coil sides. An external electric circuit is created by coupling the connection points of the coils to the commutator segments. A current is fed to the winding via brushes dragging along the commutator. The commutator switches the coils in turns to the brushes acting thus as a mechanical inverter or

rectifier depending on the operating mode of the machine. This is called commutating. In the design of a winding, the construction of a reliable commutating arrangement is a demanding task.

Commutator windings are always double-layer windings. One coil side of each coil is always in the upper layer and the other in the bottom layer approximately at a distance of a pole pair from each other. Because of problems in commutating, the voltage difference between the commutator segments must not be too high, and thus the number of segments and coils has always to be high enough. On the other hand, the number of slots is restricted by the minimum width of the teeth. Therefore, usually more than two coil sides are placed in each slot. In the slot of the upper diagram of Fig. 2.44, there are two coil sides, and in the lower diagram, the number of coil sides is four. The coil sides are often numbered so that the sides of the bottom layer are even numbers, and the slots of the upper layer are odd numbers. If the number of coils is z_c, $2z_c$ coil sides have to be mounted in Q slots, and thus there are $2u = 2z_c/Q$ sides in a slot. The symbol u gives the number of coil sides in one layer. In each side, there are N_v conductors. The total number of conductors z in the armature is

$$z = Qz_Q = 2uN_vQ = 2z_cN_v. \tag{2.104}$$

Here

Q is the number of slots,
z_Q is the number of conductors in a slot,
u is the number of coil sides in a layer,
z_c is the number of coils

N_v, number of conductors in a coil side, $2uN_v = z_Q$, because $z_Q = \frac{z}{Q} = \frac{2uN_vQ}{Q} = 2uN_v$, see (2.104).

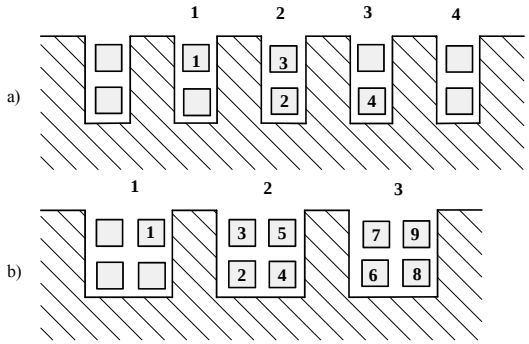

Figure 2.44. Two examples of commutator winding coil sides mounted in the slots. a) Two coil sides in a slot, one side in a layer, u = 1 b) four coil sides in a slot, two coil sides in a layer, u = 2. Even-numbered coil sides are located at the bottom of the slots. There has to be a large enough number of coils and commutator segments to keep the voltage between commutator segments small enough.

Commutator windings may be used both in AC and DC machines. Multi-phase commutator AC machines are, however, becoming rare. DC machines, instead, are built and used also in the present-day industry even though DC drives are gradually replaced by power electronic AC drives. Nevertheless, it is advisable to briefly look also at the DC windings.

The AC and DC commutator windings are in principle equal. For simplicity, the configuration of the winding is investigated with a voltage phasor diagram of a DC machine. Here, it suffices to investigate a two-pole machine, since the winding of machines with multiple poles is repeated unchanged with each pole pair. The rotor of Figure 2.45, with Q = 16, u = 1, is assumed to rotate clockwise at an angular speed Ω in a constant magnetic field between the poles N and S.

The magnetic field rotates to the positive direction with respect to the conductors in the slots, that is, counterclockwise. Now, a coil voltage phasor diagram is constructed for a winding, in which we

have already calculated the difference of the coil side voltages given by the coil voltage phasor diagram. By applying the numbering system of Fig. 2.44, we have in the slot 1 the coil sides 1 and 32, and in the slot 9 the coil sides 16 and 17. With this system, the coil voltage phasor diagram can be illustrated as in Fig. 2.45b.

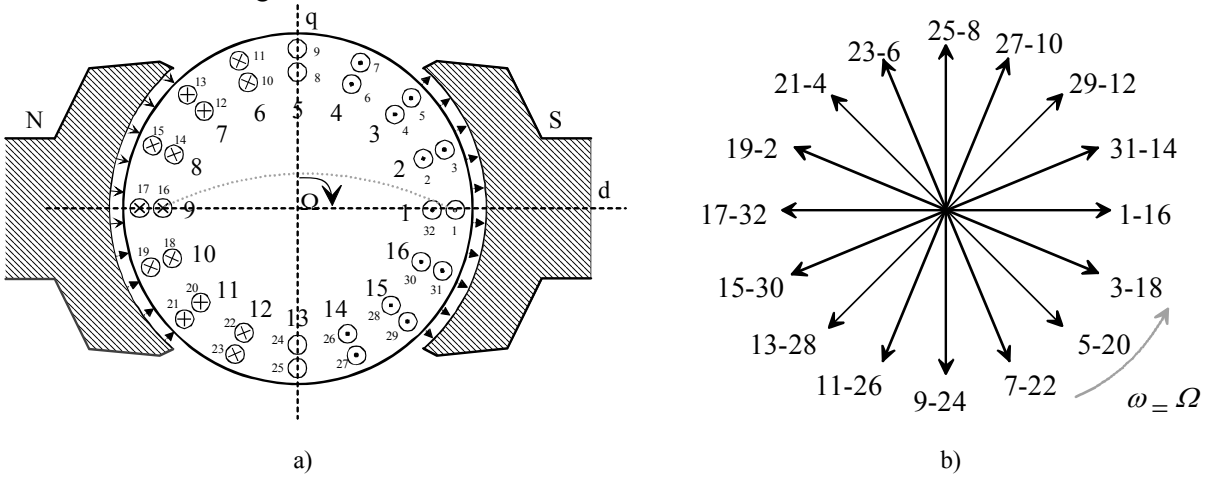

a) b)

Figure 2.45. a) Principle of a two-pole double-layer commutator armature. The armature rotates at an angular speed Ω clockwise generating an emf to the conductors in the slots. The emf tends to create the current directions illustrated in the figure. b) A coil voltage phasor diagram of the armature. It is a full-pitch winding, which does not normally occur as a commutator winding. Nevertheless, a full-pitch winding is here given as a clarifying example. $Q = 16$, $u = 1$ (one coil side per layer).

Figure 2.45 shows that if the induced emf decides the direction of the armature current, the produced torque is opposite to the direction of rotation (counterclockwise in Fig. 2.45), and mechanical power has to be supplied to the machine, which is acting as a generator. Now, if the armature current is forced to flow against the emf with the assistance of an external voltage or current source, the torque is to the direction of rotation, and the machine acts as a motor.

There are $z_c = Qu = 16 \times 1 = 16$ coils in the winding, the ends of which should next be connected to the commutator. Depending on the way they are connected, different kinds of windings are produced. Each connection point of the coil ends is connected to the commutator. There are two main types of commutator winding s, viz. lap windings and wave windings. A lap winding has coils, creating loop-like patterns. The ends of coils are connected to adjacent commutator segments. A wave winding has a wave-like drawing-pattern when presented in a plane.

The number of commutator segments is given by

$$K = uQ, \tag{2.105}$$

because each coil side begins and ends at the commutator segment. The number of commutator segments, therefore, depends on the conductor arrangement in the slot, eventually on the number of coil sides in one layer. Further important parameters of commutator windings are:

y_Q coil span expressed in the number of slots per pole

y_1 back end connector pitch which is a coil span expressed in the number of coil sides. For the winding the coil sides of which are numbered with odd figures in the top layer and with even figures in the bottom layer is:

$$y_1 = 2uy_Q \mp 1, \tag{2.106}$$

where

− sign stands for a coil side numbering as seen in Fig. 2.44, and the + sign for a numbering, where in the slot 1 there are coil sides 1, 2, in the slot 2, coil sides 3, 4, etc, if $u = 1$, or in the top layer of the slot 1 coil sides 1, 3, and in the bottom layer 2,4, etc., if $u = 2$.

y_2 front end connector pitch; it is a pitch expressed in the number of coil sides between the right coil side of one coil and the left coil side of the next coil.

y total winding pitch expressed in the number of coil sides between two left coil sides of the two adjacent coils

y_c commutator pitch between the beginning and end of one coil expressed in the number of commutator segments.

The equation for the commutator pitch is a basic equation for the winding design because this pitch must be an integer

$$y_c = \frac{nK \pm a}{p}, \tag{2.107}$$

where a is the number of parallel paths per half armature in a commutator winding, which means $2a$ parallel paths for the whole armature.

The most often employed windings are characterized on the basis of n:

1) If $n = 0$, it results in a lap winding. The commutator pitch will be: $y_c = \pm\frac{a}{p}$, which means that a is an integer multiple of p to get an integer for the commutating pitch. If for a lap winding $2a = 2p$, this means $a = p$, $y_c = \pm 1$. Such a winding is called a parallel one. The positive sign is for a progressive winding, moving from left to right, and the negative sign for a retrogressive winding, moving from right to left. If a is a k-multiple of the pole pair number, $a = kp$, then it is a k-multiplex parallel winding. For example for $a = 2p$, the commutator pitch is $y_c = \pm 2$, and this winding is called a duplex parallel winding.

2) If $n = 1$, it results in a wave winding and a commutator pitch

$$y_c = \frac{K \pm a}{p} = \frac{uQ \pm a}{p} \tag{2.108}$$

must be an integer. The positive sign is for progressive and the negative sign for retrogressive winding. In the wave winding the number of parallel paths is always 2, there is only one pair of parallel paths, irrespective of the number of poles: $2a = 2$, $a = 1$.

Not all the combinations of K, a, p result in an integer. It is a designer's task to choose a proper number of slots, coil sides, number of poles, and type of winding to ensure an integer commutator pitch.

If the number of coils equals the number of commutator segments, then, if the coil sides are numbered with odd figures in the top layer and even figures in the bottom layer, we may write:

$$y = y_1 + y_2 = 2y_c. \tag{2.109}$$

Therefore, if the commutator pitch is determined, the total pitch expressed as a number of coil sides is given

$$y = 2y_c \tag{2.110}$$

and after y_1 is determined based on the numbers of slots per pole y_Q and number of coil sides in a layer u:

$$y_Q \cong \frac{Q}{2p}, \tag{2.111}$$

$$y_1 = 2u\, y_Q \mp 1. \tag{2.112}$$

The front end connector pitch can be determined as:

$$y_2 = y - y_1. \tag{2.113}$$

2.15.1 Lap Winding Principles

The principles of the lap winding can best be explained by an example:

EXAMPLE 2.27: Make a layout of a lap winding for a two-pole DC machine with 16 slots and one coil side in a layer.

SOLUTION: Given: $Q = 16$, $2p = 2$, $u = 1$, the number of commutator segments K is $K = uQ = 1 \cdot 16 = 16$, and for a lap winding $2a = 2p = 2$. The commutator pitch is $y_c = \pm\frac{a}{p} = \pm 1$.

We choose a progressive winding, which means that $y_c = +1$ (The winding proceeds from left to right), and the total pitch is $y = 2y_c = 2$. The coil span y_Q in the number of slots is given by the number of slots per pole:

$y_Q = \frac{Q}{2p} = \frac{16}{2} = 8$. The same pitch expressed in the number of coil sides is:

$y_1 = 2uy_Q - 1 = 2 \cdot 1 \cdot 8 - 1 = 15$. The front end connector pitch is: $y_2 = y - y_1 = 2 - 15 = -13$, which is illustrated in Fig. 2.46. The coils can be connected in series in the same order they are inserted in the slots of the rotor. The neighbouring coils are connected together, the coil 1–16 to the coil 3–18, this again to 5–20 and so on. This yields a winding diagram of Fig. 2.46.

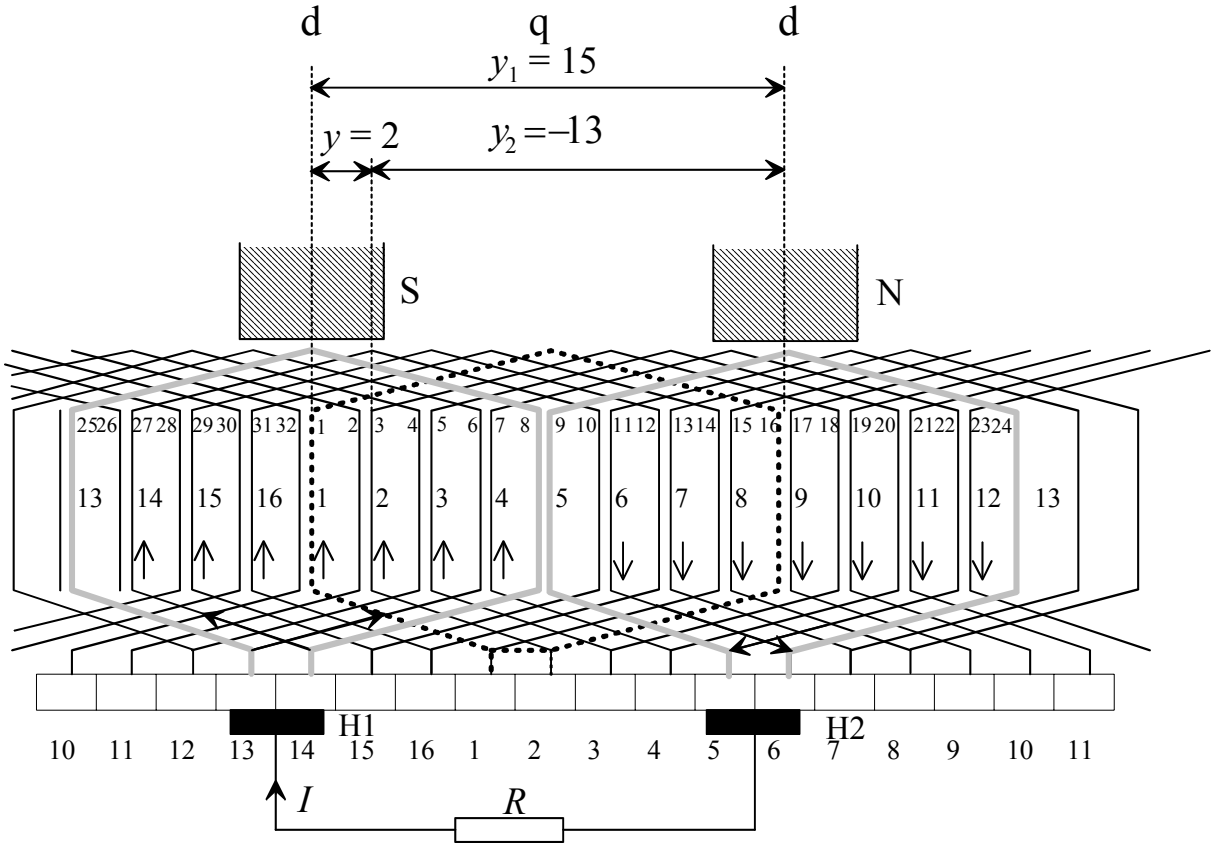

Figure 2.46. Diagram of a full-pitch lap winding. The winding is connected via brushes to an external resistance R. The pole shoes are also illustrated above the winding. In reality, they are placed above the coil sides. The laps illustrated with a thick line have been short-circuited via the brushes during commutation. The direction of current changes during the commutation. The numbers of slots (1–16) are given. The numbers of coil sides (1–32) in the slots are also given, the coil sides 1 and 32 are located in the slot 1 and e.g. the coil sides 8, 9 are located in the slot 5. The commutator segments are numbered (1–16) according to the slots. It is said that the brushes are on the quadrature axis; this is nevertheless valid only magnetically. In this figure, the brushes are physically placed close to the direct axes.

When we follow the winding by starting from the coil side 1, we can see that it proceeds one step of span $y_1 = 15$ coil sides. In the slots 1 and 9, a coil with a large enough number of winding turns is inserted. Finally, after the last coil turn the winding returns left a distance of one step of connection $y_2 = 2 - 15 = -13$ coil sides, to the upper coil side 3. We continue this way until the complete winding has been gone through, and the coil side 14 is connected to the upper coil side 1 through the commutator segment 1. The winding has now been closed as a continuum. The winding proceeds in laps from left to right; hence the name lap winding.

The pitches of a commutator winding are thus calculated by the number of coil sides, not by the number of slots, because there can be more than two coil sides in one layer, for instance four coil sides in a slot layer ($u = 1, 2, 3, 4\ldots$).

In the lap winding of Fig. 2.46, all the coil voltages are connected in series. The connection in series can be illustrated by constructing a polygon of the coil voltages, Fig. 2.47. The figure illustrates the phasors at time $t = 0$ in the coil voltage phasor diagram of Fig. 2.45. When the rotor rotates at an angular speed Ω, also the coil voltage phasor diagram rotates in a two-pole machine at an angular speed $\omega = \Omega$. Also the polygon rotates around its centre at the same angular speed. The real instantaneous value of each coil voltage may be found as a projection of the phasor on the real axis (see figure). According to the figure, the sum of all coil voltages is zero. Therefore, no circulating currents occur in the continuum.

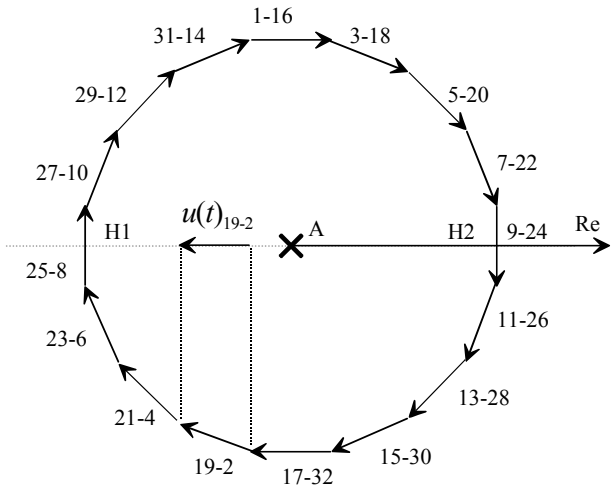

Figure 2.47. Polygon of coil voltages of the winding in Fig. 2.46. The sum of all the voltages is zero and hence the coils may be connected in series. The instantaneous value of a coil voltage $u(t)$ will be the projection of the phasor on the real axis, e.g. $u(t)_{19\text{-}2}$.

The highest value of the sum of the instantaneous values of coil voltages is equal to the diameter H1–H2 parallel to the real axis. This value remains almost constant as the polygon rotates, and thus the phasor H1–H2 represents a DC voltage without significant ripple. The voltage approaches a constant value, when the number of coils approaches infinite. A DC voltage can be connected to an external electric circuit via the brushes that are in contact with the commutator segments. At the moment $t = 0$, as illustrated, the brushes have to be in touch with the commutator segment pairs 5–6 and 13–14, that are connected to coils 9–24 and 25–8. According to Fig. 2.46, the magnetic south pole (S) is at the slot 1 and magnetic north pole (N) at the slot 9. According to Fig. 2.46, the direction of the magnetic flux is towards the observer at the south pole, and away from the observer at the north pole. As the winding moves left, a positive emf is induced to the conductors under the south pole, and a negative emf under the north pole, to the direction pointed by the arrows.

By following the laps from the segment 14 to the coil 27–10, we end up at the commutator segment 15, then gradually to the segments 16, 1, 2, 3, 4, and at last the coil 7–22, is brought to the segment 5, touched by the brush H2. We have just described one parallel path created by coils connected in series via commutator segments. An induced emf creates a current in the external part of the electric circuit from the brush H2 to the brush H1, and thus in generator drive, the H2 is a positive brush with the given direction of rotation. A half of the current I in the external part of the circuit flows the above-described path, and the other half via the coils 23–6 ... 11–26, via commutator segments 12, 11, …7 to the brush H2 and further to the external part of the circuit. In other words, there are two parallel paths in the winding. In the windings of large machines, there can be several pairs of paths in order to prevent the cross-sectional area of the conductors from increasing impractically. Because the ends of different pairs of paths touch the neighbouring commutator segments and they have no other galvanic contact, the brushes have to be made wider to keep each pair of paths always in contact to the external circuit.

If for instance in the coil voltage phasor diagram of Fig. 2.45 every other coil 1–16, 5–20, 9–24 ... 29–12 is connected in series with the first pair of paths, the lap is closed after the last turn of coil side 12 by connecting the coil to the first coil 1–16 ($12 \rightarrow 1$, from 12 to 1). The coils that remain free are connected in the order 3–18, 7–22 ... 31–14, and the lap is closed at the position $14 \rightarrow 3$. This way, a doubly-closed winding with two paths $2a = 2$ is produced. In the voltage polygon, there are two revolutions, and its diameter, that is, the brush voltage is reduced to a half of the original polygon of one revolution illustrated in Fig. 2.47. The output power of the system remains the same, because the current can be doubled when the voltage is cut into half. In general, the number of pairs of paths a always requires that $a - 1$ phasors are left between the phasors of series-connected coils in a coil voltage phasor diagram. The phasors may be similar. Because u is the number of coil sides

per layer, each phasor of the coil voltage phasor diagram represents u coil voltages. This makes it possible to skip completely similar voltage phasors. This takes place for instance when $u = 2$.

The winding of Fig. 2.46 is wound clockwise, because the voltages of the coil voltage phasor diagram are connected in series clockwise starting from the phasor 1–16. Were the coil 1–16 connected via the commutator segment 16 to the coil 31–14, the winding would have been wound counterclockwise.

The number of brushes in a lap winding is always the same as the number of poles. The brushes of the same sign are connected together. According to Fig. 2.46, the brushes always short-circuit those coils, the coil sides of which are located at the quadrature axis (in the middle, between two stator poles) of the stator, where the magnetic flux density created by the pole magnetizing is zero. This situation is also described by stating that the brushes are located at the quadrature axis of the stator independent of the real physical position of the brushes.

2.15.2 Wave Winding Principles

The winding of Fig. 2.46 can be turned into a wave winding by bending the coil ends of the commutator side according to the illustration of Fig. 2.48, as a solution of the Example 2.28 (see also Fig. 2.49).

EXAMPLE 2.28: Make a layout of a wave winding for a two-pole DC machine with 16 slots and one coil side in a layer.

SOLUTION: It is given that Q = 16, $2p$ = 2, u = 1. The number of commutator segments is $K = uQ = 1 \cdot 16 = 16$, and for a wave winding $2a$ = 2. The commutator pitch is $y_c = \frac{K \pm a}{p} = \frac{16 \pm 1}{1} = 17$, or 15. We choose $y_c = +15$ (winding proceeds from right to left), and the total winding pitch is $y = 2y_c = 30$. The coil span y_Q in the number of slots is given by the number of slots per pole: $y_Q = \frac{Q}{2p} = \frac{16}{2} = 8$. The same pitch expressed in the number of coil sides is:

$y_1 = 2uy_Q - 1 = 2 \cdot 1 \cdot 8 - 1 = 15$. The front end connector pitch is: $y_2 = y - y_1 = 30 - 15 = 15$, which is shown in Fig. 2.48.

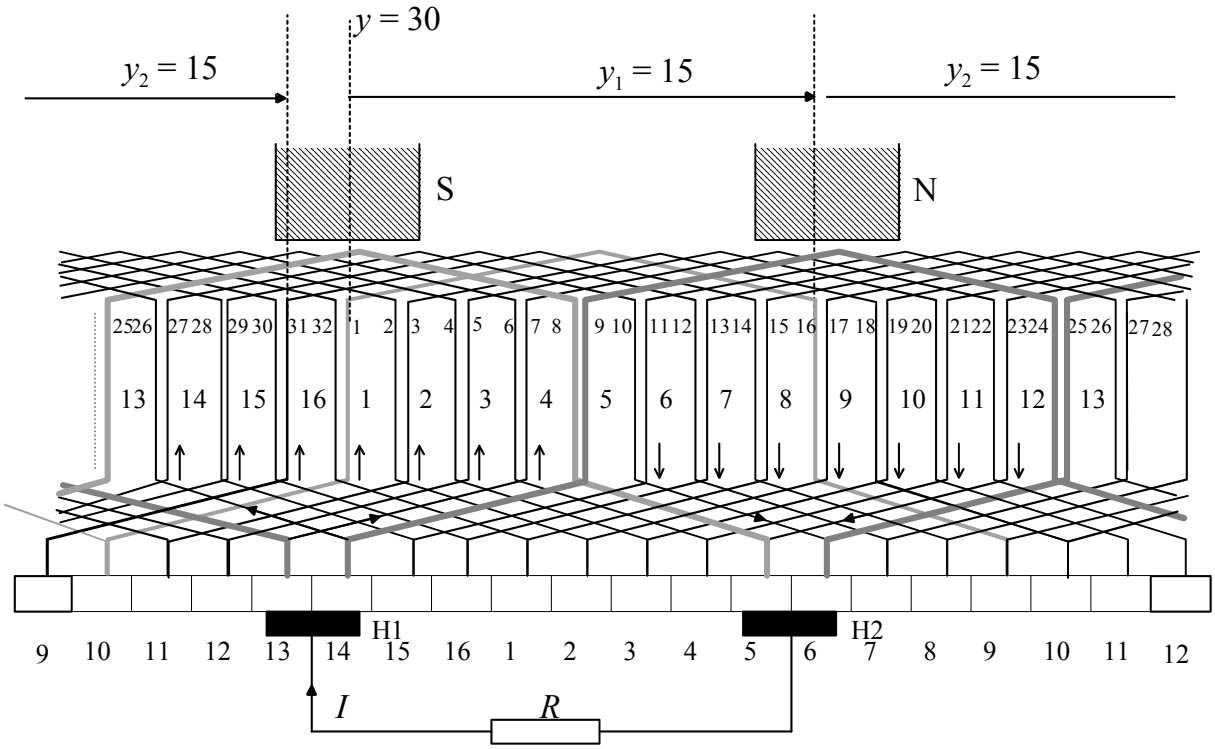

Figure 2.48. Full-pitch lap winding of Fig. 2.46 turned into a wave winding. The currents of waveforms indicated with a thick line are commutating at the moment illustrated in the figure. The commutator pitch is $y_c = 15$, which means almost two pole pitches. For instance the wave coil that starts at the commutator segment 14 ends at the segment 13, because $14 + y_c = 14 + 15 = 29$, but there are only 16 commutator segments, and therefore $29 - 16 = 13$.

In the above wave winding, the upper coil side 1 is connected to the commutator segment 10, and not to the segment 1 as in the lap winding. From the segment 10, the winding proceeds to the bottom side 18. The winding receives thus a waveform. In the figure, the winding proceeds from the right to the left, and counterclockwise in the coil voltage phasor diagram. The winding is thus rotated to the left. If the winding were turned to the right, the commutator pitch would be $y_c = 17$, $y = 34$, $y_1 = 15$, $y_2 = 19$. The coil from the bottom side 16 would have to be bent to the right to the segment 10, and further to the upper side 3, because $16 + y_2 = 16 + 19 = 35$. But there are only 32 coil sides, and therefore the coil will proceed to $35 - 32 = 3^{rd}$ coil side. The commutator ends would in that case be even longer, which would be of no use. The pitch of the winding for a wave winding follows the illustration

$$y = y_1 + y_2 . \tag{2.114}$$

The position of brushes in a wave winding is solved in the same way as in a lap winding. When comparing the lap and wave windings, we can see that the brushes short-circuit the same coils in both cases. The differences between the windings are merely structural, and the winding type is selected basically on these structural grounds. As it was written above, the pitch of winding for regular commutator windings, which equals commutator pitch is obtained from

$$y_c = \frac{nK \pm a}{p} = \frac{nuQ \pm a}{p}, \tag{2.115}$$

+ in the equation is used for progressive lap winding and retrogressive wave winding, and – is used for retrogressive lap and progressive wave winding, n is zero or a positive integer. If n is zero, it results in a lap winding, if $n = 1$, it results in a wave winding. The commutator pitch y_c must be an

integer, otherwise the winding cannot be constructed. Not all combinations of K, p, and a result in y_c as an integer, and therefore a designer must solve this problem in its complexity.

2.15.3 Commutator Winding Examples, Balancing Connectors

Nowadays, the conductors are typically inserted in slots that are on the surfaces of the armature. These windings are called drum armature windings. Drum-wound armature windings are in practice always double-layer windings, in which there are two coil sides in the slot on top of each other. Drum armature windings are constructed either as lap or wave windings. As discussed previously, the term lap winding describes a winding that is wound in laps along the periphery of the armature, the ends of one coil being connected to adjacent segments, Fig. 2.49a.

EXAMPLE 2.29: Make a layout of the lap winding for a four-pole DC machine with 23 slots and one coil side in a layer.

SOLUTION: It is given that Q = 23, $2p$ = 4, u = 1, number of commutator segment is $K = uQ = 1 \cdot 23 = 23$, and for lap winding $2a = 2p = 4$. The commutator pitch is $y_c = \pm\frac{a}{p} = \frac{2}{2} = \pm 1$. We choose a progressive winding, which means that $y_c = +1$ (winding proceeds from left to right), and the total winding pitch is $y = 2y_c = 2$. The coil span y_Q in the number of slots is given by the number of slots per pole: $y_Q = \frac{Q}{2p} = \frac{23}{4} = 5.75 \Rightarrow 6$ slots. The same pitch expressed in the number of coil sides is: $y_1 = 2uy_Q \mp 1 = 2 \cdot 1 \cdot 6 + 1 = 13$. The negative sign is used because of the coil side arrangement in the slots according to Fig. 2.44a.

The front end connector pitch is:
$y_2 = y - y_1 = 2 - 13 = -11$, which is shown in Fig. 2.49a.

In the winding of Fig. 2.49a, there are 23 armature coils (46 coil sides, two in each slot), with one turn in each, four brushes, and a commutator with 23 segments. There are four current paths in the winding ($2a$ = 4), which thereby requires four brushes. By following the winding starting from the first brush, we have to travel a fourth of the total winding to reach the next brush of opposite sign.

From the segment 1, the left coil side is put to the upper layer number 1 in the slot 1 (see Fig. 2.44a). Then, the right side is put to the bottom layer $1+y_1 = 1 + 11 = 12$ in the slot 7, from where it is led to the segment number $1 + y_c = 1 + 1 = 2$. From the segment 2 to the upper layer 3 in the slot 2, because 12 – 9 = 3. Then it proceeds to the bottom layer 14 in the slot 8, because 3 + 11 = 14, and. then to the segment 3, and continuing to the coil side 5 in the slot 3 and via 16 in the slot 9 to the segment 4, and so on.

In the figure, the brushes are broader than the segments of the commutator, the laps illustrated with thick lines being short-circuited via the brushes. In DC machines, a proper commutating requires that the brushes cover several segments. The coil sides of short-circuited coils are approximately in the middle between the poles, where the flux density is small. In these coils, the induced voltage is low, and the created short-circuit current is thus insignificant.

EXAMPLE 2.30: Make a layout of a wave winding for a four-pole DC machine with 23 slots and one coil side in a layer.

SOLUTION: It is given that Q = 23, $2p$ = 4, u = 1. The number of commutator segments is $K = uQ = 1 \cdot 23 = 23$, and for a wave winding $2a$ = 2. The commutator pitch is $y_c = \frac{K \pm a}{p} = \frac{23 \pm 1}{2} = 12$, or 11. We choose $y_c = +12$ and the total winding pitch is $y = 2y_c = 24$.

The coil span y_Q in the number of slots is given by the number of slots per pole:

$y_Q = \frac{Q}{2p} = \frac{23}{4} = 5.75 \Rightarrow 6$. The same pitch expressed in the number of coil sides is:

$y_1 = 2uy_Q - 1 = 2 \cdot 1 \cdot 6 + 1 = 13$. The negative sign is used because of the coil side arrangement in the slots according to Fig. 2.44a.

The front end connector pitch is:

$y_2 = y - y_1 = 24 - 13 = 11$, which is shown in Fig. 2.49b. Fig 2.49b illustrates the same winding as in Fig. 2.49a developed to a wave winding. In wave windings, there are only two current paths, $2a$ = 2 regardless of the number of poles. A wave winding and a lap winding can also be combined as a frog-leg winding.

We can see in Fig. 2.49b that from the commutator segment 1 the coil left side is put to the upper layer number 13 in the slot 7. Then the right side is in the lower layer 13 + y_1 = 13 + 13 = 26 in the slot 13, from where it is led to the segment number 1 + y_c = 1 + 12 = 13. From the segment 13 to the upper layer 37 (slot 19), because 24 + y_2 = 24 + 13 = 37. Then we proceed to the lower layer 2 in the slot 2, because 37 + y_1 = 37 + 11 = 48, which is over the number coil sides 46 in 23 slots; therefore, it is necessary to make a correction 48 – (2 × 23) = 50 – 46 = 2. From here we continue to the segment 2, because 13 + y_c = 13 + 12 = 25, after the correction 25 – 23 = 2, and so on.

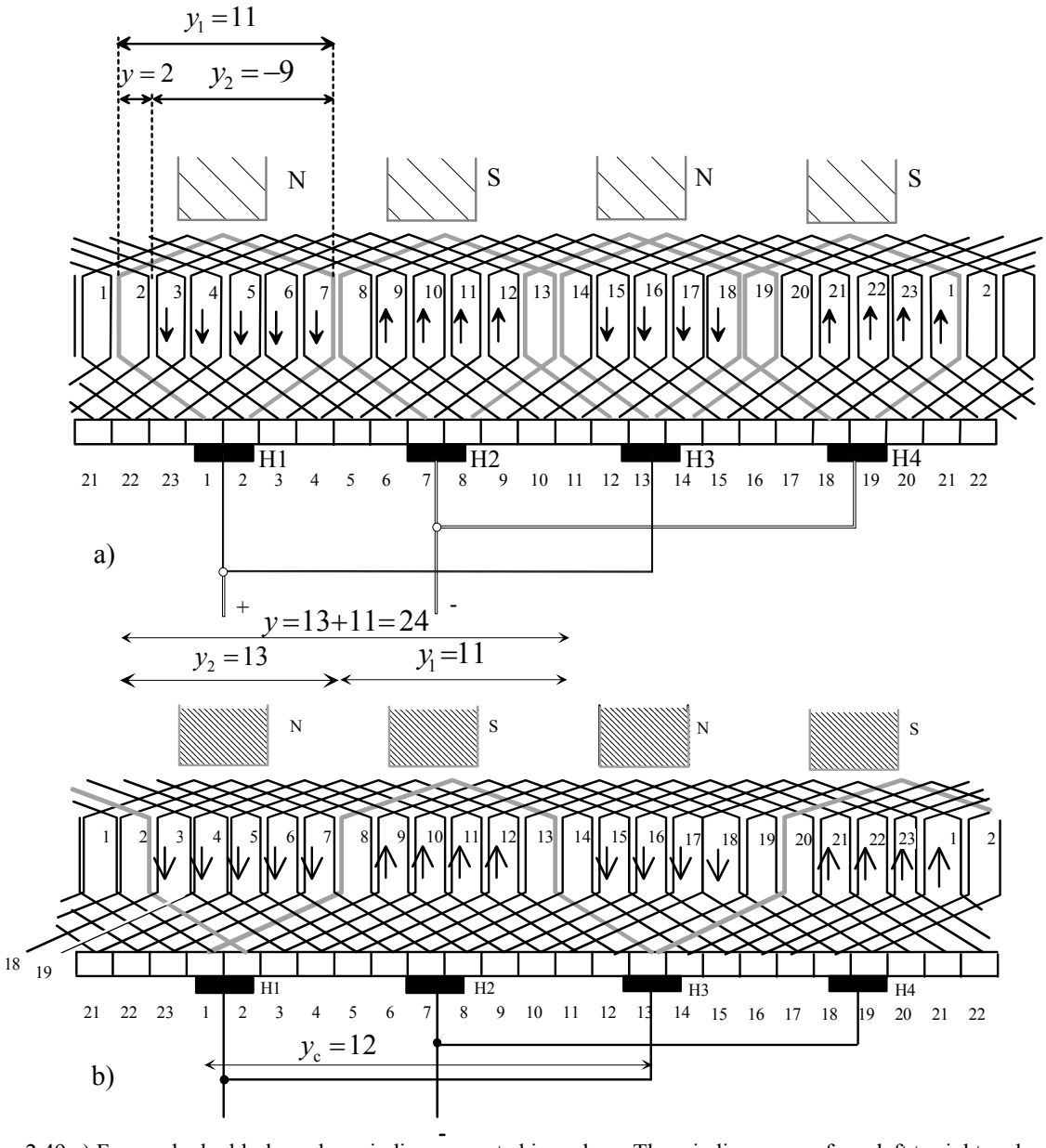

Figure 2.49 a) Four-pole double-layer lap winding presented in a plane. The winding moves from left to right and acts as a generator. The coils belonging to the commutator circuit are illustrated with a thick line. This winding is not a full-pitch winding unlike the previous ones. The illustrated winding commutates better than a full-pitch winding. b) The same winding developed to a wave winding. The wave under commutation is drawn with a thicker line than the others.

When passing through a wave winding from one brush to another brush of the opposite sign, a half of the winding and a half of the segments of the commutator are gone through. The current has thus only two paths irrespective of the number of poles. As a matter of fact, in a wave winding, only one pair of brushes is required, which is actually enough for small machines. Nevertheless, usually as many brushes are required as there are poles in the machine. This number is selected in order to reach a maximum brush area with the shortest commutator possible. One coil of a wave winding is always connected to the commutator at about a distance of two pole pitches.

A wave winding is a more common solution than a lap winding for small (< 50 kW) machines, since it is usually more cost-efficient than a lap winding. In a machine designed for a certain speed, a number of pole pairs and a flux, the wave winding requires less turns than a lap winding, a two-pole machine excluded. Correspondingly, the cross-sectional area of conductors in a wave winding has to

be larger than the area of a lap winding. Therefore, in a machine of a certain output, the copper consumption is the same irrespective of the type of winding.

The previous windings are simple examples of the various alternative constructions for commutator windings. In particular, when numerous parallel paths are employed, we must ensure that the voltages in the paths are equal, or else there will occur compensating currents flowing through the brushes. These currents create sparks and wear out the commutator and the brushes. The commutator windings have to be symmetric to avoid extra losses.

If the number of parallel pairs of paths is *a,* there are also *a* revolutions in its voltage polygon. If the revolutions are completely overlapping in the voltage polygon, the winding is symmetrical. In addition to this condition, the diameter H1–H2 has to split the polygon into two equal halves at all times. These conditions are usually met when both the number of slots Q and the number of poles $2p$ are evenly divisible with the number of parallel paths $2a$. Figure 2.50 illustrates a winding diagram of a four-pole machine. The number of slots is $Q = 16$, and the number of parallel paths is $2a$–= 4. Hence, the winding meets the above conditions of symmetry. The coil voltage phasor diagram and the voltage polygon are depicted in Fig. 2.51. Since $a = 2$, there has to be one phasor $a - 1 = 1$ of the coil voltage phasor diagram between the consequent phasors of the polygon. When starting with the phasor 1–8, the next phasor in the voltage polygon is 3–10. In between, there is a phasor 17–24, which is of the same phase as the previous one, and so on. The first circle around the voltage polygon ends up at the point of the phasor 15–22, in the winding diagram at the commutator segment 9. However, the winding is not yet closed at this point, but continues for a second, similar revolution formed by the phasors 17–24 ... 31–6. The winding is fully symmetrical, and the coils short-circuited by the brushes are placed on the quadrature axes.

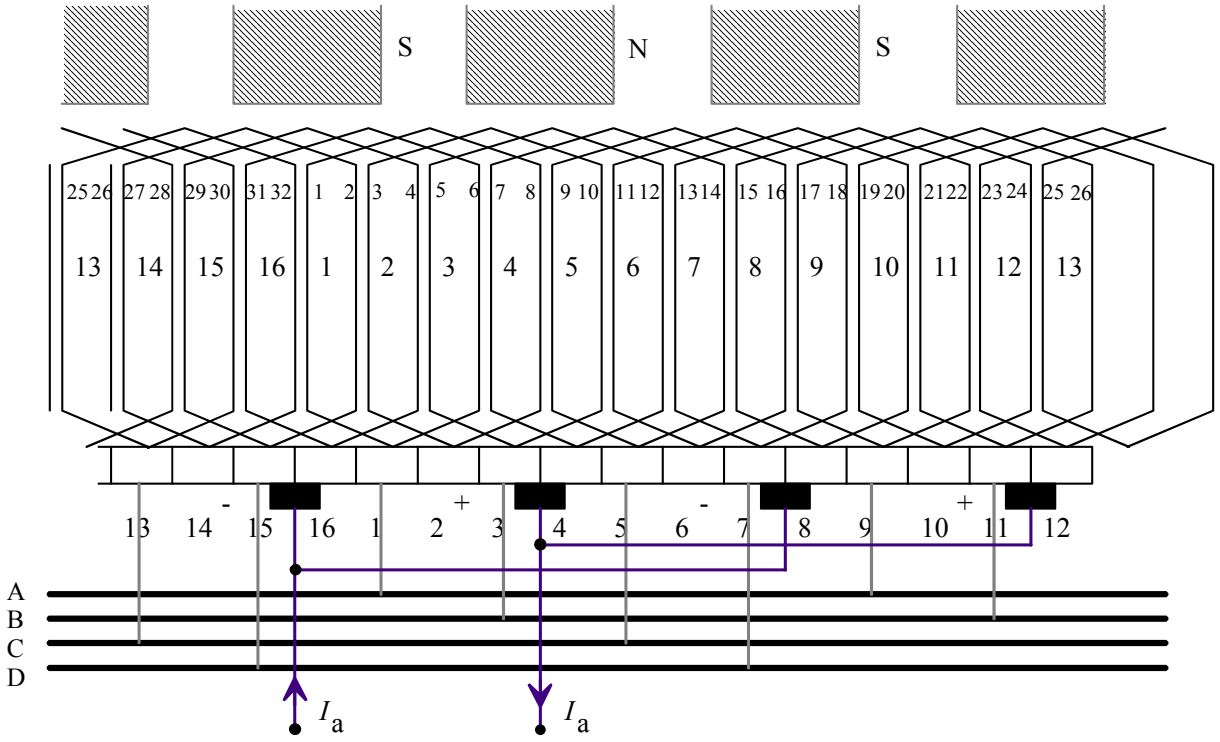

Figure 2.50. Balancing connectors or equalizer bars (Bars A, B, C, and D) of a lap winding. For instance the coil sides 29 and 13 are located in the similar magnetic positions if the machine is symmetric. Hence, the commutator segments 15 and 7 may be connected together with a balancing connector.

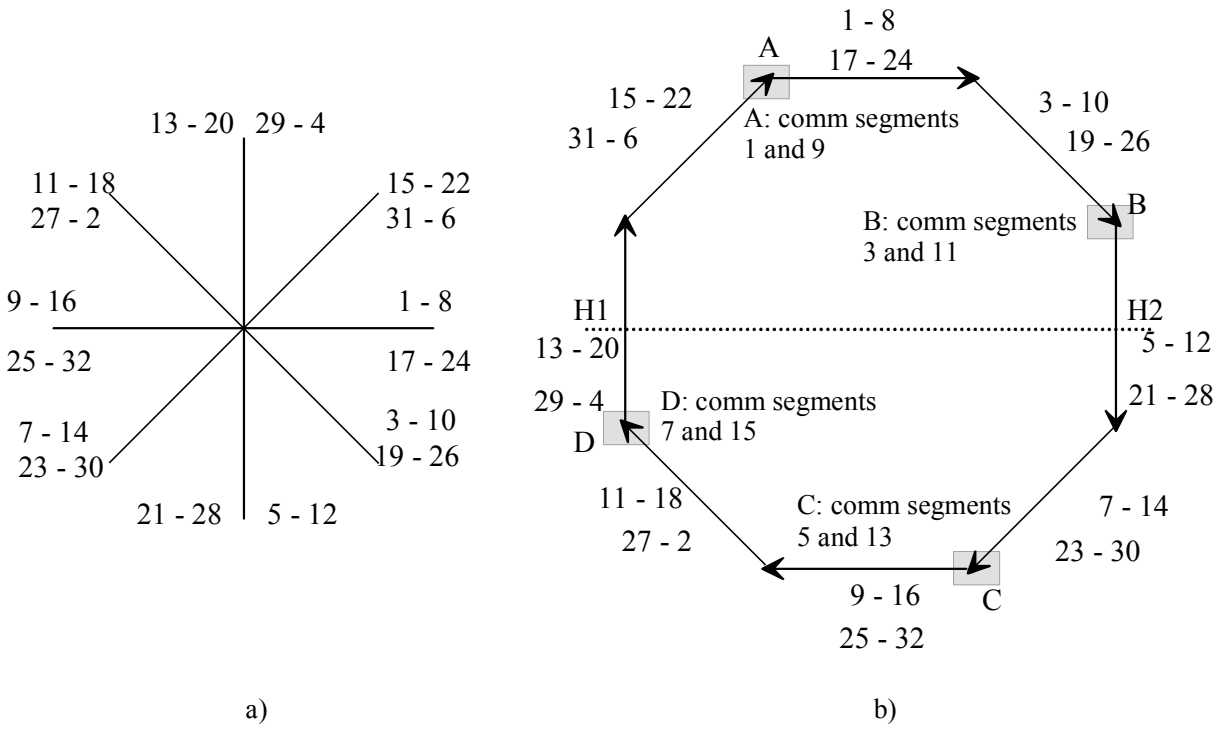

Figure 2.51. a) Coil voltage phasor diagram of the winding of Fig. 2.50, b) the coil voltage polygon of the winding of Fig. 2.50 and the connection points of the balancing connectors A, B, C, and D. There are two overlapping polygons in the illustrated voltage polygon. The phasor 1–8 is the first phasor and 3–10 the next phasor of the polygon. The phasor 17–24 is equal to the phasor 1–8 because both have their positions in the middle of poles, but it is skipped when constructing the first polygon. The first polygon is closed at the tip of the phasor 15–22. The winding continues to form another similar polygon using phasors 17–24 ... 31–6. The winding is completely symmetrical, and its brush-short-circuited coils are on the quadrature axes. The phasors 3–10 and 19–26 have a common tip point B in the polygons created by the commutator segment 3 and 11, as shown in Fig. 2.50 and in Fig. 2.51b, and the points can thus be connected by balancing connectors. The three other balancing connector points are A, C, and D.

The potential at different positions of the winding is now investigated with respect to an arbitrary position, for instance a commutator segment 1. In the voltage polygon, this zero potential is indicated by the point A of the polygon. At $t = 0$, the instant depicted by the voltage polygon, the potential of the segment 2 amounts to the amplitude of the phasor 1–8, otherwise it is a projection on the straight line H1–H2. Respectively, the potential at all other points in the polygon with respect to the segment 1 is at every instant the phasor drawn from the point A to this point, projected on the straight line H1–H2. Since for instance the phasors 3–10 and 19–26 have a common point in the voltage polygon, the potential of the respective segments 3 and 11 of the commutator is always the same, and the potential difference between them is zero at every instant. Thus, these commutator segments can be connected with conductors. All those points that correspond to the common points of the voltage polygon, can be interconnected. Figure 2.50 also depicts three other balancing connectors. The purpose of these compensating combinations is to conduct currents that are created by the structural asymmetries of the machine, such as the eccentricity of the rotor. Without balancing connectors, the compensating currents, created for various reasons, would flow through the brushes, thus impeding the commutation. There is an alternating current flowing in the compensating combinations, the resulting flux of which tends to compensate the asymmetry of the magnetic flux caused by the eccentricity of the rotor. From this we may conclude that compensating combinations are not required in machines with two brushes.

The maximum number of compensating combinations is obtained from the number of equipotential points. In the winding of Figs. 2.50 and 2.51, we could thus assemble eight combinations; however, usually only a part of the possible combinations are needed to improve the operation of the

machine. According to the illustrations, there are four possible combinations: A, B, C, and D. In machines that do not commutate easily, it may prove necessary to employ all the possible compensating combinations. In small and medium machines, the compensating combinations are placed behind the commutator. In large machines, ring rails are placed to one end of the rotor, while the commutator is at the other end.

2.15.4 AC Commutator Windings

The equipotential points A, B, C, and D of the winding in Fig. 2.51 are connected with rails in A, B, C, and D in Fig. 2.50. The voltages between the rails at time $t = 0$ are illustrated by the respective voltages in the voltage polygon. When the machine is running, the voltage polygon is rotating, and therefore the voltages between the rails form a symmetrical four-phase system. The frequency of the voltages depends on the rotation speed of the machine. The phase windings of this system, with two parallel paths in each, are connected in a square. With the same principle, with tappings, we may create other poly-phase systems connected in a polygon, Fig. 2.52.

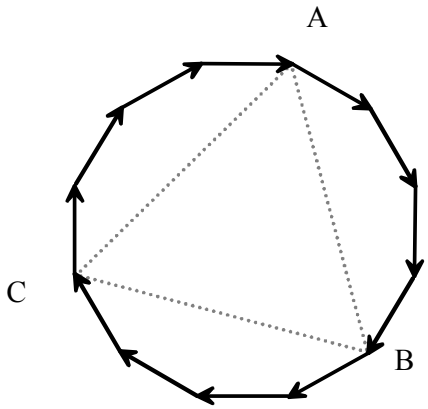

Figure 2.52. Equipotential points A, B, and C of the voltage polygon, which represents 12 coils of the commutator winding, are connected as a triangle to form a poly-phase system. The respective voltages are connected via slip rings and brushes to the terminals of the machine.

If z_c coils are connected as a closed commutator winding with a parallel path pairs, it is transformed with tappings into a m-phase AC system connected into a polygon by coupling the tappings at a distance of a step

$$y_m = \frac{z_c}{ma} \tag{2.116}$$

from each other. In a symmetrical poly-phase system, both y_m and z_c/a are integers. Windings of this type have been employed for instance in rotary converters, the windings of which have been connected both to the commutator and to the slip rings. They convert direct current into alternating current and vice versa. Closed commutator windings cannot be turned into star-connected windings, but only polygons are allowed.

2.15.5 Current Linkage of the Commutator Winding and Armature Reaction

The curve function of the current linkage created by the commutator winding is computed in the way illustrated in Fig. 2.9 for a three-phase winding. When defining the slot current I_u, the current of the short-circuited coils can be set zero. In short-pitched coils, there may be currents flowing in opposite directions in the different coil sides of a single slot. If z_b is the number of brushes, the armature current I_a is divided into brush currents $I = I_a/(z_b/2)$. Each brush current in turn is divided into two paths as conductor currents $I_s = I/2 = I_a/2a$, when a is the total number of path pairs of the winding. In a slot, there are z_Q conductors, and thus the sum current of a slot is

$$I_{\mathrm{u}} = z_{\mathrm{Q}} I_{\mathrm{s}} = \frac{z}{Q}\frac{I_{\mathrm{a}}}{2a}, \tag{2.117}$$

where z is the number of conductors in the complete winding. All the pole pairs of the armature are alike, and therefore it suffices to investigate only one of them, that is, a two-pole winding, Fig. 2.46. The curve function of the magnetic voltage follows thus the illustration of Fig. 2.53.

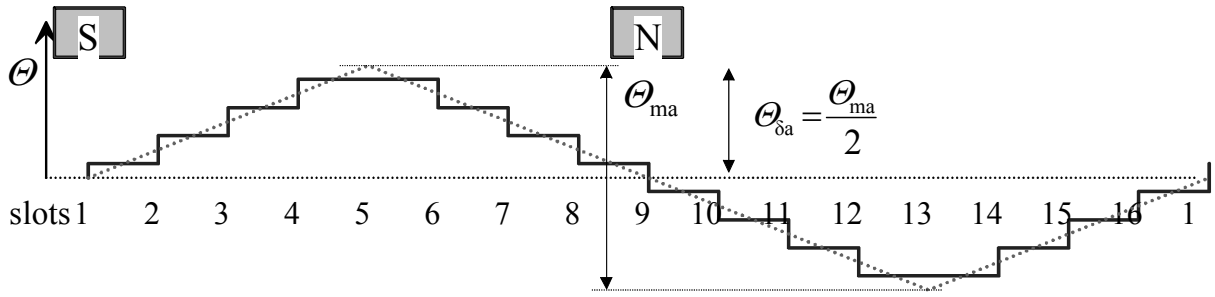

Figure 2.53. Current linkage curve of the winding of Fig. 2.46, when the commutating takes place in the coils in the slots 5 and 13.

The number of brushes of a commutator machine normally equals to the number of poles. The number of slots between the brushes is

$$q = \frac{Q}{2p}. \tag{2.118}$$

This corresponds to the number of slots per pole and phase of AC windings. The effective number of slots per pole and phase is always somewhat lower, because a part of the coils are always short circuited. The distribution factor for an armature winding is obtained from Eq. (2.33). For a fundamental, and $m = 1$ it is rewritten in the form

$$k_{\mathrm{da1}} = \frac{2p}{Q \sin\dfrac{p\pi}{Q}}. \tag{2.119}$$

Armature coils are often short pitched, and the pitch factor is thus obtained from Eq. (2.32). The fundamental winding factor of a commutator winding is thus

$$k_{\mathrm{wa1}} = k_{\mathrm{da1}} k_{\mathrm{pa1}} \approx \frac{2}{\pi}. \tag{2.120}$$

When the number of slots per pole increases, k_{da1} approaches the limit $2/\pi$. This is the ratio of the voltage circle (polygon) diameter to the circle perimeter. In ordinary machines, the ratio of short-pitching is $W/\tau_{\mathrm{p}} > 0{,}8$, and therefore $k_{\mathrm{pa1}} > 0{,}95$. As a result, the approximate value $k_{\mathrm{wa1}} = 2/\pi$ is an adequate starting point in the initial manual computation. More thorough investigations have to be based on the analysis of the curve function of the current linkage. In that case, the winding has to be observed in different positions of the brushes. Fig. 2.45 shows that at the right side of the quadrature axis q, the direction of each slot current is towards the observer, and on the left, away from the observer. In other words, the rotor becomes an electromagnet with the north pole at the bottom and the south pole at the top. The pole pair current linkage of the rotor is

$$\Theta_{\mathrm{ma}} = qI_{\mathrm{u}} = \frac{Q}{2p}\frac{z}{Q}\frac{I_{\mathrm{a}}}{2a} = \frac{z}{4ap} I_{\mathrm{a}} = N_{\mathrm{a}} I_{\mathrm{a}} . \tag{2.121}$$

The member

$$N_{\mathrm{a}} = \frac{z}{4ap} \tag{2.122}$$

of the equation is the number of coil turns per pole pair in a commutator armature in one parallel path, that is, turns connected in series, because $z/2$ is the number of all armature turns; $z/2(2a)$ is the number of turns in one parallel path, in other words, connected in series, and finally, $z/2(2a)p$ is the number of turns per pole pair. The current linkage calculated according to Eq. (2.121) is slightly higher than in reality, because the number of slots per pole and phase includes also the slots with short-circuited coil sides. In calculation, we may employ the linear current density

$$A_{\mathrm{a}} = \frac{QI_{\mathrm{u}}}{\pi D} = \frac{2p}{\pi D} N_{\mathrm{a}} I_{\mathrm{a}} = \frac{N_{\mathrm{a}} I_{\mathrm{a}}}{\tau_{\mathrm{p}}} . \tag{2.123}$$

The current linkage of the linear current density is divided into magnetic voltages of the air gaps, the peak value of which is

$$\hat{\Theta}_{\delta\mathrm{a}} = \int_0^{\frac{\tau_{\mathrm{p}}}{2}} A_{\mathrm{a}} \mathrm{d}x = \frac{1}{2} A_{\mathrm{a}} \tau_{\mathrm{p}} = \frac{1}{2}\frac{z}{2p}\frac{I_{\mathrm{a}}}{2a} = \frac{N_{\mathrm{a}} I_{\mathrm{a}}}{2} = \frac{\Theta_{\mathrm{ma}}}{2} . \tag{2.124}$$

$$\Theta_{\delta\mathrm{a}} = \Theta_{\mathrm{ma}}/2 = \frac{1}{2} A_{\mathrm{a}} \tau_{\mathrm{p}} = \frac{1}{2}\frac{z}{2p}\frac{I_{\mathrm{a}}}{2a} = \frac{1}{2} N_{\mathrm{a}} I_{\mathrm{a}} = \frac{\Theta_{\mathrm{ma}}}{2} = \Theta_{\delta\mathrm{a}} . \tag{2.125}$$

In the diagram, the peak value $\hat{\Theta}_{\delta\mathrm{a}}$ is located at the brushes (in the middle of the poles) the value varying linearly between the brushes, as illustrated with the dashed line in Fig. 2.53. $\hat{\Theta}_{\delta\mathrm{a}}$ is the armature reaction acting in the quadrature axis under one tip of a pole shoe, and it is the current linkage to be compensated. The armature current linkage also creates commutating problems because of which the brushes have to be shifted from the q-axis by and angle ε to a new position as shown in Fig 2.54.

The figure gives also the positive directions of the current I and the respective current linkage. The current linkage can be divided into two components

$$\Theta_{\mathrm{md}} = \frac{\Theta_{\mathrm{ma}}}{2} \sin\varepsilon = \Theta_{\delta\mathrm{a}} \sin\varepsilon , \tag{2.126}$$

$$\Theta_{\mathrm{mq}} = \frac{\Theta_{\mathrm{ma}}}{2} \cos\varepsilon = \Theta_{\delta\mathrm{a}} \cos\varepsilon . \tag{2.127}$$

The former is called a direct component and the latter a quadrature component. The direct component magnetizes the machine either into the parallel or opposite direction with the actual field winding of the main poles of the machine. There is demagnetizing effect, if brushes are shifted in the direction of rotation in generator mode, or in the opposite direction of rotation in motoring operation, the magnetizing effect in contrary, in generating operation opposite direction of rotation, in motoring mode in the direction of rotation. The quadrature component distorts the magnetic field

of the main poles, but neither magnetizes nor demagnetizes it. This is not a phenomenon restricted to commutator machines, but the reaction is in fact present in all rotating machines.

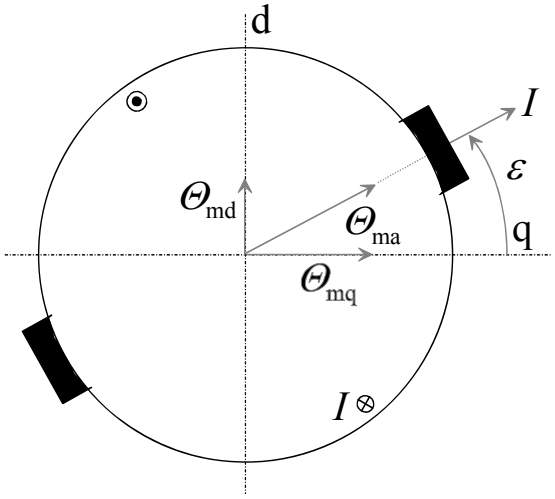

Figure 2.54. Current linkage of a commutator armature and its components. To ensure better commutation, the brushes are not placed on the q-axis.

2.16 Compensating Windings and Commutating Poles

As it was stated above, the armature current linkage (called also armature reaction) has some negative influence on the DC machine operation. The armature reaction may create commutating problems and must, therefore, be compensated. There are different methods to mitigate the armature reaction caused problems: 1) to shift brushes from their geometrical neutral axis to the new magnetically neutral axis, 2) to increase the field current to compensate the main flux decrease caused by the armature reaction, 3) to build commutating poles, and 4) to build compensating winding.

The purpose of compensating windings in DC machines is to compensate harmful flux components created by armature windings. Flux components are harmful, because they create an unfavourable air gap flux distribution in DC machines. The dimensioning of compensating windings is based on the current linkage that has to be compensated by the compensating winding. The conductors of a compensating winding have therefore to be placed close to the surface of the armature, and the current flowing in them has to be opposite to the armature current. In DC machines, the compensating winding is inserted in the slots of the pole shoes. The compensating effect has to be created in the section $\alpha_i \tau_p$ of the pole pitch, as illustrated in Fig. 2.55. If z is the total number of conductors in the armature winding, and the current flowing in them is I_s, we obtain an armature linear current density

$$A_a = \frac{z I_s}{D\pi}. \qquad (2.128)$$

The total current linkage Θ_Σ of the armature reaction and the compensating winding has to be zero in the integration path. It is possible to calculate the required compensating current linkage Θ_k by evaluating the corresponding current linkage of the armature to be compensated. The current linkage of the armature Θ_a occurring under the compensating winding at the distance $\alpha_{DC}\tau_p/2$, as it is shown in Fig. 2.55 is

$$\Theta_{\mathrm{a}}\left(\frac{\alpha_{\mathrm{i}}\tau_{\mathrm{p}}}{2}\right)=zI_{\mathrm{s}}\frac{\alpha_{\mathrm{DC}}\tau_{\mathrm{p}}}{2D\pi}=\frac{\alpha_{\mathrm{DC}}\tau_{\mathrm{p}}A_{\mathrm{a}}}{2}. \tag{2.129}$$

Since there is an armature current I_{a} flowing in the compensating winding, we obtain the current linkage of the compensating winding accordingly

$$\Theta_{\mathrm{k}}=-N_{\mathrm{k}}I_{\mathrm{a}}, \tag{2.130}$$

where N_{k} is the number of turns of the compensating winding. Since the current linkage of the armature winding has to be compensated in the integration path, the common current linkage is written

$$\Theta_{\Sigma}=\Theta_{\mathrm{k}}+\Theta_{\mathrm{a}}=-N_{\mathrm{k}}I_{\mathrm{a}}+\frac{\alpha_{\mathrm{i}}\tau_{\mathrm{p}}A_{\mathrm{a}}}{2}=0, \tag{2.131}$$

where $\Theta_{\mathrm{a}}=\frac{1}{2}\alpha_{\mathrm{i}}A_{\mathrm{a}}\tau_{\mathrm{p}}=\frac{1}{2}\alpha_{\mathrm{i}}\frac{z}{2p}\frac{I_{\mathrm{a}}}{2a}=\frac{1}{2}N_{\mathrm{a}}I_{\mathrm{a}}$. (2.132)

Now, we obtain the number of turns of the compensating winding to be inserted in the pole shoes producing demagnetizing magnetic flux in the q-axis compensating the armature reaction flux:

$$N_{\mathrm{k}}=\frac{\alpha_{\mathrm{i}}\tau_{\mathrm{p}}A_{\mathrm{a}}}{2I_{\mathrm{a}}}. \tag{2.133}$$

As N_{k} has to be an integer, Eq. (2.133) is only approximately feasible. To avoid large pulsating flux components and noise, the slot pitch of the compensating winding is set to diverge 10–15 % from the slot pitch of the armature.

Since a compensating winding cannot completely cover the surface of the armature, also commutating poles are utilized to compensate the armature reaction although their function is just to improve commutation. These commutating poles are located between the main magnetizing poles of the machine. There is an armature current flowing in the commutating poles. The number of turns on the poles is selected such that the effect of the compensating winding is strengthened appropriately. In small machines, commutating poles alone are used to compensate the armature reaction. If commutation problems still occur despite a compensating winding and commutating poles, the position of the brush rocker of the DC machine can be adjusted so that the brushes are placed on the real magnetic quadrature axis of the machine.

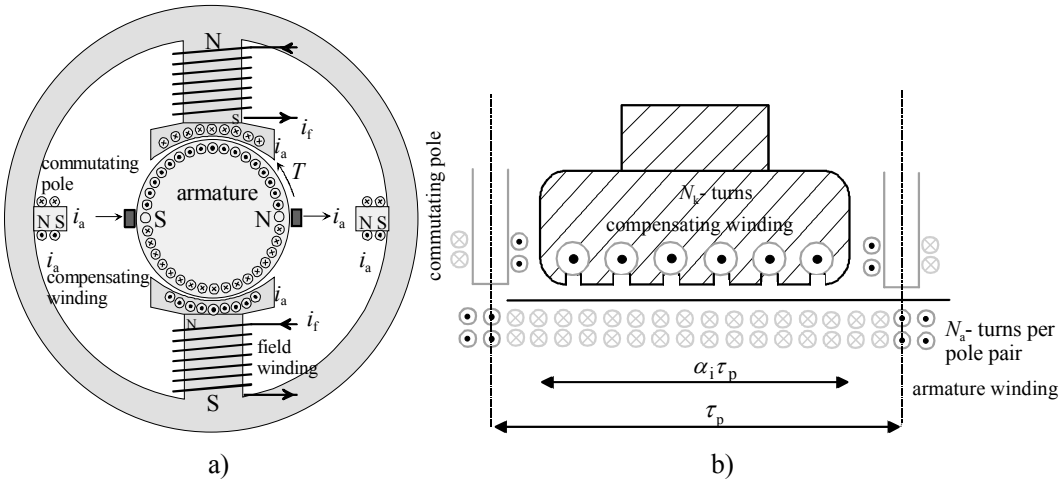

Figure 2.55. a) Location of the compensating windings and the commutating poles, b) definition of the current linkage of a compensating winding.

In principle, the dimensioning of a commutating pole winding is straightforward. Since the compensating winding covers the section $\alpha_i \tau_p$ of the pole pitch and includes N_k turns that carry the armature current I_a, the commutating pole winding should compensate the remaining current linkage of the armature $(1-\alpha_i)\tau_p$. The number of turns in the commutating pole N_{cp} should be

$$N_{cp} = \frac{1-\alpha_i}{\alpha_i} N_k . \qquad (2.133)$$

When the same armature current I_a flows both in the compensating winding and in the commutating pole, the armature reaction will be fully compensated.

If there is no compensation winding, the commutating pole winding must be dimensioned and the brushes positioned so that the flux in a commutating armature coil is at its maximum, and no voltage is induced in the coil.

2.17 Rotor Windings of Asynchronous Machines

The simplest rotor of an induction machine is a solid iron body, turned and milled to a correct shape. In general, a solid rotor is applicable to high-speed machines and in certain cases also to normal-speed drive. However, the computation of the electromagnetic characteristics of a steel rotor is a demanding task, and it is not discussed here. A solid rotor is characterized by a high resistance and a high leakage inductance of the rotor. The phase angle of the apparent power created by a waveform penetrating a linear material is 45°, but the saturation of the steel rotor reduces the phase angle. A typical value for the phase angle of a solid rotor varies between 30° and 45°, depending on the saturation. The characteristics of a solid-rotor machine are discussed for instance in Pyrhönen (1991), Huppunen (2004), and Aho (2007). The performance characteristics of a solid rotor can be improved by slotting the surface of the rotor, Fig. 2.56. Axial slots are used to control the flow of eddy currents in a direction favourable to the torque production. Radial slots increase the length of the paths of the eddy currents created by certain high-frequency phenomena. This way, eddy currents are damped and the efficiency of the machine is improved. The structure of the rotor is of great significance in torque production, Fig. 2.57. An advantage of common cage winding rotors is that they produce the highest torque with small values of slip, whereas solid rotors yield a good starting torque.

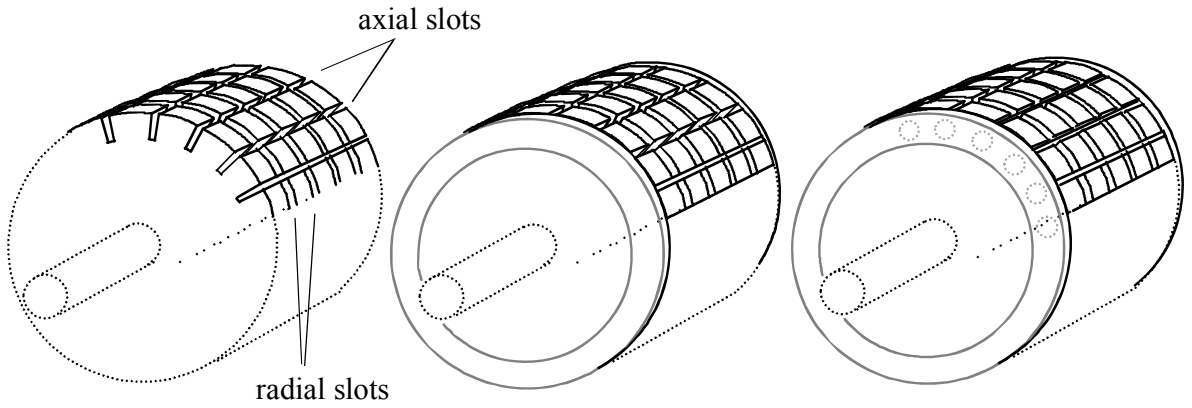

Figure 2.56. Different solid rotors. a) A solid rotor with axial and radial slots (in this model, short-circuit rings are required. They can be constructed either by leaving the part of the rotor that extends from the stator without slots, or by equipping it with aluminium or copper rings, b) a rotor equipped with short-circuit rings in addition to slots, c) a slotted and cage-wound rotor. A completely smooth rotor can also be employed.

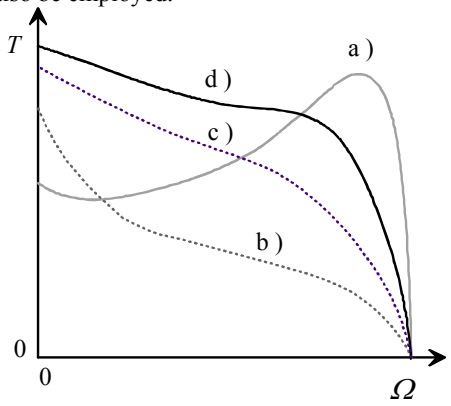

Figure 2.57. Torque curves of different induction rotors as a function of mechanical angular speed Ω. a) A normal double-cage winding rotor, b) a smooth solid rotor without short-circuit rings, c) a smooth solid rotor equipped with copper short-circuit rings, d) axially and radially slitted solid rotor equipped with copper short-circuit rings.

In small machines, a Ferraris rotor can be employed. It is constructed of a laminated steel core covered with a thin layer of copper. The copper covering provides a suitable path for eddy currents induced to it. The copper covering takes up a certain space in the air gap, the electric value of which increases notably because of the covering, since the relative permeability of copper is μ_r = 0.9999926. As a diamagnetic material, copper is thus even a somewhat weaker path for the magnetic flux than the air.

The rotor of an induction machine can be produced as a normal slot winding by following the principles discussed in the previous sections. A wound rotor has to be equipped with the same number of pole pairs as the stator, and therefore it is not in practice suitable for machines permitting a varying number of poles. The phase number of the rotor may differ from the phase number of the stator. For instance, a two-phase rotor can be employed in slip-ring machines with a three-phase stator. The rotor winding is connected to an external circuit via slip rings.

The most common short-circuit winding is the cage winding, Fig. 2.58. The rotor is produced of electric steel sheets and it is provided with slots containing non-insulated bars, the ends of which are connected either by welding or brazing to the end rings, that is, to the short-circuit rings. The short-circuit rings are often equipped with fins that together act as a cooling fan as the rotor rotates. The cage winding of small machines is produced of pure aluminium by simultaneously pressure casting the short-circuit rings, the cooling ribs and the bars of the rotor.

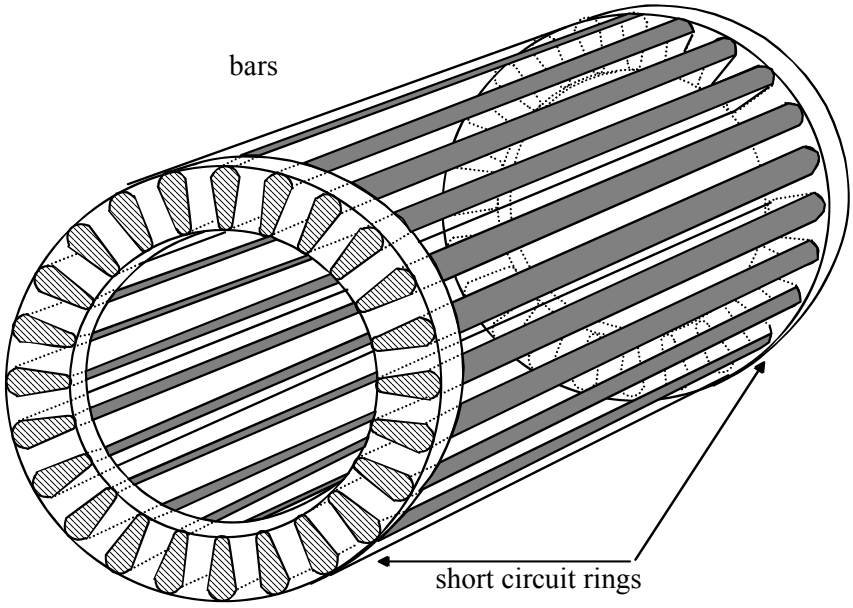

Figure 2.58. Simple cage winding. Cooling fans are not illustrated. $Q_r = 24$.

Fig. 2.59 illustrates a full-pitch winding of a two-pole machine observed from the rotor end. Each coil of the rotor constitutes also a complete phase coil, since the number of slots in the rotor is $Q_r = 6$. The star point 0 forms, based on symmetry, a neutral point. If there is only one turn in each coil, the coils can be connected at this point. The magnetic voltage created by the rotor depends only on the current flowing in the slot, and therefore the connection of the windings at the star point is of no influence. However, the connection of the star point at one end of the rotor turns the winding into a six-phase star connection with one bar, that is, half a turn, in each phase. The six-phase winding is then short circuited also at the other end. Since also the shaft of the machine takes some room, the star point has to be created with a short-circuit ring as illustrated in Fig. 2.58. We can now see that Fig. 2.59 depicts a star-connected, short-circuited poly-phase winding, for which the number of phase coils is in a two-pole case equal to the number of bars in the rotor: $m_r = Q_r$.

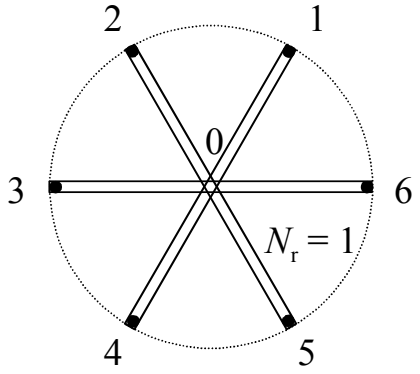

Figure 2.59. Three-phase winding of a two-pole rotor. The number of turns in the phase coil is $N_r = 1$. If the winding is connected in star at point 0 and it is short-circuited at the other end, a six-phase, short-circuited winding is created, for which the number of turns is $N_r = ½$, $k_{wr} = 1$.

In machine design, it is often assumed that the analysis of the fundamental $\nu = 1$ alone gives an adequate description of the characteristics of the machine. However, this is valid for cage windings only if we consider also the conditions related to its number of bars. A cage winding acts differently with respect to different harmonics ν. Therefore, a cage winding has to be analyzed with respect to the general harmonic ν. This is discussed in more detail in Chapter 7, in which different types of machines are investigated separately.

2.18 Damper Windings

The damper windings of synchronous machines are usually short-circuit windings, which in non-salient pole machines are contained in the same slots with magnetizing windings, and in salient pole machines in particular, in the slots at the surfaces of pole shoes. There are no bars in the damper windings on the quadrature axes of salient pole machines, but only the short-circuit rings encircle the machine. The resistances and inductances of the damper winding of the rotor are thus quite different in the d-direction and q-direction. In a salient pole machine constructed of solid steel, the material of the rotor core itself may suffice as a damper winding. In that case, an asynchronous operation resembles the operation of a solid rotor induction machine. Figure 2.60 illustrates a damper winding of a salient pole synchronous machine.

Damper windings improve the performance characteristics of synchronous machines especially during the transients. Like in asynchronous machines, thanks to damper windings, synchronous machines can in principle be started direct-on-line. Also a stationary asynchronous drive is in some cases a possible choice. Especially in single-phase synchronous machines and in the unbalanced load situations of three-phase machines, the function of damper windings is to damp the counter-rotating fields of the air gap which otherwise cause great losses. In particular, the function of damper windings is to damp the fluctuation of the rotation speed of a synchronous machine when rotating loads with pulsating torques, such as piston compressors.

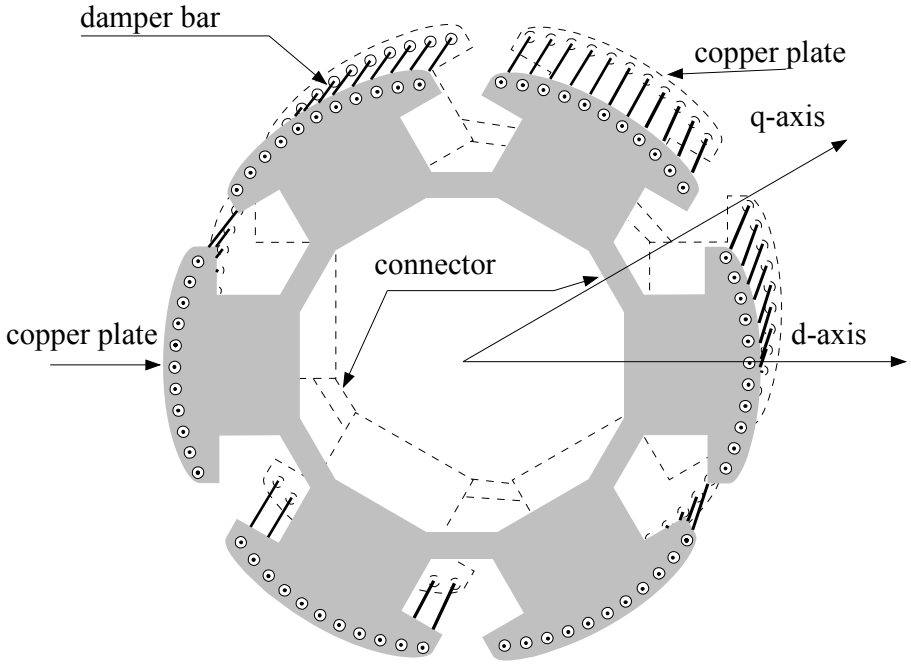

Figure 2.60. Structure of the damper winding of a six-pole salient pole synchronous machine. The copper end plates are connected with a suitable copper connector to form a ring for the damper currents. Sometimes also real rings connect the damper bars.

The effective mechanisms of damper windings are relatively complicated and diverse, and therefore their mathematically accurate design is difficult. That is why damper windings are usually constructed by drawing upon empirical knowledge. However, the inductances and resistances of the selected winding can usually be evaluated with normal methods to define the time constants of the winding.

When the damper windings of salient pole machines are placed in the slots, the slot pitch has to be selected to diverge 10–15 % from the slot pitch of the stator to avoid the pulsation of the flux and

noise. If the slots are skewed (usually for an amount of a single stator slot pitch), the same slot pitch can be selected both for the stator and the rotor. Damper winding comes into effect only when the bars of the winding are connected with short-circuit rings. If the pole shoes are solid, they may, similarly as the solid rotor of a non-salient pole machine, act as a damper winding as long as the ends of the pole shoes are connected with durable short-circuit rings. In non-salient pole machines, an individual damper winding is seldom used. However, in non-salient pole machines, conductors may be mounted under slot wedges, or the slot wedges themselves are used as the bars of the damper winding.

In synchronous generators, the function of damper windings is to damp for instance counter-rotating fields. To minimize losses, the resistance is kept to a minimum in damper windings. The cross-sectional area of the damper bars is selected to be 20–30 % of the cross-sectional bar area of the armature winding. The windings are made of copper. In single-phase generators, damper bar cross-sectional areas larger than 30 % of the stator copper area are employed. The frequency of the voltages induced by counter-rotating fields to the damper bars is double when compared with the network frequency. Therefore, it has to be considered whether special actions are required with respect to the skin effect of the damper windings (for instance the utilization of the Roebel bars (braided conductors) to avoid skin effect). The cross-sectional area of the short-circuit rings is selected to be approximately 30–50 % of the cross-sectional area of the damper bars per pole.

The damper bars have to damp the fluctuations of the rotation speed caused by the pulsating torque loads. They also have to guarantee a good starting torque when the machine is starting as an asynchronous machine. Thus, brass bars or small-diameter copper damper bars are employed to increase the rotor resistance. The cross-sectional area of copper bars is typically only 10 % of the cross-sectional area of the copper of the armature winding.

In permanent magnet synchronous machines, in axial flux machines in particular, the damper winding may be easily constructed by placing a suitable copper or aluminium plate on the surface of the rotor, on top of the magnets. However, achieving a total conducting surface in the range of 20 – 30 % of the stator copper surface may be somewhat difficult as the plate thickness easily increases too large and limits the air gap flux density created by the magnets.

References and Further Reading

Aho, T. 2007. *Electromagnetic design of a solid steel rotor motor for demanding operational environments.* Dissertation. Acta Universitatis Lappeenrantaensis 134. Lappeenranta University of Technology. (https://oa.doria.fi/)

Heikkilä, T. 2002. *Permanent magnet synchronous motor for industrial inverter applications – analysis and design*. Dissertation. Acta Universitatis Lappeenrantaensis 134. Lappeenranta University of Technology. (https://oa.doria.fi/)

Hindmarsh, J. 1988. *Electrical Machines and Drives. Worked Examples.* Second edition. Oxford: Pergamon Press.

Huppunen, J. 2004. *High-speed solid-rotor induction machine – electromagnetic calculation and design.* Acta Universitatis Lappeenrantaensis 197. Lappeenranta University of Technology. (https://oa.doria.fi/)

IEC 60050-411. 1996. *International electrotechnical vocabulary (IEC). Rotating machines.* Geneva: International Electrotechnical Commission.

Pyrhönen, J. 1991. *The high-speed induction motor: calculating the effects of solid-rotor material on machine characteristics*. Acta Polytechnica Scandinavica, Electrical Engineering Series 68. (https://oa.doria.fi/)

Richter, R. 1954. *Electrical machines.* (*Elektrische Maschinen*.) Volume IV. *Induction machines.* (*Die Induktionsmaschinen.*) Second edition. Basel and Stuttgart: Birkhäuser Verlag.

Richter, R. 1963. *Electrical machines.* (*Elektrische Maschinen*.) Volume II. *Synchronous machines and rotary converters. (Synchronmaschinen und Einankerumformer*.) Third edition. Basel and Stuttgart: Birkhäuser Verlag.
Richter, R. 1967. *Electrical machines.* (*Elektrische Maschinen*.) Volume I. *General calculation elements. DC machines.* (*Allgemeine Berechnungselemente. Die Gleichstrommaschinen*.) Third edition. Basel and Stuttgart: Birkhäuser Verlag.
Salminen, P. 2004. *Fractional slot permanent magnet synchronous motors for low speed applications*. Dissertation. Acta Universitatis Lappeenrantaensis 198. Lappeenranta University of Technology.
Vogt, K. 1996. *Design of electrical machines.* (*Berechnung elektrischer Maschinen*.) Weinheim: VCH Verlag.